Molecular mechanisms of CD8+ T cell mediated control of HIV-1 infection in peripheral blood and lymphoid tissues

By: Funsho J. Ogunshola

MSc Immunology

Submitted in fulfilment of the academic requirements of the degree Doctor of Philosophy in Immunology

School of Laboratory Medicine and Medical Sciences

Nelson R Mandela School of Medicine

University of KwaZulu-Natal

Durban, South Africa

Supervisor: Prof. Zaza M. Ndhlovu

Co-supervisor: Prof. Thumbi Ndung'u

PREFACE

The experimental work described in this dissertation was carried out at the Africa Health Research Institute (AHRI) and HIV Pathogenesis Programme (HPP), School of Laboratory Medicine and Medical Sciences, Nelson R. Mandela School of Medicine, University of KwaZulu-Natal, Durban, South Africa, from April 2014 to June 2019, under the supervision of Prof. Zaza M. Ndhlovu and Prof. Thumbi Ndung'u.

These studies represent original work by the author and have not otherwise been submitted in any form for any degree or diploma to any University. Where use has been made of the work of others, it is duly acknowledged in the text.

Funsho J. Ogunshola (candidate

Prof. Zaza M. Ndhlovu (supervisor)

Prof. Thumbi Ndung'u (co-supervisor)

DECLARATION 1: PLAGIARISM

I, Funsho J. Ogunshola, declare that

(i)   The research reported in this dissertation, except otherwise indicated, is my original research work.

(ii)   This dissertation has not been submitted for any degree or examination at any other university.

(iii)   This dissertation does not contain other persons' data pictures, graphs or other information, unless specifically acknowledged as being sourced from other persons.

(iv)   This dissertation does not contain other persons' writing, unless specifically acknowledged as being sourced from other researchers. Where other written sources have been quoted, their words have been re-written but the general information attributed to them has been referenced.

(v)   Where I have reproduced a publication of which I am not the author, co-author or editor, I have fully referenced such publications.

(vi)   This dissertation does not contain text, graphics or table copied and pasted from internet unless specifically acknowledged, and the source being detailed in dissertation and in the references sections.

Signed: --------------------------   **Date:** ------------------------------

The manuscripts that constitute this thesis are listed below and the contributions that I and other co-authors made to each manuscript are declared here:

Manuscript 1: Funsho Ogunshola, Gursev Anmole, Rachel Miller, Emily Goering, Thandeka Nkosi, Daniel Muema, Jaclyn Mann, Nasreen Ismail, Denis Chopera, Thumbi Ndung'u, Mark Brockman, and Zaza Ndhlovu. Dual HLA B*42:01 and B*81:01-reactive T cell receptor clonotypes display broad recognition of HIV-1 Gag escape variants. *Nature Communications* 2018 Nov 27;9(1):5023. doi: 10.1038/s41467-018-07209-7. PMID: 30479346.

Authors' contributions: Prof. Zaza Ndhlovu and Prof. Thumbi Ndung'u initiated the study cohorts. Prof. Zaza Ndhlovu conceived the idea. Prof. Zaza Ndhlovu, Prof. Mark Brockman and I designed the experiments. Gursev Anmole and I conducted the TCR sequencing and reporter assay and generated the TCR clones. I performed the rest of the laboratory experiments and analyzed the data. Gursev and I wrote the manuscript under the supervision of Prof. Zaza. Ndhlovu and Prof. Mark Brockman. All authors approved of the manuscript before it was submitted and published in *Nature Communications*.

Manuscript 2: Funsho J. Ogunshola, Werner Smidt, Anneta F. Naidoo, Thandeka Nkosi, Thandekile Ngubane, Trevor Khaba, Omolara O. Baiyegunhi, Sam Rasehlo, Ismail Jajbhay, Krista L. Dong, Veron Ramsuran, Johan Pansegrouw, Thumbi Ndung'u, Bruce D. Walker, Tulio Oliveria and Zaza M. Ndhlovu* ***CXCR5* gene**

expression in human CD8$^+$ T cells is regulated by DNA methylation and nucleosomal occupancy.

Authors' contributions: Prof. Zaza Ndhlovu conceived the idea. Prof. Zaza Ndhlovu and I designed the experiments. Thandekile Ngubane, Ismail Jajbhay, Johan Pansegrouw performed the lymph node excisions. Thandeka Nkosi processed the lymph node samples. I performed majority of the experiments described in this study under the supervision of Prof. Zaza Ndhlovu with technical assistance from Veron Ramsuran on drug treatment assay, Omolara Baiyegunhi, and Trevor Khaba on tissue staining. Anneta Naidoo and I performed the Next Generation Sequencing (NGS). Werner Smidt wrote the scripts used to perform NGS analysis under the supervision of Tulio Oliveria. I analysed other data reported in this study. Werner and I wrote the manuscript under the supervision of Prof. Zaza Ndhlovu. Prof. Zaza Ndhlovu, Prof. Tulio Oliveria, Prof. Bruce Walker and Prof. Thumbi Ndung'u, provided critical edits to the manuscript. All authors reviewed the manuscript.

Funsho J. Ogunshola (candidate): ----------------- **Date:** ------------------------

Prof. Zaza Ndhlovu (Supervisor): ----------------- **Date:** ------------------------

Prof. Thumbi Ndung'u (Co-supervisor): ----------------- **Date:** ------------------------

PRESENTATIONS AND SCHOLARSHIP AWARDS

Oral Presentations

1. South Africa Immunology Society (SAIS), March 2016. Antiviral Activity of HIV-Specific CD8$^+$ T cells when presented with identical TL9-epitope restricted by HLA-B*81:01 and HLA-B*42:01.

2. Sub-Saharan African Network for TB/HIV Research Excellence (SANTHE), Annual Consortium Meeting, September 2016. Phenotypic and Functional Characterization of CD8$^+$ T cells from lymphoid tissues excised from HIV infected Subjects.

3. Sub-Saharan African Network for TB/HIV Research Excellence (SANTHE), Annual Consortium Meeting, September 2017. Epigenetic Regulation of lymphoid tissues CD8$^+$ T cells during HIV infection.

4. DELTAS Annual Consortium Meeting, July 2019. Mechanism of CD8$^+$ T cells mediated control of HIV: Implication for HIV vaccine.

Poster Presentations

1. Keystone Symposia conference-C9, HIV Vaccine, March 2017. Phenotypic and Functional Characterization of CD8$^+$ T cells from lymphoid tissues excised from HIV infected Subjects.

2. Indian Alliance Network Meeting, May 2017. CXCR5 Expression in human CD8$^+$ T cells is tightly regulated by DNA methylation.

3. Sub-Saharan African Network for TB/HIV Research Excellence (SANTHE), Annual Consortium Meeting, September 2017. Epigenetic modifications dictate the expression of CXCR5 on CD8$^+$ T cells in lymphoid tissues.

4. Keystone Symposia conference, HIV and co-infection: Pathogenesis, Inflammation and Persistence (X8), March 2018. Tetramer cross-reactivity defines a public TCR clonotype with broad recognition against HIV Gag TL9 variants.

Scholarship Awards

1. South Africa Immunology Society (SAIS) Student scholarship award (March 2016).

2. SANTHE PhD fellowship Award (March 2016).

3. SANTHE Consumable Award (January 2017).

4. Keystone Symposia scholarship for C9, HIV Vaccine, (March 2017).

DEDICATION

This project is dedicated to the Almighty God for His unconditional love upon my life and His help I received all through my PhD programme.

ACKNOWLEDGEMENTS

I would like to express my sincere gratitude and appreciation to the following people:

My supervisor, Professor Zaza M. Ndhlovu, for his guidance, encouragement, believing in me, and giving me a reason to believe in myself, I feel honoured to be under his mentorship. I would also like to acknowledge my dear co-supervisor, Professor Thumbi Ndung'u for all his support throughout my PhD programme.

Many thanks to my wife Dr (Mrs). Sarah Opeyemi Ogunshola, for bringing me so much joy and for her support at all times. To my dear mother, Mrs Foluke Ogunshola and parents in the Lord, Mr and Mrs Gbile Akanni, Mr and Mrs Lanre Adeboye, and many others. I want to say a big thank you to them all for their immense inputs to my career development. To my special friends, Prof. Gbenga Johnson, Dr. Joshua Edokpayi, Dr. Samson Adeyemi, Mr Ntuthuko Mbonambi, Miss Yonela Vukapi, Miss Phiwe Nota, Mr Someleze Makubalo, Dr. Daniel Muema and Dr. Shola Olagoke and Mr Seyi Olagoke, thanks for being there for me through thick and thin. I will forever be grateful for your love. God Bless you all!

I also offer my regards to my colleagues in the laboratory who offered assistance in any form, supported and showered me with words of encouragement during the course of my studies. Special thanks to Dr. Omolara Baiyegunhi, Dr. Faatima Laher, Miss Thandeka Nkosi, Miss Bongiwe Mahlobo. I love you all, God bless you all!

The honour of God is to hide a thing, and the honour of the kings to search out the thing **(Proverb 25:2).**

I can do all things through Christ that strengthen me **(Philippians 4:13).**

Table of Contents

List of Figures

List of Tables

xvii

Abstracts

Naturally induced CD8^{+} T cells do not clear human immunodeficiency virus (HIV) infection, partly because the virus rapidly escapes CD8^{+} T cell responses and the effector cells are excluded from HIV reservoirs sites. However, optimizing CD8^{+} T cell responses could potentially be leveraged in HIV vaccine or cure efforts if epitope escape and barriers to effector CD8^{+} T cells infiltrating the sites of HIV reservoirs are overcome. In our first study, we described a potential mechanism of HIV-1 control by CD8^{+} T cells targeting different variants in individuals infected with HIV-1. Our second study focused on describing the molecular regulation of CXCR5 expression in human CD8^{+} T cells.

Study 1

HLA-B*81 is associated with control of HIV-1 subtype C infection, while the closely related allele B*42 is not. Interestingly, both alleles present the immunodominant Gag TL9 epitope, and the magnitude of this response correlates negatively with viral load. To examine the role of T cell receptor (TCR) in this process, we characterized the sequence and function of TL9-specific CD8^{+} TCR in B*81 and B*42 individuals.

TL9-specific CD8^{+} T cells were identified and isolated using B*81 and/or B*42 TL9 tetramers. TCR beta genes were amplified from single sorted cells and sequenced. Paired alpha genes were identified for selected clones. TCR function was tested using

a reporter cell assay where TCR$^+$ Jurkat cells were co-cultured with peptide-pulsed or HIV-1 infected B*81 or B*42 target cells, and signalling quantified by luminescence. TCR recognition was assessed against all single amino acid TL9 variants and results were compared to HIV-1 subtype C sequences.

A population of dual-reactive T cells was detected by both B*81- and B*42-TL9 tetramers in 7/9 (78%) B*81 and 4/11 (36%) B*42 individuals; and this population was associated with lower viremia. Mono- and dual-reactive TCR beta sequences were collected from six individuals. In B*81 individuals, all TCRs were highly restricted to TRBV12-3. In B*42 individuals, mono-reactive TCRs encoded a variety of V beta genes, while dual-reactive TCRs were restricted to TRBV12-3 and enriched for public clones. Functional analyses indicated that B*81 TCRs (1 mono, 2 dual) and a dual-reactive public B*42 TCR displayed similar TL9 cross-reactivity profiles and enhanced capacity to recognize HIV-1 escape mutations compared to mono-reactive B*42 TCRs. This work highlights the impact of TCR promiscuity on T cell-mediated control of HIV-1.

Study 2

HIV-1 infection is difficult to cure even with effective antiretroviral therapy (ART) because of persistent viral replication in immune privileged sites such as the B cell follicles of secondary lymphoid tissues. CD8$^+$ T cells are generally excluded from B cell follicles, partially due to a lack of expression of the follicular homing receptor CXCR5. Recent murine studies have identified CXCR5$^+$ CD8$^+$ T cells, referred to as

follicular CD8^{+} T cells (fCD8s), that localize in B cell follicles. However, the mechanisms governing expression of CXCR5 on human CD8^{+} T cells are not known. We investigated the epigenetic and transcriptional mechanisms involved in the regulation of CXCR5 expression in human CD8^{+} T cells.

We FACS-sorted CXCR5^{+}CD8^{+} (fCD8s), CXCR5^{-}CD8^{+} (non-fCD8s), naïve CD8^{+} T cells and germinal center T follicular helper cells (GCTfh) from the lymph node of HIV-1 infected individuals and performed RNA-sequencing (RNA-Seq), DNA methylation assays and the assay for transposase-accessible chromatin using sequencing (ATAC-Seq). RNA-Seq was used to quantify the expressed genes in FACS-sorted subsets and to determine transcriptional modules governing CXCR5 expression in CD8^{+} T cells. ATAC-Seq was used to quantify accessible genes, identify the transcriptional factors footprinting and determine epigenetic modules governing CXCR5 expression. DNA methylation, a major epigenetic gene silencing mechanism, was used to profile methylation pattern of the *CXCR5* gene region in the sorted subsets.

We observed hypermethylation of DNA around the transcriptional start site (*TSS*) of the *CXCR5* gene in non-fCD8s but not in fCD8s. ATAC-Seq analysis revealed a closed chromatin conformation at the *TSS* in non-fCD8s, but not in fCD8s. Our gene expression data revealed significant differences in the CXCR5 associated factors between GCTfh and fCD8s. Computational analysis further revealed the presence of a nucleosome at the *TSS* of fCD8s, which could be a plausible explanation for lower expression of CXCR5 in fCD8s as compared to GCTfh.

Together, we identified epigenetic regulations involved in CXCR5 expression in human CD8^{+} T cells and propose that DNA methylation, chromatin structure and nucleosome positioning cooperatively regulate the expression of CXCR5 in CD8^{+} T

cells. Our data open up the possibility of using epigenetic manipulation as a novel strategy for redirecting CD8+ T cells to B cell follicles where they are needed to eradicate HIV-1 infected cells.

CHAPTER 1: INTRODUCTION

1.1 The HIV/AIDS Epidemic

Human immunodeficiency virus (HIV) is the aetiological agent of acquired immune deficiency syndrome (AIDS) and is one of the most devastating pathogens known to man. Following its isolation in 1983, HIV has evolved to become a threat to global health [1] and over 25 million AIDS related deaths have been recorded since its discovery. In 2018, an estimate of 37 million people were living with HIV globally, with almost 70% of that figure living in sub-Saharan Africa [2]. Furthermore, South Africa bears the highest burden of the HIV epidemic globally (Figure 1.1) [2]. There are two types of HIV, namely HIV-1 and HIV-2. Although both HIV-1 and HIV-2 have similar modes of transmission and replication pathways, they are genetically different viruses with different ancestral origins [3]. HIV has intrinsic mechanisms that ensure rapid viral evolution. The resultant HIV diversity has implications for possible differential rates of disease progression and vaccine development. For example, HIV-1 recombination can lead to further viral diversity and occurs when one person is co-infected with two separate strains of virus [4]. HIV-1 has been divided into subtypes, denoted with letters for subtypes: A, B, C, D, F, G, H, J and K are currently recognized. The present study was conducted in South Africa where the HIV-1 subtype C is prevalent [5]. Thus, the focus hereon will be on HIV-1 subtype C infection.
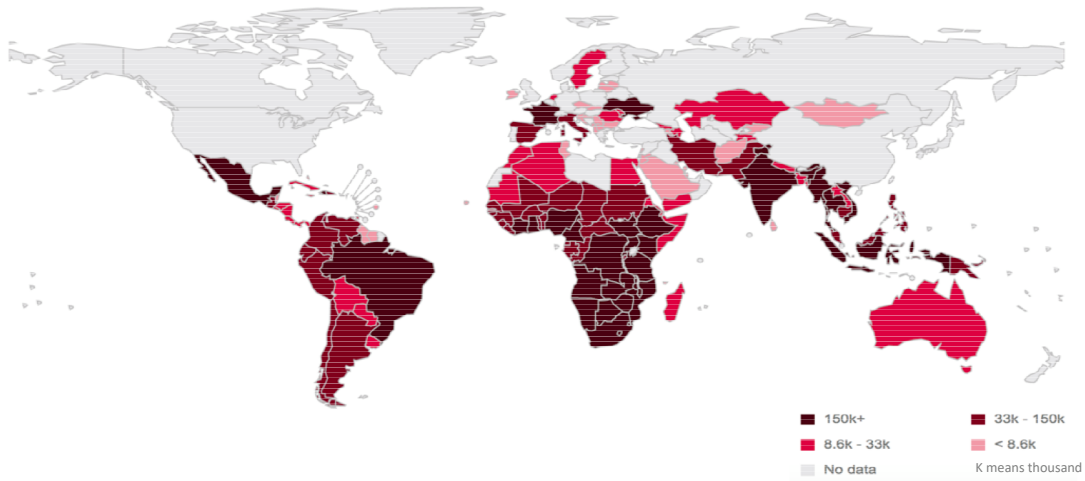
2

Figure 1.1: Global HIV prevalence in 2018.

1.2   HIV-1 Pathogenesis

Exposure to HIV-1 is primarily through the mucosal route of either the gastrointestinal or the reproductive tract, which results in initial local replication of the virus within target cells of the mucosal tissue [6]. This is followed by a systematic spread with considerable dissemination in the gut-associated lymphoid tissue (GALT) [7]. The establishment of HIV-1 infection is dependent on the target cells expression of CD4 and a chemokine receptor, majorly, CCR5 or CXCR4 [8]. The course of HIV-1 infection can be categorized into 3 phases as illustrated in (Figure 1.2); (1) the acute phase, (2) the asymptomatic phase and (3) the AIDS phase.
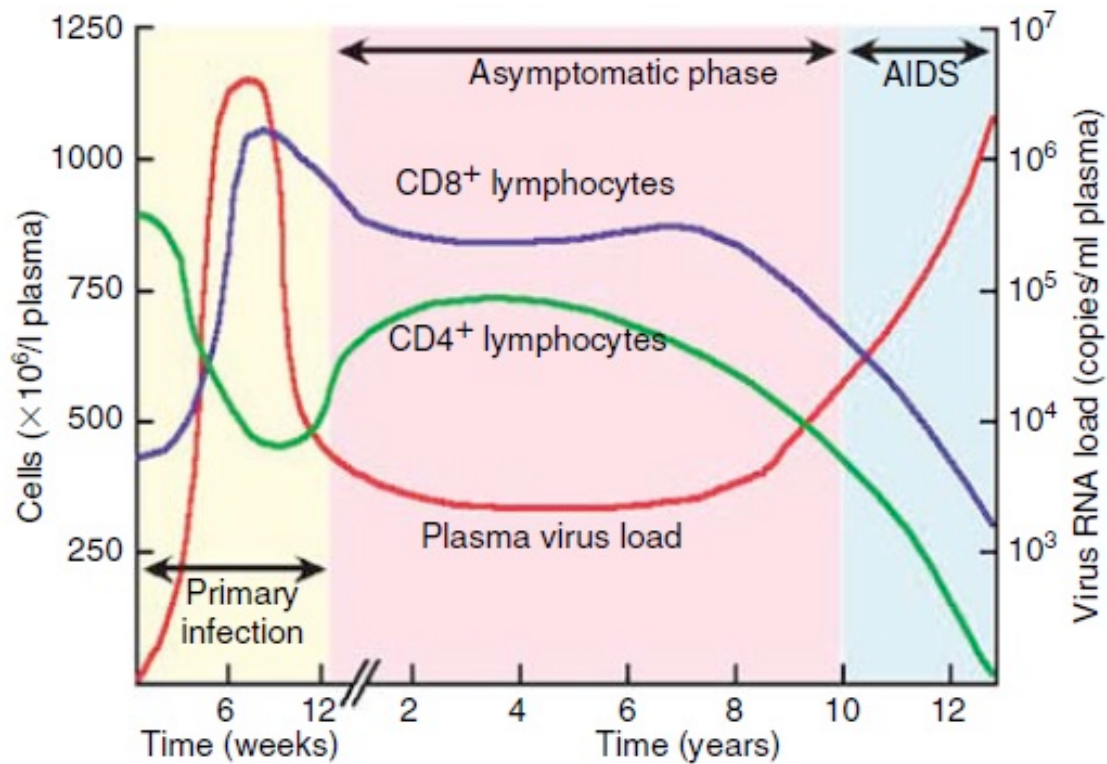
9.

Figure 1.2: HIV-1 pathogenesis.

Representation of a typical course of HIV-1 infection showing CD8$^+$ T and CD4$^+$ T cells dynamics and viral load changes over time of infection.

1.2.1 The Acute Phase

Following transmission of HIV-1, approximately 10 days are required for viral RNA to be detectable in the plasma [10]. During this acute phase, diagnosis of acute HIV-1 infection is often missed because the symptoms are similar to many other infections [11]. HIV-1 replicates rapidly during the acute phase of infection with viral titres reaching a peak of usually more than 100 million RNA copies per millilitre of blood. Also, CD4$^+$

T cells numbers are significantly lowered at the time of peak viremia [10]. Subsequently, the emergence of CD8^{+} T cells responses coincides with a decrease in viremia [12], suggesting that the suppression of viral replication is largely mediated by CD8^{+} T cells [10].

A few studies have measured HIV-1 specific CD8^{+} T cells responses during early HIV-1 infection [13-17]. The HIV-1 specific CD8^{+} T cell responses peaks at about 1-2 weeks after viremia declines [10,18]. Following the peak in HIV-1 specific CD8^{+} T cell responses, the virus sequence starts to change dramatically [10]. Due to rapid selection of mutations at discrete sites in the virus genome [19,20]. There is still a lot to learn on the early events during the acute phase of HIV-1 infection which determine the course of HIV disease progression.

1.2.2 Asymptomatic Phase

The asymptomatic phase of HIV-1 infection is characterized by the establishment of a viral set-point [10]. During this phase, there is a gradual decline in the circulating CD4^{+} T cells and loss of immune function. The decline in the CD4^{+} T cells is not only caused by direct infection but also as a result of chronic immune activation and inflammation [21]. The steady replication of HIV-1 results in progressive exhaustion of HIV-1 specific CD8^{+} T cells as a result of continuous exposure to HIV-1 antigens, thus impairing the ability of the immune system to control the virus [10,21].

1.2.3 The AIDS Phase

In the absence of antiretroviral treatment, HIV-1 establishes a chronic, progressive infection of the host's immune cells that, invariably, over the course of the years, leads

to its destruction and severe immunodeficiency [6]. The AIDS phase is defined by the rapid decline in CD4^{+} T cell count with an increase in viral load. At this stage, the host becomes highly susceptible to opportunistic infections (e.g. tuberculosis, pneumococcal infections, oral candidiasis) and certain cancers (e.g. Kaposi's sarcoma) [22]. The average time from infection to full blown AIDS is 8-10 years, but this may vary considerably due to host and viral factors [23,24]. During advanced disease, the immune cells are severely compromised, and death ensues as a result of opportunistic infections. [25,26].

Both viral and host factors influence HIV-1 disease progression [27]. In fact, emerging data now provide evidence that the immune system is a key player in the outcome of HIV-1 infection [28]. As previously mentioned, a critical component of the adaptive immune response to HIV-1 infection is the CD8^{+} T cell response. CD8^{+} T cells directed against HIV-1 are commonly detectable in HIV-infected individuals and have been shown to effectively inhibit HIV-1 replication through several mechanisms that are increasingly being elucidated.

1.3 CD8^{+} T Cells

CD8^{+} T cells also referred to as cytotoxic T lymphocytes (CTLs), are the host's major defence mechanism against invading intracellular pathogens [29]. CD8^{+} T cells control HIV-1 replication and help to maintain clinical stability in infected individuals through a number of mechanisms [13,14]. The role of CD8^{+} T cells in controlling HIV replication will be discussed in the subsequent chapters.

1.3.1 History of HIV-1 Specific CD8^{+} T Cells

HIV-1 specific CD8^{+} T cells were first reported in 1987 by Walker *et al*., [30] and Plata *et al*., [31] where they measured the ability of freshly isolated peripheral blood mononuclear cells (PBMCs) to lyse autologous B cells infected with recombinant vaccinia-HIV vector [30] or by peptide-pulsed targets [32]. Subsequent studies using other approaches such as detection of interferon-γ by enzyme-linked immune absorbent spot (ELISPOT) [33] and intracellular cytokines (ICS) [34] were used to confirm HIV-1 specific CD8^{+} T cells responses in HIV-1 infected individuals. Tetramer assay has also been developed to measure absolute number of cells that recognize a particular HIV-1 epitope, without providing any information regarding the functionality of CD8^{+} T cells. [35,36]. Thus, most of these assays are used in concert to measure the quality and quantity of CD8^{+} T cells responses isolated from HIV-1 infected individuals.

1.3.2 Mechanism of Action of CD8^{+} T Cells during Viral Infection

During viral infections, CD8^{+} T cells are able to recognize the complex of class I human leukocyte antigen (HLA) molecules and viral peptides via CD8^{+} T cell receptors (Figure 1.3). The recognition triggers signalling cascade via the CD8^{+} T cell receptor (TCR), resulting in the release of cytolytic molecules such as perforin and granzymes that cooperatively lyse the infected cell [37]. These effector molecules are capable of direct killing of infected cells by inducing cellular apoptosis [38]. CD8^{+} T cell responses in an individual mainly dependant on the TCR repertoire that recognise restricted peptides by class I HLA alleles. But, CD8^{+} T cells can also eliminate viral infected cells through the engagement of death-inducing ligands (FasL) [39,40]. FasL expressed by activated CD8^{+} T cells interacts with the Fas receptors expressed on the surface of infected

cells. The binding causes trimerizing of the Fas molecules on the surface of target cells. The resultant activation of a caspase cascade leads to apoptosis of the target cell [41]. In addition, CD8^{+} T cells can also secrete soluble antiviral factors that suppress viral replication [42-44].
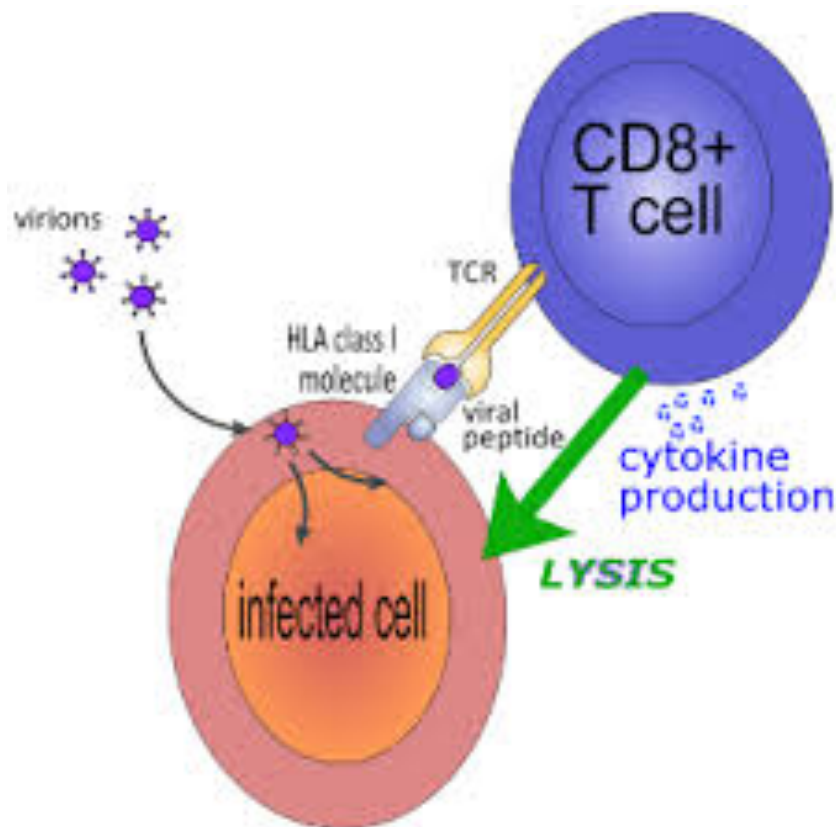
Figure 1.3: Schematic representation of CD8^{+} T cell killing mechanism and secretion of antiviral factors. The infected cell processes the viral peptide and presents it to a CD8^{+} T cell via a class I HLA molecule. The CD8^{+} T cell recognizes the presented peptide through the TCR and releases cytotoxic molecules into the infected cell, thereby resulting in the killing of the infected cell. CD8^{+} T cell also secrets antiviral factors that inhibit viral replication [45,46].

1.3.3 CD8^{+} T Cell Receptors

The CD8^{+} T cell receptors (TCRs) are surface heterodimers consisting of disulphide-linked α- and β-chains. Each TCR chain is composed of variable and constant Ig-like domains, followed by a transmembrane domain and a short cytoplasmic tail [47]. CD8^{+} T cells recognize peptides presented by the infected cell through the α/β binding site of the TCR [48]. Binding of the peptide fragment takes place through the third loop region on each of α and β chains and the complementarity determining regions (CDRs). The CDR is composed of three domains; CDR1, CDR2 and CDR3. The CDR3 is mainly involved in the interactions with the peptide fragment, while CDR2 interacts with the heavy chain of class I HLA molecule (Figure 1.4). In most TCRs, CDR1 has limited interaction with the peptide fragment and the class I HLA molecule [49]. Studies have suggested that engineered TCRs might provide a means of generating HIV-1 specific polyfunctional T-cell responses and can engage epitope variants presented by the infected cells [50-52]. Hence, engagement of TCRs could modulate viral inhibitory capacity and recognition of naturally occurring HIV-1 peptides.
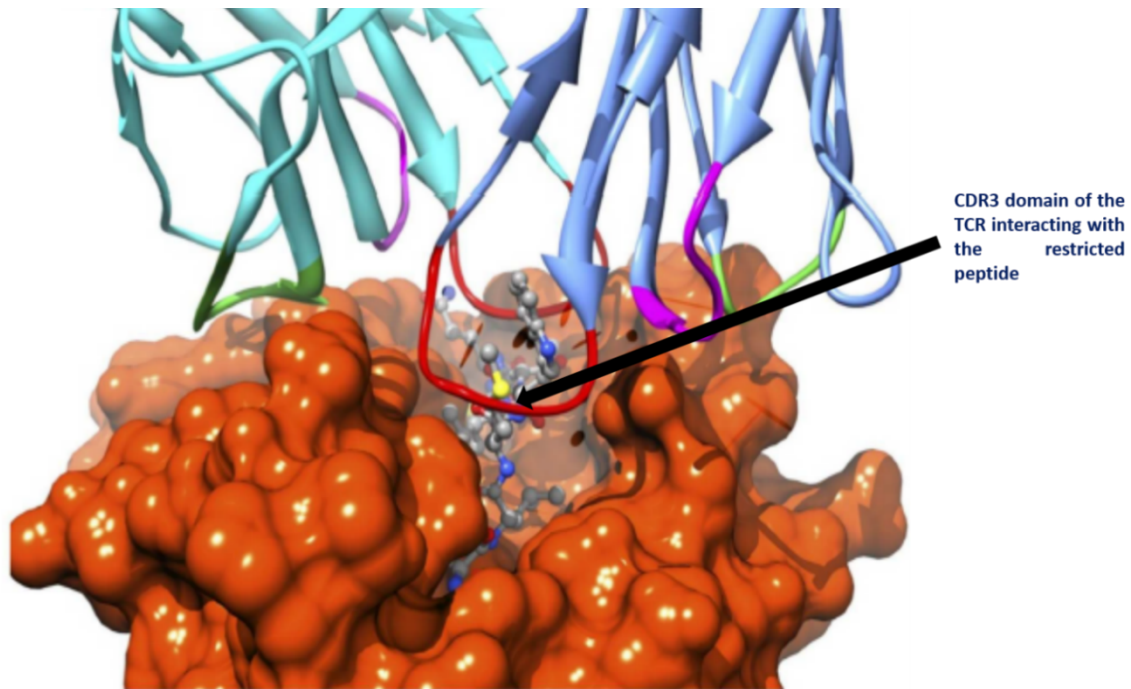
Figure 1.4: Interaction of the TCR CDRs with the class I HLA allele/peptide complex. CDR1, CDR2 and CDR3 are colored in magenta, green and red respectively [53]. CDR3 (red) is mainly involved in the interraction with the peptide presented by the class I HLA molecule.

1.4   Human Leukocyte Antigen (HLA)

The major histocompatibility complex (MHC) coding region, known as HLA in humans is located on the short arm of chromosome 6, and is the most polymorphic region of the entire human genome [54,55]. Genes in this complex are categorized into three groups: class I, class II and class III. Functional MHC molecules are made of a heavy (α) chain and a β_2-microglobulin chain genes encoding class I loci [56]. Peptide binding by MHC class I molecules is accomplished by interaction of the peptide amino acid side chains with discrete pockets within the peptide-binding groove of the MHC

molecule formed by the α_1 and α_2 domain of the heavy chain, (Figure 1.5), [56]. The main binding energy of a peptide to the class I HLA molecule is provided by the interaction of residues in position 2 and the C-terminus of the peptide with the B and F binding pockets respectively, (Figure 1.6), [57].
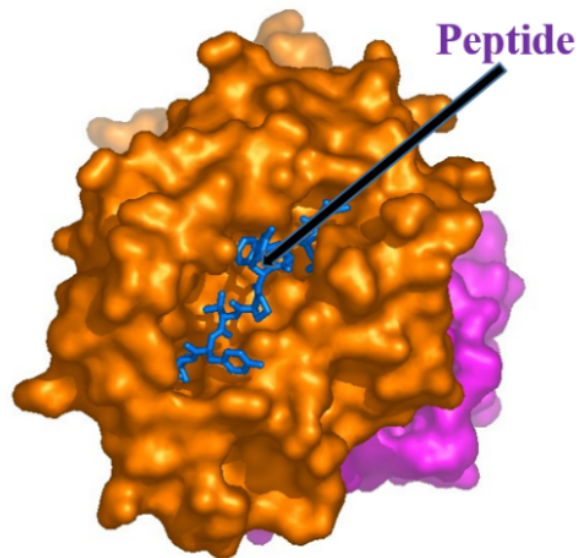
Figure 1.5: Schematic representation of HLA molecule housing a peptide. The peptide (blue) is the amino acid sequence sitting in the peptide binding pocket of HLA molecule [58].

Of the three MHC class I loci in humans (HLA-A, HLA-B and HLA-C), HLA-B is the most polymorphic, with 817 different HLA-B molecules described, compared to 486 distinct HLA-A and 263 distinct HLA-C molecules [59]. The polymorphism of HLA molecules influences the peptide-binding repertoire. However, multiple class I HLA alleles can bind identical peptides due to the similarity in their peptide binding motifs.

HLA alleles sharing similar peptide binding motifs have therefore been referred to as HLA supertypes, (Figure 1.6), [60]. Polymorphisms of class I HLA molecules have been shown to contribute to differences in disease outcome [54].
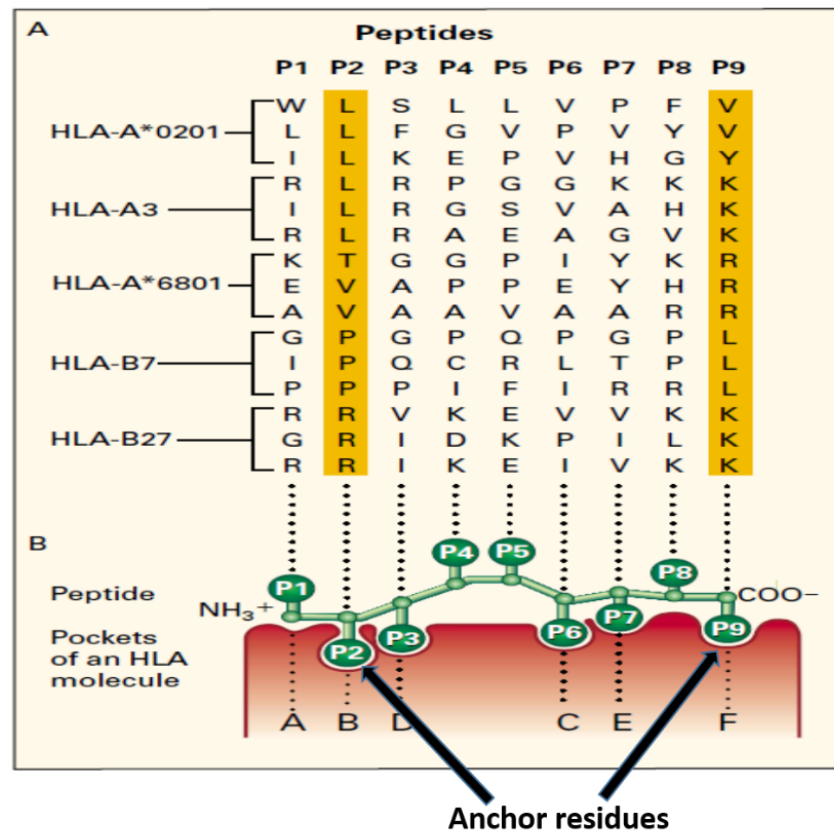
Figure 1.6: Interactions between HLA molecules and peptides. Panel A illustrates examples of peptide motifs. The listed amino acids as well as many others have been found to complex with the respective HLA class I molecules. The anchor residues are highlighted in yellow. Panel B is a longitudinal section through the peptide-binding groove of pocket A to F. Pocket B and F bind the peptide residue P2 and P9 respectively. Some of the peptide residues pointing into the HLA molecule have a greater influence over binding while the residues that point outward interact with the T-cell receptor [61].

1.5   Role of CD8^{+} T Cells in HIV-1 Infection

Numerous lines of evidence suggest that HIV-1 specific CD8^{+} T cells exert potent antiviral effect in HIV-1 infected individuals reviewed by [62]. The magnitude and rapidity of HIV-1 specific CD8^{+} T cell activation in hyperacute infection correlate inversely with the viral load set point [18], indicating that these cells mediate antiviral pressure during peak viremia [13,63]. The antiviral activity of HIV-1 specific CD8^{+} T cell is further indicated by rapid evolution of escape variants within targeted viral CD8^{+} T cell epitopes following acute infection [64,65]. *In vitro* models provide additional evidence for an antiviral effect of CD8^{+} T cells, showing that these cells potently inhibit viral replication [66,67]. In addition, *in-vivo* studies on the control of viremia in macaques during primary simian immunodeficiency virus (SIV) infection show that the depletion of CD8^{+} T cells abrogates their ability to control primary viremia [68-70]. However, the factors influencing the effectiveness of the HIV-1 specific CD8^{+} T cells responses in controlling viral replication and in subsequently establishing different viral set points in individuals are poorly understood.

The relationship between the earliest CD8^{+} T cells responses, viral set point and disease progression remains controversial [62]. Studies have suggested that the initial CD8^{+} T cells responses are low in magnitude and narrowly directed towards specific viral proteins [33,71-73]. The responses may be localized at the T cell zone within the lymphoid tissue [74], and are most effective in controlling viral replication as they have the greatest antiviral activity [72]. The responses detected in lymph nodes precede those detected in peripheral blood and are of higher magnitude [74]. Although most of these detectable responses persist even in the chronic phase of infection [75], they are largely

ineffective at further reducing the viral load [76]. Thus, there is a need to better understand the causes of ineffectiveness of the persistent responses at the chronic phase of HIV-1 infection.

1.6   Activation of CD8+ T Cells in Lymph Nodes

Lymph nodes (LN) represent immunological sites where lymphocytes are primed with antigens [77]. Activation of CD8+ T cells is initiated within a specialized region of the LN, often referred to as the paracortex [78]. Upon priming with antigen, naïve CD8+ T cells undergo activation, proliferation, clonal expansion and differentiation into effector CD8+ T cells [79]. The effect of activated CD8+ T cells is seen in the vigorous destruction of infected cells presenting cognate peptides. Most of these activated CD8+ T cells die by apoptosis after eliciting their effector function. A few of the effector CD8+ T cells mature into memory CD8+ T cells, which can respond faster and more effectively upon re-encountering their cognate antigen [80].

The majority of HIV-1 replication takes place in the lymphoid tissues, and it is not clear if HIV-1-specific CD8+ T cell responses found in the blood are representative of responses found in the lymphoid tissues [40]. As such, we need to broaden our understanding of CD8+ T cell function and trafficking within lymphoid tissues to pinpoint mechanism of control. Data from lymph nodes are controversial. While Altfeld *et al*. 2002 reported a greater magnitude of HIV-1-specific CD8+ T cells in the lymph nodes than in peripheral blood, Connick *et al*. 2007 demonstrated that CD8+ T cells have limited access to lymphoid follicles, the primary site of HIV-1 replication within lymphoid tissues. Furthermore, Andersson *et al*. 2009 reported perforin expressing CD8+ T cells within the follicles, whereas subsequent studies have found no perforin

expression by lymph node-resident CD8^{+} T cells [81], particularly by those that do gain access to the follicle [82]. It will be important to determine the true contribution of antiviral CD8^{+} T cell responses at lymph node sites given their role in HIV-1 replication and dissemination. This is of particular importance given publications reporting lymph node CD4^{+} T follicular helper cells as a new major reservoir of HIV-1 infection [83,84].

1.7   CD8^{+} T Cell Differentiation

During infection, many factors coordinate the induction, expansion and differentiation of CD8^{+} T cells either to effector or memory phenotypes, which help mediate pathogen clearance and provide long-term immunity [85]. In the well characterized murine model systems of infection, such as lymphocytic choriomeningitis virus (LCMV), a small subset of effector CD8^{+} T cells that is enriched for memory precursor cells has been distinguished based on the increased expression of IL-7, CD27 and BCL-2, and decreased expression of KLRG1 [86,87]. After acute infection, CD8^{+} T cells are maintained in an antigen-independent, cytokine-dependent manner mainly through the action of IL-7 and IL-15, which promote memory CD8^{+} T cell survival and proliferation [88]. Several potential mechanisms have been proposed to explain how a heterogenous pool of effector and memory CD8^{+} T cells arise during viral infections Reviewed in [85]. Nevertheless, the question about how antigen-experienced CD8^{+} T cells maintain a balance to enable the formation of cells with different phenotypes, functions and short- or long-term fates remain unanswered.

1.7.1 Transcriptional Regulation of CD8^{+} T Cell Differentiation

Several transcriptional factors that regulate the differentiation of CD8^{+} T cells to effector or memory phenotype have been identified. Interestingly, a number of them function in pairs that form counter-regulatory axes to simultaneously produce different types of antigen experienced CD8^{+} T cells that can provide both short- and long term protection [85]. T-bet and eomesodermin (EOMES) play crucial roles in the generation of effector and memory CD8^{+} T cells with unique phenotype and function. In activated CD8^{+} T cells, T-bet and EOMES cooperate to create cytotoxic CD8^{+} T cells with the expression of CXCR3 and CXCR4, inflammatory chemokine receptors that guide effector CD8^{+} T cells towards inflamed tissues [89-93]. Although T-bet and EOMES cooperate in many regards, their expression is somewhat reciprocal. For example, T-bet expression is highest in early effector CD8^{+} T cells, but progressively declines as memory cells form [85,94]. Conversely, EOMES is upregulated in early effector CD8^{+} T cells by IL-2, but in keeping with its role in memory T cell homeostasis its expression increases further during the effector to memory cell transition [91,94,95]. Thus, transcriptional regulation may be crucial in the determination of phenotype and function of antigen specific CD8^{+} T cells.

1.7.2 Epigenetic Regulation of CD8^{+} T Cell Differentiation

Epigenetic changes occurring during CD8^{+} T cell differentiation provide a means for the initiation of transcriptional changes that drive the differentiation and maintenance of either effector or memory CD8^{+} T cells [96]. Epigenetic changes such as DNA methylation and histone post-translational modification represent two major epigenetic mechanisms that guide differentiation of CD8^{+} T cells. DNA methylation is associated

with transcriptional repression, although it is also associated with transcriptional activation when found within gene bodies [97,98]. This concept holds during CD8^{+} T cell differentiation, where genome-wide DNA methylation profiles indicate that methylation marks are lost at the promoters of genes whose expression increases during differentiation and are gained at the promoters of genes whose expression decreases [99-101].

Within the nucleus, DNA is organized into structural units termed nucleosomes that consist of eight histone subunits (two copies each of H2A, H2B, H3 and H4) that are subject to covalent post-translational modification [96]. Histone modification profiles in CD8^{+} T cell subsets indicate that, as with DNA methylation, promoters and gene bodies undergo progressive changes in the distribution and accumulation of histone modifications during differentiation that correlate with gene expression patterns [100,102,103]. The initiation of epigenetic changes in CD8^{+} T cells following antigenic stimulation is illustrative of one of the functions of epigenetics, which is to facilitate transcriptional changes in response to external stimulus [101].

1.7.3 Epigenetic Regulation of CD8^{+} T Cell during HIV-1 infection

In order to develop strategies to boost CD8^{+} T cell function, we need a better understanding of the epigenetic changes in immune cells during HIV-1 infection. CD8^{+} T cells have been shown to be epigenetically modified during HIV-1 infection (Figure 1.7), [104,105]. For example, the expression of the inhibitory PD-1 molecules is regulated by methylation of the PD-1 promoter. CD8^{+} T cells from HIV-1 infected subjects with fully suppressed plasma viremia by ART have an unmethylated PD-1 promoter [104]. Another study also reported that inability of the exhausted CD8^{+} T cells to produce

IFN-ϒ and IL-2 positively correlates with low levels of di-acetyl-Histone-3 (diAcH3) in the regulatory regions of the *Ifng* and *Il2* genes [106]. These data imply that CD8$^+$ T cells function is epigenetically controlled during HIV-1 infection. Further understanding of the epigenetic mechanisms regulating CD8$^+$ T cell differentiation and dysfunctionality during HIV-1 infection have implications for CD8$^+$ T cell biology.
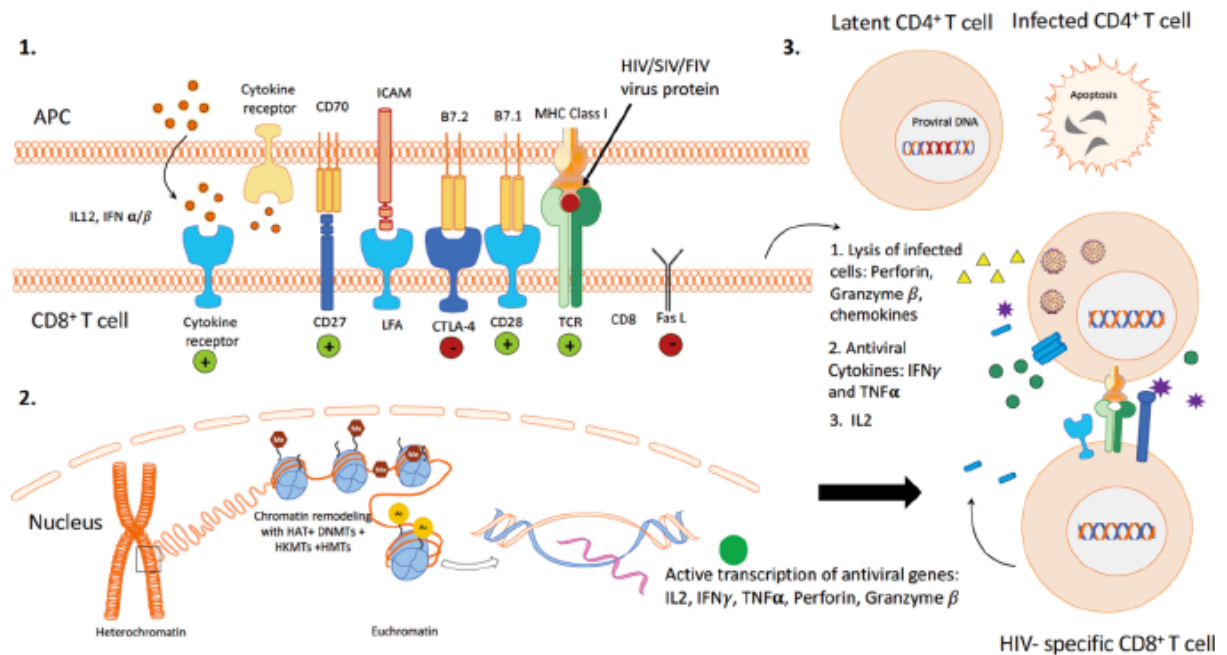
[107]

Figure 1.7: Epigenetic regulation of CD8$^+$ T cell responses to HIV-1.

(1) The antigen presenting cell (APC) presents the viral antigens on the surface via major histocompatibility complex (MHC) Class I molecules for recognition by the T-cell receptor (TCR) on CD8$^+$ T cells. As the CD8$^+$ T cell becomes activated, they also begin upregulating cytotoxic T lymphocyte-associated molecule (CTLA)-4. CTLA-4 binding with CD86 (B7.2) on APCs delivers an inhibitory signal to maintain immune homeostasis. (2) Upon CD8$^+$ T cell activation, the chromatin within the nucleus "relaxes" into euchromatin conformation to allow the binding of various factors of the

transcriptional machinery. Chromatin remodelling enzymes such as histone acetyltransferases (HAT), histone methyltransferases (HMTs), DNA methyltransferases (DNMTs) and histone lysine methyltransferases (HKMTs) alter the accessibility of chromatin at specific sites based on the signals provided to direct the specific response. During HIV-1 infection, "relaxed" chromatin in gene promoter regions allows for the active transcription of antiviral genes such interleukin IL-2 and IFN-Υ, TNF-α, perforin and granzyme B . (3) Illustrates the interaction of activated HIV-specific CD8$^+$ T cell with productively HIV-infected CD4$^+$ T cell. Upon recognition, the infected CD4$^+$ T cell undergo lysis and apoptosis due to the action of perforin, granzyme B [107].

1.8   Trafficking of Effector CD8$^+$ T Cells

When naïve CD8$^+$ T cells are primed and become effector CD8$^+$ T cells, they display a dramatic shift in the expression of genes, surface proteins and inflammatory-specific receptors [108]. Effector CD8$^+$ T cells lose expression of CD62L and CCR7, thereby losing their ability to access lymph nodes through the high endothelial venues [109]. Instead, effector CD8$^+$ T cells gain expression of a cohort of homing molecules that enables them to traffic to infected tissues. The recruitment of CD8$^+$ T cells to the site of infection requires changes in the expression of adhesion molecules on the vascular endothelium [110]. Effector CD8$^+$ T cells upregulate chemokine receptor CXCR3 that binds inflammatory chemokines CXCL9 and CXCL10 secreted by infected tissues. The binding of CXCR3 receptor to these chemokines causes activation of lymphocyte function-associated antigen 1 (LFA-1) and newly expressed integrins, which enable rolling of effector CD8$^+$ T cells on endothelium [108]. Further expression of chemokines

by infected tissue facilitates extravasation of effector CD8$^+$ T cells into the tissues to exert their antiviral effect. Thus, chemokines and chemokines receptors are crucial for trafficking of CD8$^+$ T cells to the site of infection.

1.9   Thesis Outline

HIV-1 is essentially an infection of the immune system. It infects and depletes CD4$^+$ T cells that normally coordinate the adaptive T and B cell responses that defend against both intracellular and extracellular pathogens, respectively. Studies have demonstrated the role of CD8$^+$ T cells in HIV-1 control Reviewed in [62]. It has also become clear that among the strongest association with disease outcome, is the expression of certain class I HLA alleles [111], thus, implicating class I HLA restricted CD8$^+$ T cells responses as a major modulator of disease progression. Studies on viral fitness, particularly those in epitopes restricted by protective alleles such as HLA-B*81:01 in HIV-1 subtype C [55,112] and HLA-B*27:01 in HIV-1 subtype B [113] infections, further suggest a persisting antiviral effect. Although, the relationship between the immune function of CD8$^+$ T cells and viral control have been demonstrated, the precise role of CD8$^+$ T cells in HIV-1 control, and the precise phenotype and function that should be harnessed in HIV-1 vaccine or curative strategies remain unclear. The first part of this thesis focuses on understanding the mechanisms of HIV-1 control by HIV-1 specific CD8$^+$ T cells in peripheral blood.

Effective antiviral CD8$^+$ T cells responses depend on the ability of CD8$^+$ T cells to traffic into tissue sites of active viral replication [114,115]. Chemokines and their receptors

direct the movement of CD8^{+} T cells between the circulatory system and specific tissues throughout the body [116]. The established model of CD8^{+} T cell trafficking is that naïve CD8^{+} T cells home to lymphoid tissues guided by chemokines CCL19 and CCL21 and their receptor, CCR7. In contrast, effector CD8^{+} T cells exit lymphoid tissues and traffic to peripheral sites of infection guided by inflammatory chemokines and chemokine receptors, such as CXCR3 [117]. In HIV-1 infection, B cell follicles within the lymphoid tissues are major sites of viral replication [118-120]. Persistence of HIV in B cells follicle is largely due to exclusion of CD8^{+} T cell from this microanatomical tissue site [121]. Several studies have focussed on developing novel strategies for attracting CD8^{+} T cells to B cells follicles. For effector CD8^{+} T cells to achieve this, they must express CXCR5, a chemokine receptor that is normally present on B cells, CD4^{+} T follicular helper (Tfh) cells and other follicular homing cells. Recent studies have described some CD8^{+} T cells that express CXCR5 but the molecular mechanism regulating the expression of CXCR5 on human CD8^{+} T cells, is largely unknown. The second part of this thesis describes the transcriptional and epigenetic regulation of CXCR5 in human CD8^{+} T cells isolated from the lymphoid tissue of HIV-1 infected individuals. By elucidating molecular mechanisms that regulate CXCR5, these studies might lead to the development of novel strategies for increasing trafficking into the B cells follicles where they are needed to control HIV-1 infection.

The aims of the present study are as follows:

Aim 1: To investigate the mechanisms associated with CD8^{+} T cell mediated control of HIV-1 subtype C infection by characterizing peripheral blood (PB) HIV-1 specific CD8^{+} T cell responses in individuals expressing protective and less protective alleles.

Aim 2: To define the molecular regulation of CXCR5 expression in human CD8$^+$ T cells isolated from the lymphoid tissues of HIV-1 infected individuals.

Chapter 1 is the introduction of the thesis. It includes a review of relevant topics related to the defined aims of the study.

In chapter 2, we conducted a detailed characterization of PB CD8$^+$ T cell responses to the HIV-1 Gag epitope TL9 (TPQDLNTML$_{180-188}$), which is immunodominant in the context of both HLA B*81:01 and B*42:01 alleles.

In chapter 3, we extended our study to lymphoid tissues and described the molecular regulation of CXCR5 expression in human CD8$^+$ T cells.

Chapter 4 is a general discussion and overall implications of our findings and future directions of our studies.

CHAPTER 2

Aim: To investigate the mechanisms associated with CD8^{+} T cell mediated control of HIV-1 subtype C infection by characterizing peripheral blood (PB) CD8^{+} T cell responses in individuals expressing protective and non-protective alleles.

Chapter 2 Overview

Host genetic variation and the considerable genetic diversity of HIV-1 are the major obstacles to designing an effective HIV-1 vaccine. Although several studies have demonstrated the crucial role of CD8^{+} T cells in immune mediated control of HIV-1 infection, developing a broadly cross-reactive T cell-based vaccine remains an elusive goal. In chapter 2, we present a study conducted to determine the mechanism by which protective HLA-B*81:01 mediates natural control of HIV-1 subtype C while closely related HLA-B*42:01 does not. We identified an unexpected population of T cells that responded to TL9 when presented by B*81:01 and B*42:01, even in monoallelic individuals. The dual-HLA reactive response was more common in B*81:01-expressing individuals and it was associated with lower plasma viral loads, indicating that it contributes to the control of infection. In-depth analysis of TL9-specific T cell receptors (TCR) uncovered genetic and functional similarities between B*81:01-derived T cell responses and dual-HLA reactive responses from B*42:01 individuals. In addition, mono-reactive responses from B*42:01 individuals were genetically and functionally distinct. Notably, TCR clones isolated from dual-reactive cells from B*42:01 individuals displayed a broader ability to recognize TL9 polymorphisms that

contribute to immune evasion, providing a mechanism to explain their association with lower viremia. These results have been published in Nature Communications, 2018 Nov 27; 9(1):5023. doi:10.1038/s41467-018-07209-7. PMID: 30479346.

CHAPTER 2: Dual HLA B*42 and B*81-reactive T cell receptors recognize more diverse HIV-1 Gag escape variants

Funsho Ogunshola[1,5,#], Gursev Anmole[2,#], Rachel L. Miller[3], Emily Goering[4], Thandeka Nkosi[1,5,], Daniel Muema[1], Jaclyn Mann[5], Nasreen Ismail[5], Denis Chopera[1], Thumbi Ndung'u[1,4,5,7], Mark A. Brockman[2,3,6,*], Zaza Ndhlovu[1,4,5,*]

[1]Africa Health Research Institute, University of KwaZulu-Natal, Durban, South Africa

[2]Department of Molecular Biology and Biochemistry, Simon Fraser University, Burnaby, BC V5A 1S6, Canada

[3]Faculty of Health Sciences, Simon Fraser University, Burnaby BC V5A 1S6, Canada

[4]Ragon Institute of MGH, MIT, and Harvard, Cambridge MA 02139, USA

[5]HIV Pathogenesis Programme, Doris Duke Medical Research Institute, University of KwaZulu-Natal, Durban, South Africa

[6]British Columbia Centre for Excellence in HIV/AIDS, Vancouver, BC V6Z 1Y6, Canada

[7]Max Planck Institute for Infection Biology, Berlin, Germany

*Corresponding author

2.1　Abstract

Some closely related human leukocyte antigen (HLA) alleles are associated with variable clinical outcomes following HIV-1 infection despite presenting the same viral epitopes. Mechanisms underlying these differences remain unclear but may be due to intrinsic characteristics of the HLA alleles or responding T cell repertoires. Here we examine CD8$^+$ T cell responses against the immunodominant HIV-1 Gag epitope TL9 (TPQDLNTML$_{180-188}$) in the context of the protective allele B*81:01 and the less protective allele B*42:01. We observe a population of dual-reactive T cells that recognize TL9 presented by both B*81:01 and B*42:01 in individuals lacking one allele. The presence of dual-reactive T cells is associated with lower plasma viremia, suggesting a clinical benefit. In B*42:01 expressing individuals, the dual-reactive phenotype defines public T cell receptor (TCR) clones that recognize a wider range of TL9 escape variants, consistent with enhanced control of viral infection through containment of HIV-1 sequence adaptation.

2.2 Introduction

The rate of clinical progression following human immunodeficiency virus type 1 (HIV-1) infection is variable, with rare individuals maintaining plasma viral loads below 50 RNA copies mL^{-1} in the absence of therapy [122,123]. Host and viral mechanisms associated with relative control of infection indicate that the ability of HIV-1 to adapt to a new host is a critical determinant of pathogenesis [124,125]. Multiple lines of evidence support the central role of CD8$^+$ T cells in this process [13,14,62]. Expression of certain class I human leukocyte antigen (HLA) alleles, particularly at the HLA-B locus [111,126], is associated with lower plasma viral loads, higher CD4$^+$ T cell counts and delayed onset of AIDS [127,128]. Interaction between CD8$^+$ T cells and viral peptide epitopes presented on HLA determines breadth and other characteristics of the antiviral response [129,130], while rapid development of viral mutations in targeted epitopes facilitates evasion from host immunity [124,131,132]. CD8$^+$ T cells that target epitopes derived from p24 Gag are associated with better control [64,133], likely due to their relative immunodominance and greater fitness constraints on this major viral structural protein [112,132,134,135].

Recognition of a peptide/HLA (pHLA) ligand by a CD8$^+$ T cell is determined by the sequence and functional characteristics of its T cell receptor (TCR) [47,48]. The exceptional diversity of the TCR repertoire, generated by somatic recombination of variable (V), diversity (D), and joining (J) gene segments, junctional modifications, and differential pairing of α and β chains, has profound implications for immune coverage [136]. In addition to defining antigen specificity, TCR affinity for pHLA can dictate the strength of intracellular signaling events that modulate T cell effector functions, including cytotoxicity and proliferative capacity [137]. Characteristics of TCR clonotypes

that contribute most effectively to CD8^{+} T cell-mediated control of HIV-1 infection are largely unknown, since data linking individual TCR sequences with measures of antiviral function remains limited. In previous studies of p24 Gag epitopes TW10 (TSTLQEQIGW$_{240-249}$) and KK10 (KRWIILGLNK$_{263-272}$), presented on protective HLA alleles B*57:01 and B*27:05, respectively, CD8^{+} T cell clones displaying higher functional avidity or greater ability to cross-recognize epitope variants were shown to have enhanced antiviral activity [52,138-140]. In the case of B*27-KK10, public TCR clonotypes, defined as having identical (or nearly identical) TCR β sequences in the antigen-specific repertoire of at least two unrelated individuals [48,141], displaying high avidity against the consensus epitope were also associated with a more effective T cell response [140,142].

Following infection with HIV-1 subtype C strains that are prevalent in sub-Saharan Africa, expression of HLA allele B*81:01 is associated with improved clinical outcomes [111,143], while the genetically-related allele B*42:01 is less protective [133,143-148]. Both alleles belong to the HLA B7 supertype [60,149] and present similar viral peptides, including the immunodominant p24 Gag epitope TL9 (TPQDLNTML$_{180-188}$) [146,150-153]. The magnitude of the TL9 response has been associated with lower plasma viremia and improved clinical outcome in the case of B*81:01 [154]. TL9 is located on helix 3 of the p24 protein, which is critical to form the mature viral capsid. Circulating subtype C strains display >99% sequence identity at all TL9 residues except positions 3 (88.5%) and 7 (93.5%) (HIV Databases; www.hiv.lanl.gov). Positions 3 and 7 are the principal sites for viral escape from CD8^{+} T cell pressure [124,151,152,155]; however, mutations at these residues also impair fitness [55], indicating that HIV-1 adaptation at TL9 must balance these counteracting pressures. Structural studies indicate that the TL9 residues exposed to T cells differ in its bound conformations with B*81:01 and B*42:01

[156], and some evidence suggests that enhanced antiviral T cell function is related to distinct TCR sequences elicited in the context of B*81:01 [151]. These observations are consistent with delayed viral escape in B*81:01 expressing individuals compared to B*42:01 expressing individuals [155] and selection of TL9 escape mutations by B*81:01 that tend to be more difficult to compensate for [55]. An improved understanding of clonotypic differences among CD8^{+} T cells responding to TL9 could highlight features that contribute to HIV-1 control in the context of B*81:01 and B*42:01.

Here we investigate the mechanisms associated with immune-mediated control of HIV-1 subtype C infection by examining the CD8^{+} T cell response to the immunodominant p24 Gag epitope TL9 in virus-infected individuals expressing HLA B*81:01 or B*42:01 alleles. We identify a subset of T cells that recognize TL9 epitope presented on both B*81:01 and B*42:01 alleles, despite individuals lacking one allele. The presence of a dual-reactive T cell population is associated with lower plasma viral loads after controlling for differences in HLA expression. Notably, the dual-reactive population in B*42:01 expressing individuals is dominated by several public TCR clonotypes that encoded *TRBV12-3*. In contrast, while mono- and dual-reactive populations in B*81:01 expressing individuals are enriched for *TRBV12-3* usage, no public clonotypes are observed. Comprehensive *in vitro* functional analyses of selected TCR clones demonstrated that B*81:01-derived clones and public dual-reactive B*42:01-derived clones display greater ability to cross-recognize HIV-1 Gag TL9 escape pathways compare to mono-reactive TCR clones isolated from B*42:01 expressing individuals. These results illustrate a use of HLA-tetramers and *in vitro* functional assays to identify and characterize TCR clonotypes that display enhanced ability to recognize a rapidly evolving HIV-1 infection.

2.3   Materials and Methods

2.3.1   Study subjects

Twenty-one antiretroviral naïve individuals were enrolled in Durban, South Africa through the HIV Pathogenesis Programme (HPP) acute infection cohorts. The clinical characteristics are shown in Table 1. All individuals were infected with HIV-1 subtype C. The Biomedical Research Ethics Committee of the University of KwaZulu-Natal and the Massachusetts General Hospital Ethics committee approved this study. All subjects provided written informed consent.

2.3.2   HLA typing

HLA typing was conducted by the laboratory of Dr. Mary Carrington (National Cancer Institute, Fredrick, USA), as previously described [111]. DNA samples obtained from peripheral blood mononuclear cells (PBMC) were first oligo-typed using Dynal RELITM reverse Sequence Specific Oligonucleotide (SSO) kits for the HLA-A, HLA-B and HLA-C loci (Dynal Biotech). Genotypes were refined to the allelic level using the Dynal Biotech Sequence Specific priming (SSP) kits in conjunction with the previous SSO type. In cases where alleles were still not well-defined at the allelic level, sequence-specific primers were used [157]. All class I HLA alleles in the IMGT allele release 24.0 were considered in the typing.

2.3.3 Tetramer staining, cell sorting and cell line generation

To identify and characterize TL9-specific CD8^{+} T cell populations, PBMC were first stained with a cell-viability dye (Fixable Blue Dead Cell Stain Kit, Invitrogen) for 10 minutes at room temperature. Cells were washed with 2% fetal calf serum (FCS) in phosphate buffered saline (PBS) and then stained with B*42:01-APC and/or B*81:01-PE TL9 HLA class I tetramers (obtained from the laboratory of Dr. Soren Buus), for 30 mins at room temperature. Subsequently, cells were washed, and surface stained with anti-CD8-BV786, CD3-BV711 and CD4-BV650 for 20 minutes at room temperature. Stained cells were analyzed by flow cytometry and/or tetramer-specific CD8^{+} T-cells were sorted for TCR sequencing. To generate TL9-specific CD8^{+} T-cell lines, cells were pulsed with 5 µl (200 µg ml^{-1}) of TL9 peptide at 37 ºC for 3 hours and subsequently cultured in RPMI medium containing 10% heat-inactivated fetal calf serum (R10 medium) supplemented with 50 units ml^{-1} of recombinant human interleukin 2 (IL-2) (R10/50 medium) for 2 weeks. Expanded TL9-specific CD8^{+} T cells were validated for specificity by tetramer staining and isolated using a cell sorter (BD FACSAria, Germany).

2.3.4 Tetramer intracellular cytokine staining and ELISPOT assay

To assess the functional quality of TL9-specific CD8^{+} T cells, PBMC from B*81:01 and B*42:01 subjects were stimulated with 1.2 µl (200 µg ml^{-1}) of TL9 peptide for 6 hours. After stimulation, cells were stained with an equal mixture of B*81:01 and B*42:01 TL9 tetramers for 30 minutes at room temperature, washed in PBS containing 2% FCS and then stained with viability dye, anti-CD8-BV786, CD3-BV711, and CD4-BV650 for 20 minutes at room temperature. Cells were fixed, permeabilized, stained

intracellularly with anti-IFN-γ-PE-Cy7 and analyzed on the BD LSRFortessa. HIV-1 immune responses were enumerated by IFN-γ enzyme-linked immunosorbent spot (ELISPOT) assay as previously described [111,158]. Briefly, PBMCs were stimulated with optimal HIV-1 subtype C peptide corresponding to each patient's HLA-A, B and C alleles at a final concentration of 2 μg ml^{-1} peptide.

2.3.5 TCR Vβ antibody staining

TCR Variable β (Vβ) expression on mono- and dual-tetramer$^+$ cells was assessed by flow cytometry as described previously [159]. PBMC were stained with B*81:01 and/or B*42:01 TL9 tetramers conjugated to different fluorochromes, followed by TCR Vβ family labeling using IOTest Beta Mark TCR Vβ repertoire Kit (Beckman Coulter, Pasadena, United States) for 30 minutes at room temperature. Subsequently, cells were stained with viability dye, anti-CD8-BV786, CD3-BV711, and CD4-BV650. The percentage of each Vβ family was determined for a minimum of 100,000 CD8$^+$ T cells using FlowJo software (Treestar, Ashland, United States). TCR Vβ staining was also performed on expanded mono- and dual- TL9 tetramer$^+$ cell lines.

2.3.6 TCR sequencing

Amplification of TCR β CDR3 coding regions from single T cells was performed as described previously by Han et al [160] with modifications to obtain ~230 bp amplicons for Sanger sequencing (ABI 3130xl). Primers are included in Supplementary Tables 2 and 3. The one-step SuperScript III kit (ThermoFisher) was used for RT-PCR and

Expand High Fidelity PCR system (Roche) was used for subsequent rounds. TCR α amplicons were TOPO cloned and screened to ensure productive CDR3 rearrangement. Sequences were examined using the ImMunoGeneTics (IMGT)/V-quest tool (www.imgt.org) to characterize Variable gene usage and CDR3 diversity. Full-length TCR alleles were reconstructed using Variable and Constant gene sequences obtained from the IMGT database, codon-optimized using the CodonOpt tool (Integrated DNA Technologies; www.idtdna.com) and synthesized as double-stranded DNA gBlocks by IDT. Full-length genes were cloned into pSELECT_GFPzeo (Invivogen) for functional studies.

2.3.7 TCR reporter assay

TCR antigen recognition was examined using a previously described *in vitro* reporter T cell assay [161]. Briefly, Jurkat T cells were co-transfected with TCR α, TCR β, CD8 α and NFAT-driven luciferase reporter plasmids by electroporation (BioRad MxCell). Target cells consisted of a CEM-derived GXR cell line [162] stably expressing either HLA-B*42:01 or B*81:01. TCR-transfected Jurkat effector cells (50,000 cells) were co-cultured with 50,000 target cells either pulsed with 20 µM TL9 peptide (purchased from GenScript at >90% purity) or infected with HIV-1 in a total volume of 100 µL, and TCR recognition activity was quantified by luminescence after 6 hours (Tecan M200). Viral stocks were generated by co-transfection of HEK293T cells with pBR4.3ΔNefΔEnv and pVSV-g using Lipofectamine 2000 (ThermoFisher Scientific). Infected GXR target cells were isolated by FACS based on GFP expression prior to co-culture with Jurkat T cells. To screen antigen cross-recognition, a peptide panel consisting of all single amino acid TL9 variants (180 total peptides) was purchased from GenScript. This

panel was prepared using microscale synthesis methods and individual peptides were aliquoted to 96-well plates at 0.5 to 2.0 mg total weight and >75% purity. Target cells were pulsed with ~20 μM peptide; however, due to variations in peptide sequence, total weight, Molar weights and purity, actual concentrations were anticipated to range between 8.4 and 20 μM.

2.3.8 HIV sequence analysis

To determine the frequency of naturally occurring Gag TL9 variants in HIV-1 subtype C infection, all subtype C TL9 amino acid sequences (N=5,481) were downloaded from the Los Alamos National Laboratory (LANL) HIV sequence database (www.hiv.lanl.gov) and analyzed. Sequences encoding consensus TL9 (N=4,526), multiple substitutions or mixed residues (combined N=217) and those appearing fewer than five times (N=53) were removed to generate a list of the most probable single amino acid TL9 variants (N=685). The proportion of each variant within this population was calculated to determine the likelihood of viral escape. Critical transition mutations (i.e. those that must to occur for consensus TL9 to evolve into escape variants) were identified using the standard amino acid codon table for eukaryotes. Sequence conservation frequencies for TL9 residues were estimated using the QuickAlign tool on the LANL web site (based on N=1,865 protein sequences).

2.3.9 Statistical analysis

Statistical analyses were conducted using Prism software, version 6.0 (GraphPad, Inc.). Two-tailed tests were employed, and p-values less than 0.05 were considered

to be significant. Comparisons between groups of continuous variables were assessed using parametric (unpaired Student's T) or non-parametric (Mann-Whitney U) tests. Differences in categorical variables between groups were assessed using Fisher's exact test. A multivariable linear regression analyses was conducted using Stata, version 14 (Stata Corp), to assess the independent predictive ability of HLA and dual reactivity on plasma viral loads. Hierarchical clustering analysis was performed using pvclust software [163] (http://stat.sys.i.kyoto-u.ac.jp/prog/pvclust), implemented in R. Data was grouped according to correlation distances using single linkage methods. Approximately unbiased (au) p-values and bootstrap probability (bp) values were based on 5,000 iterations.

2.4 Results

2.4.1 Characterizing CD8^{+} T cell responses in study participants

Population-level studies have demonstrated that HLA-B*81:01 is associated with better control of HIV-1 subtype C infection than the closely related allele B*42:01 [111,124]; however, mechanisms to explain this remain unclear. To examine this, we recruited 21 treatment-naïve HIV-infected individuals expressing B*81:01 (n = 9), B*42:01 (n = 11), or both alleles (n = 1) from Durban, South Africa. Individuals co-expressing other protective class I HLA alleles (namely B*57:03, B*58:01 and B*39:01) were excluded from this study. The clinical characteristics and class I HLA genotypes of participants are shown in Table 2.1 and 2.2, respectively. Consistent with prior reports [151,164,165], we observed that untreated B*81:01 expressing individuals displayed lower plasma viral loads (median 3.38 $\log_{10}$ RNA copies ml^{-1} [IQR 2.36-3.99]) compared to untreated B*42:01 expressing individuals (4.15 $\log_{10}$ RNA copies ml^{-1} [IQR 3.40-4.84]) (p=0.03, Mann-Whitney U-test) (Fig. 2.1A). The difference in CD4 counts between groups was not statistically significant (median 625 cells µl^{-1} in B*81:01 vs. 555 cells µl^{-1} in B*42:01; p = 0.14, Mann-Whitney U-test). While the individual who co-expressed HLA-B*81:01 and B*42:01 alleles was not included in our analysis of clinical correlations, this participant displayed the lowest plasma viral load (2.11 $\log_{10}$ RNA copies ml^{-1}) and highest CD4 count (1,002 cells µl^{-1}).

Table 2.1: Demographic and clinical characteristics of the study participants.

HLA	B*81:01/B*42:01	B*81:01	B*42:01	(B*81:01 vs B*42:01) Pvalue
n	1	9	11	N/A
Female n (%)	1 (100%)	7 (77.8%)	10 (90.9%)	0.57[b]
Age (yr)	24	22.5 (22.25-28.5)[a]	22 (20.5-28.5)[a]	0.75[c]
CD4 counts, cells/mm^3	1002	625 (495-802)[a]	588 (479-673)[a]	0.14[c]
Viral load, log$_{10}$ RNA copies/ml	2.11	3.38 (2.36-3.99)[a]	4.15 (3.40-4.84)[a]	0.03[c]

[a] Values expressed as median (interquartile range)
[b] Statistical test used: Fisher's exact test
[c] Statistical test used: Mann Whitney test
Excluded alleles: HLA-B*57:03; B*58:01; B*39:01
N/A means not applicable

All values in parenthesis were expressed as inter-quartile range. Participants with other protective alleles present in the cohort of study were excluded in the study.

Immune targeting of dominant CD8$^+$ T cell epitopes contributes to long-term suppression of HIV-1 viremia [166-168]. The p24 Gag-derived epitope TL9 is immunodominant in both B*81:01 and B*42:01 expressing individuals [150,151], and the magnitude of the TL9 response has been associated with improved clinical outcome in the context of B*81:01 [154]. To characterize the TL9 response in our cohort, we quantified antigen specific CD8$^+$ T cells using B*81:01 and B*42:01 tetramers. We observed no difference in the frequency of tetramer$^+$ CD8$^+$ T cells between individuals expressing B*81:01 (median 2.08%) compared to B*42:01 (1.14%) (p=0.50; Student's T test) (Fig. 2.1B). Notably, intra-patient comparison of responses in either B*81:01 or B*42:01 participants showed that TL9 was the most dominant response compared to

other responses (p=<0.0001, Student's T test) by both tetramer staining and ELISPOT (Supplementary Fig. 2.1A-C and Supplementary Table 2.1). These data are consistent with previous studies [151,156]. The proportion of TL9-specific CD8+ T cells expressing IFN-γ following peptide stimulation was also not significantly different between individuals expressing B*81:01 (median 47%) and B*42:01 (27%) (p=0.09, Student's T test) (Fig. 2.1C); however, the observed trend in favor of B*81:01 participants is consistent with prior work describing moderately higher TL9-specific IFN-γ secretion and higher functional avidity in the context of B*81:01 [151].

2.4.2 Dual HLA reactivity is associated with lower viral load

To investigate if there were any qualitative differences in TL9-specific CD8$^+$ T cells restricted by these two HLA alleles, we first made a direct comparison between antigen-specific T cells in the individual who co-expressed B*81:01 and B*42:01. Intriguingly, when we double-stained cells from this individual with both HLA tetramers, we observed a dominant T cell subset that was labelled using the B*81:01-TL9 tetramer as well as a secondary subset that was labelled by both B*81:01-TL9 and B*42:01-TL9 tetramers, which we will refer to as the dual-reactive population (Fig. 2.1D).

Table 2.2: List of class I HLA type of the study participants

Participants	HLA-A	HLA-B	HLA-C
PT1	33:03/34:02	53:01/81:01	04:01/04:01
PT2	02:00/34:00	14:01/81:01	08:00/08:00
PT3	01:01/30:01	81:01/81:01	04:01/18:00
PT4	23:01/29:02	53:01/42:01	03:04/17:00
PT5	30:01/34:02	35:01/42:01	02:10/17:01
PT6	43:01/74:01	57:01/81:01	04:01/07:01
PT7	01:01/29:11	13:02/81:01	06:02/18:01
PT8	01:01/29:02	45:01/81:01	06:02/18:01
PT9	23:01/68:02	14:02/81:01	08:02/18:00
PT10	02:05/33:01	42:01/58:02	07:01/17:01
PT11	29:02/29:02	42:01/45:01	06:02/17:01
PT12	26:01/30:02	15:18/42:01	17:01/18:00
PT13	30:01/32:01	42:01/58:02	06:02/17:01
PT14	02:01/30:01	42:01/45:07	16:01/17:01
PT15	01:01/74:01	35:01/81:01	04:01/18:01
PT16	02:05/29:02	42:01/45:07	16:01/17:01
PT17	29:01/30:01	15:22/42:01	04:01/17:01
PT18	30:01/68:02	14:02/42:01	08:02/17:01
PT19	23:01/30:01	42:01/57:02	07:01/17:00
PT20	02:00/34:00	14:01/81:01	08:00/08:00
PT21	30:01/68:01	42:01/81:01	04:01/17:01

Detail class I HLA profiles of the study participants.

To explore whether the dual-reactive T cell population was unique to this individual, we re-examined all study participants using both class I HLA tetramers. We observed dual-reactive TL9 responses in the majority of participants, indicating that a subset of CD8$^+$ T cells elicited in the context of both B*81:01 and B*42:01 could cross-recognize

TL9 bound to the other class I HLA allele, even when it was not expressed by the host. Representative results for two individuals are also shown in Fig. 2.1D. The dual-reactive population was seen more frequently in individuals expressing B*81:01 (7 of 9; 78%) compared to B*42:01 (5 of 11; 46%) (Fig. 2.1E), but this difference was not statistically significant (p=0.19, Student's T test). While CD8^{+} T cell promiscuity is frequently observed towards peptide variants presented on the same HLA allele, we know of only one prior report that described CD8^{+} T cell cross-reactivity to the same peptide presented on two different class I HLA alleles [169]. In a multivariable linear regression model, we identified dual-reactivity, but not HLA, as a significant independent predictor of lower plasma viral load in our participants (p=0.02) (Fig. 2.1F), suggesting that this T cell phenotype is associated with a clinical benefit. We therefore hypothesized that features associated with dual-reactive CD8^{+} T cells could provide insight into mechanisms of HIV-1 control.
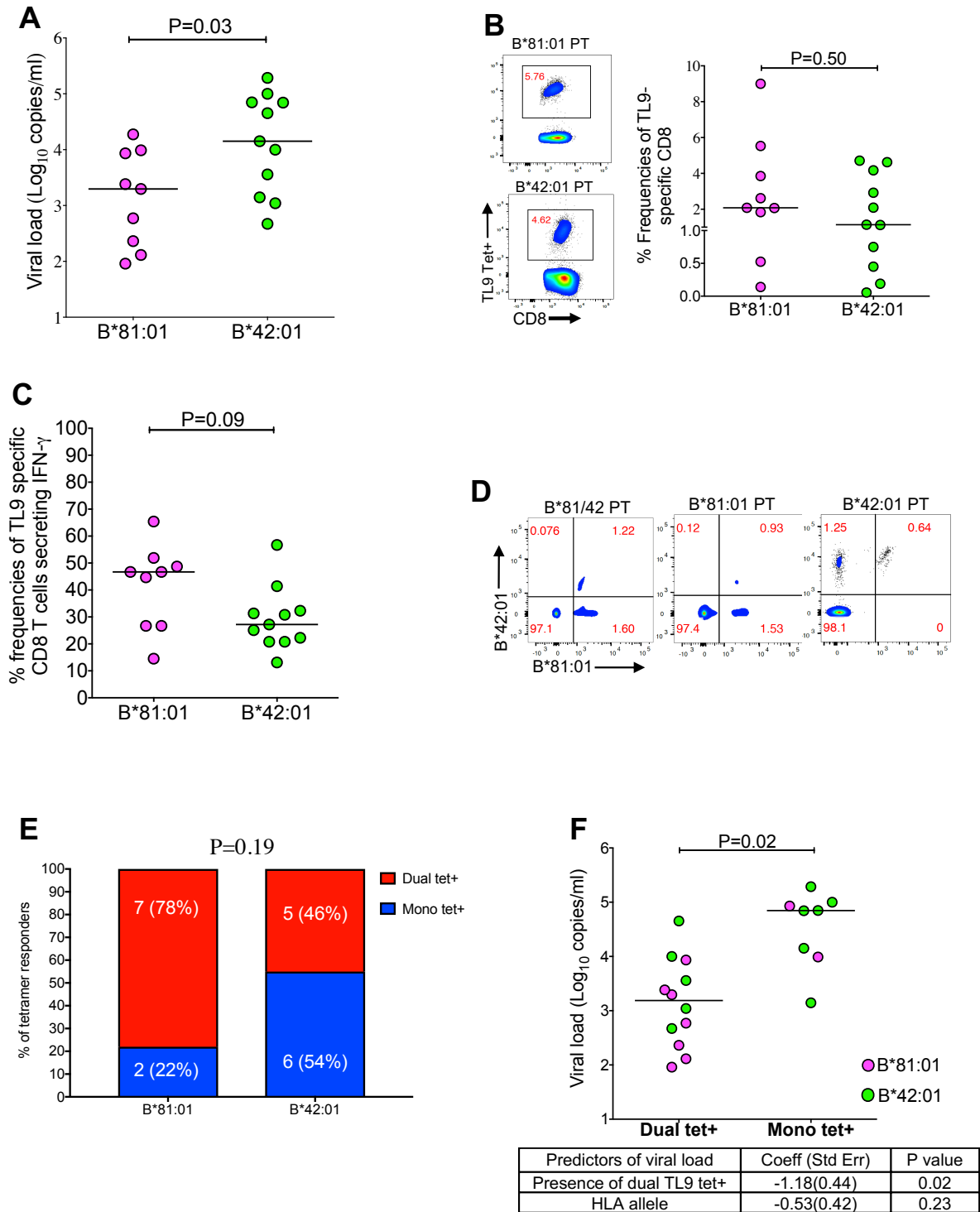
Figure 2.1: A dual TL9 tetramer+ response is associated with lower plasma viral load.

A comparative analysis indicated lower plasma viral loads (log10) among participants expressing B*81:01 compared to participants expressing B*42:01 (p=0.03, Mann-

Whitney U-test test) (A). Representative flow plots display TL9 tetramer responses observed in one B*81:01 expressing individual (top) and one B*42:01 expressing individual (bottom). A comparative analysis of TL9 tetramer+ frequencies observed no difference between participants expressing B*81:01 compared to those expressing B*42:01 (p=0.5; Mann-Whitney U-test) (B). A comparative analysis of IFN-γ secretion following stimulation with TL9 peptide indicated a trend towards higher activity among individuals expressing B*81:01 versus B*42:01 (p=0.09, Mann-Whitney U-test) (C). Representative flow plots display the dual TL9 tetramer-reactive T cell population in B*81/42:01 expressing participant, one B*81:01 expressing participant and one B*42:01 expressing participant (D). A higher proportion of B*81:01 expressing participants displayed dual tetramer reactivity (p=0.19, Chi-square test) (E). Multivariable linear regression analyses that included HLA allele and presence of dual tetramer-reactive T cells as independent variables indicated that dual-reactivity (p=0.02) but not HLA (p=0.23) was a significant determinant of plasma viral load (F).

2.4.3 Constrained Vβ genes in B*42-derived dual-reactive TCR

The ability of dual-reactive CD8$^+$ T cells to recognize TL9 bound to different, albeit related, class I HLA alleles suggested that they harbored distinct characteristics. Since individual TCR clonotypes have been associated with improved control of HIV-1 [52,139,140,170-173], we analyzed the TCR repertoire found in mono- and dual-reactive TL9-specific T cells. First, we investigated TCR β expression using flow cytometry by co-staining PBMC with B*81:01- and B*42:01-TL9 tetramers plus a cocktail of Vβ-specific antibodies. Representative results for one B*42:01 expressing individual are shown in Fig. 2.2A. Consistent with prior studies that described a high frequency of *TRBV12-3*

gene usage among TL9-specific T cells [151,152], we observed that both mono- and dual-reactive T cells from B*81:01 expressing individuals were highly enriched for Vβ 12-3/12-4 (Fig. 2.2B). In contrast, while mono-reactive T cells from B*42:01 individuals expressed multiple Vβ families, the dual-reactive T cells from these individuals were highly enriched for Vβ 12-3/12-4 (Fig. 2.2C). These results suggested that TCR clonotypes expressed by dual-reactive CD8$^+$ T cells elicited in the context of HLA B*42:01 shared distinct features with T cells that dominated TL9 responses elicited by the more protective B*81:01 allele. To confirm these observations, we sorted mono- and dual-reactive T cells using FACS and generated separate TL9-specific cell lines. Similar Vβ staining profiles were observed following *ex vivo* expansion (Supplementary Fig. 2.2), confirming that dual-reactive T cells were a *bona fide* population and not an artifact of tetramer staining.
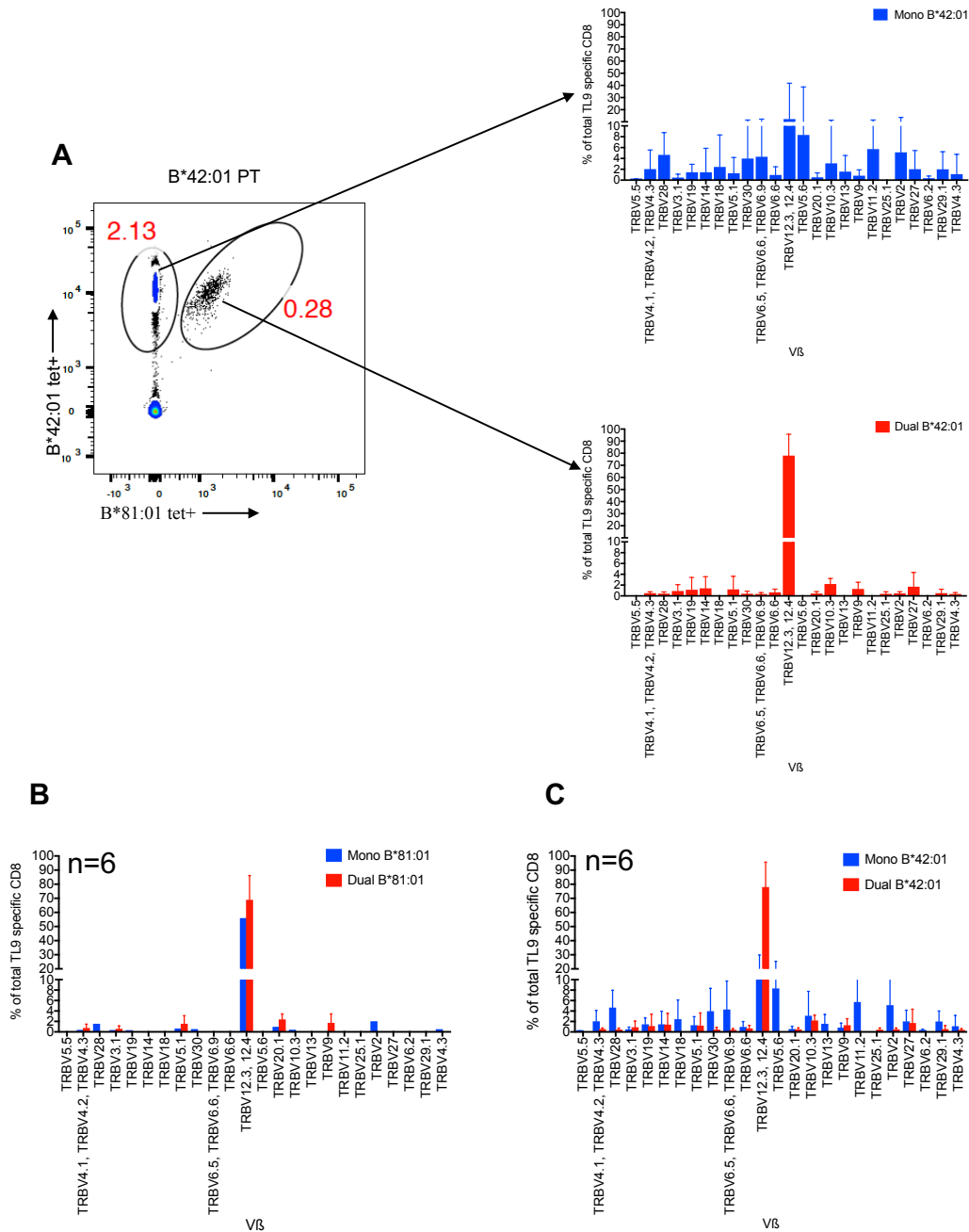
Figure 2.2: Enrichment of TCR Vβ 12-3/12-4 in dual-reactive T cells.

A representative flow plot for one B*42:01 expressing individual displays mono- and dual-TL9 tetramer reactive T cell populations and linked TCR Vβ expression profiles based on antibody staining (**A**). Aggregate results for TCR Vβ usage are shown for

mono- (blue) and dual-reactive (red) T cells from six B*81:01 expressing individuals (**B**) or six B*42:01 expressing individuals (**C**).

To gain additional molecular insight into the TCR clonotypes present within each TL9-specific T cell population, we sequenced the TCR β gene repertoire in single tetramer-labeled T cells isolated by FACS from three B*81:01 and three B*42:01 expressing individuals who displayed mono- and dual-reactive responses. Consistent with antibody staining results, Vβ gene usage for mono- and dual-reactive B*81:01-derived populations, as well as dual-reactive B*42:01-derived populations, was highly restricted to *TRBV12-3/12-4* (Fig. 2.3A, B). In contrast, while the mono-reactive population in one B*42:01 expressing individual (participant 11) was comprised largely of T cells encoding *TRBV12-3/12-4*, the primary Vβ gene present in the other two individuals (participants 13 and 17) was *TRBV7-9* (Fig. 2.3B). Notably, we observed that the dual-reactive population in all three B*42:01 expressing individuals was dominated by four public Vβ sequences (highlighted CDR3 regions in Fig. 2.3B) that were never observed in B*81:01-derived TCR sequences. Enrichment of *TRBV12-3/12-4* usage by TL9-specific TCR in the context of B*81:01 as well as the public dual-reactive TCR in B*42:01 expressing individuals suggested that features of these TCR clonotypes contribute to control of HIV-1 infection.
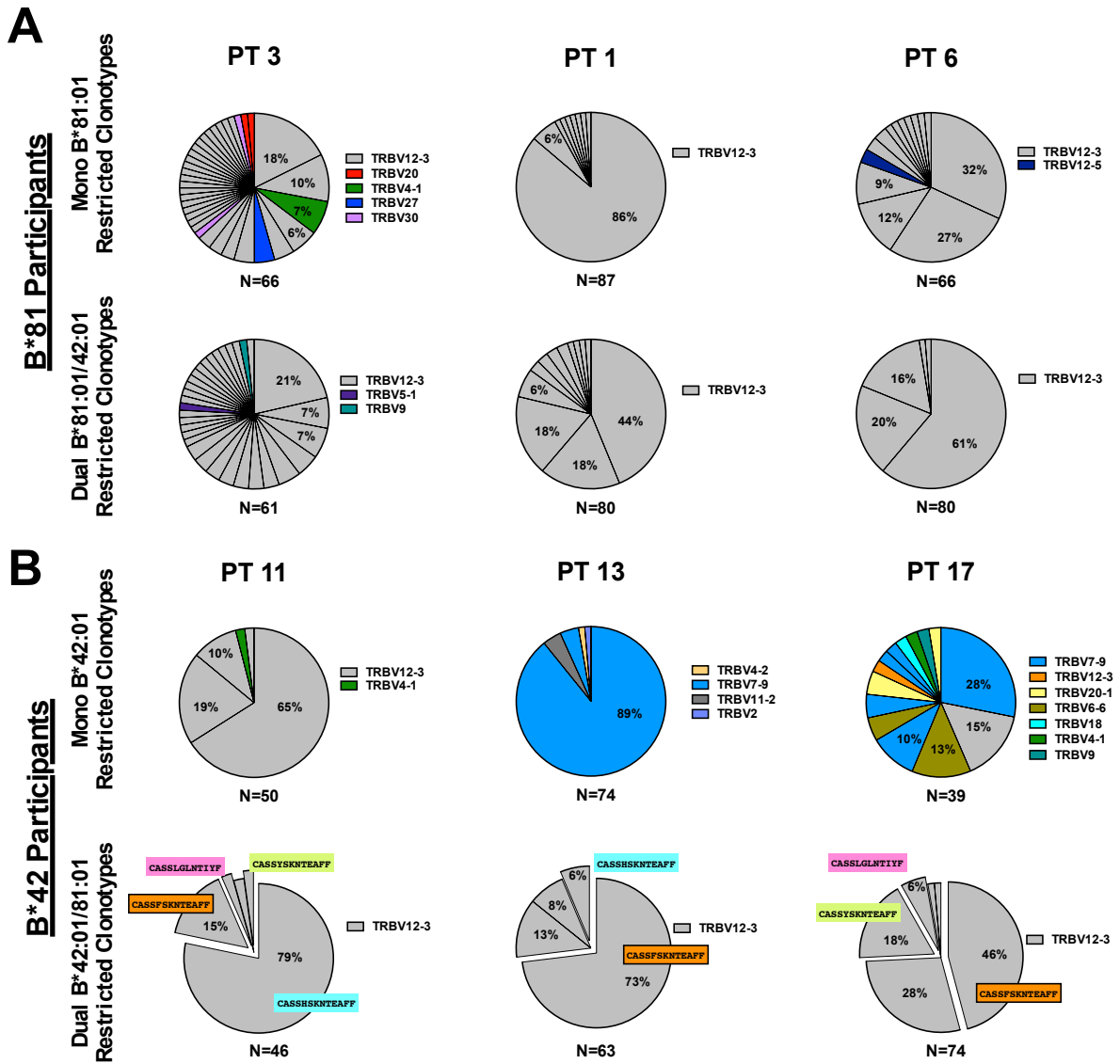
Figure 2.3: Molecular analysis of TCR β clonotypes in mono- and dual-reactive T cells. TCR β sequencing was performed on single FACS-sorted mono- and dual-TL9 tetramer reactive T cells from three B*81:01 expressing participants (A) and three B*42:01 expressing participants (B). TRBV and CDR3 sequences were determined using the IMGT V-quest tool (www.imgt.org). The total number of sequences collected per population is indicated under each pie chart. Unique TCR β clones are displayed as wedges in the pie chart. The size of the wedge indicates the frequency of each sequence within the population and the color represents TRBV usage. TCR β sequences in mono- and dual-reactive populations from B*81:01 expressing

individuals were highly enriched for TRBV12-3/12-4 usage (indicated in grey); however, no public sequences were observed among these individuals. Mono-reactive populations from B*42:01 expressing individuals encoded diverse TRBV and also lacked public sequences. In contrast, dual-reactive populations from B*42:01 expressing individuals were enriched for TRBV12-3/12-4 usage (grey), and these sequences were comprised predominately of four identical (public) TCR β clones (highlighted by colored boxes). Notably, these public clones were distinct from any TCR observed in B*81:01 individuals.

2.4.4 Isolation and validation of TL9-specific TCR clones

To provide a more complete understanding of mono- and dual-reactive CD8^{+} T cell phenotypes, we identified the paired TCR α gene from eight dominant TCR clones representing the mono- and dual-reactive populations from B*81:01 and B*42:01 expressing individuals (Fig. 2.4A) and directly assessed TCR function using a previously described *in vitro* reporter T cell assay [161]. Briefly, full-length TCR α/β genes were reconstructed and transiently expressed in Jurkat T cells. TCR-mediated NFAT signaling was quantified by luminescence following co-culture with HLA-expressing target cells presenting the TL9 epitope. Since methods used for TCR staining and sequencing could not distinguish between *TRBV12-3* and *TRBV12-4*, which differ by two amino acids in the CDR1, TCR β genes were synthesized encoding both alleles; however, only *TRBV12-3* constructs were functional (Supplementary Fig. 2.3). TCR clones displayed dose-dependent responses to consensus TL9 over a range of peptide concentrations (5 nM to 20 μM) (Supplementary Fig. 2.4), indicating that the reporter assay was sensitive and specific. Furthermore, reconstructed TCR

maintained mono- or dual-reactivity against TL9 peptide-pulsed (Fig. 2.4B) and HIV-infected (Fig. 2.4C) target cells expressing B*81:01 or B*42:01, confirming that dual-reactive T cells were a distinct population in both B*81:01 and B*42:01 expressing individuals, and that phenotypic differences in pHLA specificity were due to TCR sequence.

A

TCR ID	Restriction	TRAV	TRAJ	CDR3 Alpha	TRBV	TRBJ	CDR3 Beta
7A10	B*42- Mono B*42 TL9	12-1*01	31*01	CVVNIRGNARLMF	12-3*01	2-1*01	CASSLGTLNEQFF
13A10	B*42- Mono B*42 TL9	16*01	18*01	CALRGRGSTLGRLYF	7-9*01	1-3*01	CASSSSLTGVTSYNEQFF
14A4	B*42- Dual B*42/81 TL9	13-1*01	38*01	CAATNAGNNRKLIW	12-3*01	1-1*01	CASSFSKNTEAFF
14D7	B*42- Dual B*42/81 TL9	13-1*01	38*01	CAATNAGNNRKLIW	12-3*01	1-1*01	CASSHSKNTEAFF
16A11	B*42- Dual B*42/81 TL9	13-1*01	38*01	CAACNAGNNRKLIW	12-3*01	1-1*01	CASSYSKNTEAFF
11A10	B*81- Mono B*81 TL9	26-1*01	23*01	CIVRGTYNQGGKLIF	12-3*01	2-1*01	CASSLGTLNEQFF
12A11	B*81- Dual B*81/42 TL9	26-2*01	30*01	CILRGLMNRDDKIIF	12-3*01	1-1*01	CASKQGVAEAFF
18A2	B*81- Dual B*81/42 TL9	26-1*01	39*01	CIVRGLNNAGNMLTF	12-3*01	1-3*01	CASSLGIDAIYF

B

Legend:
- Mono reactive B*42 7A10
- Mono reactive B*42 13A10
- Dual reactive B*42 14A4
- Dual reactive B*42 14D7
- Dual reactive B*42 16A11
- Mono reactive B*81 TCR 11A10
- Dual reactive B*81 TCR 12A11
- Dual reactive B*81 TCR 18A2

C

68

Figure 2.4: In vitro validation of TCR specificity and dual reactivity. Details for the eight TL9-specific TCR clones investigated in this study are shown, including donor HLA, mono- or dual-reactivity phenotype, paired TCR α/β V gene usage and CDR3 sequences (A). Jurkat T cells were co-transfected with TCR α/β, CD8 α and an NFAT-driven luciferase reporter vector, and then co-cultured with TL9 peptide-pulsed (B) or HIV-infected (C) target cells stably expressing B*81:01 or B*42:01. TCR-dependent NFAT signaling was quantified by luminescence. The expected mono- or dual-reactive phenotype was observed for all reconstructed TCR clones, as indicated by greater luminescence (absolute light units, y-axis) in the presence of TL9-pulsed or virus-infected target cells compared to no-peptide or uninfected controls. Assays were conducted at least three times. Results from a representative experiment are shown as the mean of three co-culture reactions, plus standard deviation.

2.4.5 Analyses of TL9 variant recognition by TCR clones

The ability of TCR to cross-recognize epitope variants is associated with enhanced antiviral activity of CD8^{+} T cells [52,139,174]. If indeed the dual-reactive population contributes to control of HIV-1, we hypothesized that it should be able to respond to a variety of TL9 variants. To explore this, we assessed the ability of each reconstructed TCR to respond to a panel of 180 peptides representing TL9 and all possible single amino-acid TL9 variants. These results are displayed as heat maps in Fig. 2.5. Collectively, the eight TCR clones recognized 114 (of 171, 67%) TL9 variants at a normalized luminescence value of 0.1 or greater (which was ~10-fold above negative control wells). In addition to consensus TL9, individual B*81:01-derived clones responded to 67 (11A10, mono-reactive), 53 (12A11, dual), and 94 (18A2, dual)

variant peptides, while B*42:01-derived clones responded to 48 (7A10, mono), 46 (13A10, mono), 54 (14A4, public dual), 34 (16A11, public dual), and 34 (14D7, public dual) variant peptides. No correlation was observed between the total breadth of TL9 variant recognition and dual-reactivity, suggesting that qualitative features of TCR function contributed to this phenotype. The three TCR clones isolated from B*81:01 expressing individuals (one mono- and two dual-reactive) displayed similar overall TL9 variant cross-recognition profiles, as demonstrated by Spearman R-values >0.80 for all pair-wise associations; however, greater breadth against variants at position 4 (aspartic acid) was seen for clone 18A2. In contrast, the five TCR clones isolated from B*42:01 expressing individuals displayed more disparate cross-recognition profiles, which was reflected by pair-wise Spearman R-values between 0.12 and 0.67. Notable differences were observed among B*42:01-derived TCR clones for recognition of TL9 peptide variants at positions 3 and 7, which are discussed below. To further evaluate the degree of functional similarity among these TCR clones, we performed a hierarchical clustering analysis based on their TL9 variant recognition profiles. Results are shown as a dendrogram in Figure 2.5. We observed that all three of the public dual-reactive B*42:01-derived clones grouped together with bootstrap values of 100. Furthermore, this group of public clones clustered more closely with the three B*81:01-derived clones (bootstrap value of 97), compared to the two mono-reactive B*42:01-derived clones. Together, these results indicate that the epitope binding properties of the public dual-reactive B*42:01-derived TCR clones are more similar to those of clones elicited in the context of the more protective B*81:01 allele, despite TL9 peptide being presented on a different HLA allele.
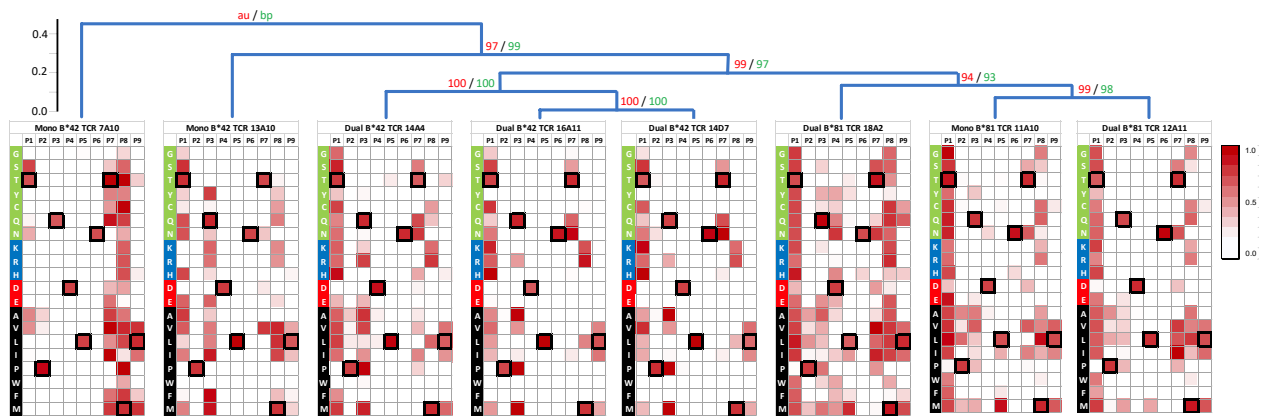
Figure 2.5: Functional clustering of TCR clones based on TL9 variant recognition profiles. TCR recognition of TL9 variants was assessed by pulsing target cells expressing the donor HLA (B*81:01 or B*42:01) with a panel of 180 peptides encompassing all single amino acid substitutions at epitope positions 1 through 9 prior to co-culture with Jurkat T cells expressing the TCR of interest. TCR-dependent NFAT signalling was quantified by luminescence. Values were normalized to the mean signal obtained for consensus TL9 (set to 1.0), which was tested nine times in each experiment. Results are displayed as heatmaps, where the warmer color reflects higher relative luminescence values indicative of better TCR recognition. Peptide positions are shown at the top of each heatmap; amino acid substitutions on the consensus TL9 backbone are shown on the left-hand side. Amino acids are grouped according to chemical properties: polar residues (G, S, T, Y, C, Q, N) are highlighted in green; basic residues (K, R, H) are blue; acidic residues (D, E) are red; and hydrophobic residues (A, V, L, I, P, W, F, M) are black. For reference, the consensus TL9 residue at each position is indicated using a box. TCR were grouped according to their functional profiles by hierarchical clustering using correlation distances and single linkage methods (5,000 iterations) implemented in pvclust (http://stat.sys.i.kyoto-u.ac.jp/ prog/pvclust/). The dendrogram (top) displays approximately unbiased (au) p-values in red text and bootstrap probability (bp) values in green text. The three

B*81:01-derived TCR clustered with bp values of 93 or higher. The three public dual-reactive B*42:01-derived TCR clustered with bp values of 100; and, notably, they grouped more closely with B*81:01 clones (bp value of 97), rather than mono-reactive B*42:01-derived TCR.

2.4.6 Dual-reactive TCR recognize more TL9 escape mutations

We observed substantial differences in TL9 variant recognition among TCR clones, particularly at epitope positions 3 and 7. To examine the impact of these differences on viral adaptation, we restricted our analysis to 19 TL9 polymorphisms present in circulating HIV-1 subtype C sequences at a prevalence of ~0.1% or greater, which were considered as viable escape mutations. The ability of each TCR to recognize this panel of mutants is illustrated as a SequenceLogo in Figure 2.6 (panels A-H). Collectively, the eight TCR clones recognized 16 (of 19, or 84%) TL9 escape mutants; none responded to a threonine, glycine or aspartic acid substitution at position 3, which together accounted for 26.1% of circulating variant sequences. These results were highly consistent with prior studies of T cell cross-reactivity based on IFN-γ ELISPOT assays using PBMC [151,152,154], with 7 (of 8; 88%) TCR clones recognizing serine at position 7 or alanine at position 3, whereas responsiveness to other natural polymorphisms at position 3 (histidine, 13%; serine, 13%; threonine, 0%) and position 7 (valine, 75%; methionine, 25%) were less common. While the total number of TL9 escape mutants recognized by B*81:01-derived TCR clones (range, 8-14), public dual-reactive B*42:01-derived clones (6-9) and mono-reactive B*42:01-derived clones (6-7) was not significantly different between groups, we observed that the two mono-reactive B*42:01-derived TCR clones responded primarily to variants located at either

position 7 (for 7A10) (Fig. 6A) or position 3 (for 13A10) (Fig. 2.6B), indicating a limited ability to control escape mutations that occur at the other residue. In contrast, B*81:01-derived TCR clones and public dual-reactive B*42:01-derived clones each displayed broader recognition of variants at both position 3 and 7 (Fig. 2.6C-H), suggesting a distinct mechanism(s) of binding that accommodated changes at these residues. B*81:01-derived TCR clones also displayed broader recognition of TL9 variants at position 5. These results demonstrate functional differences among TCR clonotypes that may contribute to control of naturally occurring TL9 variants, particularly at epitope positions 3 and 7.

HIV-1 adaptation to CD8^{+} T cells is highly dynamic [175,176], but escape in TL9 is limited by functional constraints [55]. Since common TL9 variants, such as serine at position 7 (S7; 23.4% of non-consensus sequences in LANL), are presumed to encounter a relatively lower barrier for escape compared to rare variants, such as isoleucine at this position (I7: 0.7%), we reasoned that TCR recognition of more common TL9 variants would be beneficial for viral control. To explore this, we plotted these 19 TL9 polymorphisms using pie charts with wedges sized according to their prevalence in subtype C sequences (Fig. 2.6I-P) and then determined the percent coverage of TL9 escape mutations for each TCR by calculating the proportion of total sequence variation that was recognized (see wedges highlighted in Red). Based on this frequency-adjusted analysis, individual clones displayed 22% (Fig. 2.6J) to 67% (Fig. 2.6P) coverage of TL9 variants. While differences between groups were not statistically significant, B*81:01-derived TCR clones and public dual-reactive B*42:01 clones tended to display greater coverage (40-67% and 36-41%, respectively) compared to the mono-reactive B*42:01 clones (22% and 32%). These results indicate

that individual TCR clonotypes display variable capacity to recognize more common

TL9 variants that are likely to constitute preferential escape mutants.

A TCR 7A10
Mono-B*42:01
TRBV12-3

I

Variant Epitope Recognition (R): 32%
Escape Pathway Recognition (Y+R): 32%

B TCR 13A10
Mono-B*42:01
TRBV7-9

J

Variant Epitope Recognition (R): 22%
Escape Pathway Recognition (Y+R): 32%

C TCR 14A4
Dual-B*42:01
TRBV12-3

K

Variant Epitope Recognition (R): 41%
Escape Pathway Recognition (Y+R): 83%

D TCR 14D7
Dual-B*42:01
TRBV12-3

L

Variant Epitope Recognition (R): 36%
Escape Pathway Recognition (Y+R): 52%

E TCR 16A11
Dual-B*42:01
TRBV12-3

M

Variant Epitope Recognition (R): 36%
Escape Pathway Recognition (Y+R): 52%

F TCR 11A10
Mono-B*81:01
TRBV12-3

N

Variant Epitope Recognition (R): 42%
Escape Pathway Recognition (Y+R): 58%

G TCR 12A11
Dual-B*81:01
TRBV12-3

O

Variant Epitope Recognition (R): 40%
Escape Pathway Recognition (Y+R): 57%

H TCR 18A2
Dual-B*81:01
TRBV12-3

P

Variant Epitope Recognition (R): 67%
Escape Pathway Recognition (Y+R): 83%

Figure 2.6: Enhanced recognition of TL9 escape by B*81:01-derived and B*42:01-derived dual-reactive TCR clones. The ability of each TCR clone to respond to HIV-1 escape mutants was determined by comparing its recognition profile to a panel of 19 naturally occurring subtype C TL9 variants, found at a prevalence of ~0.1% or greater in the LANL HIV Sequence Database (HIV Databases; http://www.hiv.lanl.gov). Recognition breadth for each TCR is illustrated as a SequenceLogo, demonstrating variable responsiveness towards relevant TL9 mutations located primarily at epitope positions 3 and 7. Mono-reactive TCR from B*42:01 expressing individuals displayed narrower profiles that recognized TL9 variants at either position 7 (7A10, A) or position 3 (13A10, B), whereas public dual-reactive B*42:01-derived clones (C-E) and B*81:01-derived clones (F-H) demonstrated broader ability to recognize TL9 variants at both positions 3 and 7. To account for constraints on TL9 escape, epitope variants were displayed using pie charts where the size of each wedge is proportional to variant frequency in circulating subtype C isolates (I-P). Serine at position 7 (S7), serine at position 3 (S3), and threonine at position 3 (T3) accounted for the majority (55%) of population-level variation. For each chart, the wedge is shaded in Red (R) if the TCR responded to the escape mutant or in Yellow (Y) if the TCR recognized all transitional mutations required to generate that escape mutant from consensus TL9. The sum of all Red wedges is displayed under each chart as the total percentage of Variant Epitope Recognition and the sum of all shaded wedges, Red plus Yellow, is displayed as the total percentage of Escape Pathway Recognition, where recognition of all circulating TL9 variants would be 100%. Overall, B*81:01-derived TCR (N-P) and public dual-reactive B*42:01-derived TCR (K-M) displayed better ability to cross-recognize circulating TL9 escape variants and pathways compared to mono-reactive B*42:01-derived clones (I-J).

Since codon usage places additional constraints on viral sequence evolution, we reasoned that TCR recognition of transitional variants would hinder the development of TL9 escape . For example, substitution of glutamine at position 3 (Q3) with serine (S3) requires a minimum of two nucleotide changes with transition through proline (P3) or a stop codon. Thus, TCR recognition of the P3 variant would be expected to prevent formation of S3, even in cases where the TCR did not respond to the S3 variant itself. For each TCR clone, we determined which TL9 escape mutations were inhibited due to recognition of critical transitional variants (see Yellow wedges in Figures 2.6I-P). We then calculated the total coverage of TL9 escape pathways by summing the proportion of variant sequences that were recognized or prevented by each TCR (i.e. Red plus Yellow wedges). Based on this pathway-adjusted analysis, individual TCR clones displayed 32% to 83% coverage of TL9 escape mechanisms. Notably, B*81:01-derived clones (range, 57-83%, Fig. 2.6N-P) and public dual-reactive B*42:01-derived clones (range, 52-83%, Fig. 2.6K-M) displayed broader coverage compared to mono-reactive B*42:01-derived clones (both 32%, Fig. 6I-J) (p = 0.05 and p = 0.11, respectively; Student's T test); highlighted by one public dual-reactive B*42:01-derived clone (14A4) and one B*81:01-derived clone (18A2). Notably, extended coverage of TL9 escape pathways was due mainly to the ability of TCR clones 14A4 (**K**), 14D7 (**L**), 16A11 (**M**), 11A10 (**N**), and 12A11 (**O**) to respond to the P3 variant, which is anticipated to impair development of the S3 escape mutation that accounts for 16.5% of TL9 variant sequences. Together, these results illustrate the functional diversity that exists among antigen-specific T cells and demonstrate the impact of TCR sequence on recognition of HIV-1 Gag TL9 escape mutations. This

work highlights the role of TCR clonotype differences as a correlate of HIV-1 control in the context of HLA B*81:01 and B*42:01.

2.5 Discussion

The characteristics that determine effectiveness of adaptive host immune responses to rapidly evolving pathogens such as HIV-1 are not fully defined. In this study, we examined the CD8^{+} T cell response against the immunodominant HIV-1 p24 Gag TL9 epitope in the context of two closely related class I HLA alleles, B*81:01 and B*42:01, that both display differential abilities to control viral subtype C infection [111]. We identified a population of dual HLA tetramer-reactive T cells that recognized TL9 presented in the context of either B*42:01 or B*81:01 alleles and observed that the presence of this dual-reactive population was an independent predictor of lower plasma viral load. In B*42:01 expressing individuals, dual-reactive populations were dominated by public TCR clonotypes that encoded *TRBV12-3*. A comprehensive *in vitro* functional analysis of selected TCR clones indicated that B*81:01-derived clones (regardless of mono- or dual-reactive phenotype) and public dual-reactive B*42:01-derived TCR clones displayed greater ability to recognize TL9 escape pathways, compared to mono-reactive clones from B*42:01 expressing individuals. While the dual-reactive T cell phenotype reported here is a phenomenon of tetramer binding to pHLA that is not expressed by the host, our results indicate that it identifies T cell subsets within diverse antigen-specific repertoires that share important features, including Vβ gene sequences and the ability to recognize HIV-1 epitope variants. A similar dual HLA-reactive phenotype has been described for one CTL clone [169], but here we demonstrate the extent to which dual-reactive T cells exist *in vivo* and link this phenotype to functional characteristics of individual TCR clonotypes. It will be critical to examine this phenomenon further to see if it is a common feature of T cell responses elicited in the context of other HLA supertypes, such as members of the B57 family that also show differential abilities to control HIV-1 infection [111].

It is important to note that antigen sensitivity appeared to be independent of cross-reactivity for TCRs examined in this study. While more detailed biochemical analyses will be necessary to fully assess the affinity of TL9-specific TCR clones, our reporter assay provides a surrogate measure of antigen sensitivity based on strength of NFAT signalling. The activities of dual-reactive B*42:01-derived TCR clones were lower compared to those of mono-reactive B*42:01-derived clones. We observed similar differences in the sensitivity of representative TCR clones tested over a range of TL9 concentrations (Supplementary Fig. 3), indicating that this result was not an artefact of peptide dose. In addition, TCR sensitivity towards consensus TL9 did not correlate with cross-recognition of TL9 variants in our more comprehensive analysis, although it will be important to confirm this observation using a larger panel of TL9-specific TCR clones.

Although B*81:01 and B*42:01 are both members of the B7 supertype and known to present many of the same HIV-1 peptides, the dual-reactive T cell phenotype is unexpected since structural data indicated that TL9 adopts a distinct conformation upon binding to each allele [156]. Our analysis demonstrated that B*81:01-derived TCR clones and public dual-reactive B*42:01-derived clones recognized TL9 variants at both principal sites of viral escape, position 3 and 7. This is interesting since both residues are buried in the B*81:01 structure, while position 7 is solvent-exposed in the context of B*42:01 [156]. It remains to be determined whether TCR recognition reflects direct binding to these TL9 variants, or rather is due to conformational changes in the pHLA or indirect effects on other TL9 residues. In contrast, mono-reactive B*42:01-derived TCR displayed breadth against TL9 variants at either position 3 or position 7, but not both. While both types of mono-reactive TCR may be present within the repertoire of B*42:01 expressing individuals, skewing of the immune response towards

either mono-reactive TCR subset could facilitate viral escape at the alternative TL9 position.

Our detailed functional data provides insight into characteristics of TL9-specific TCR clones that might be overlooked using more conventional methods based on HIV-1 sequences alone. For example, all TCR clones were sensitive to changes at TL9 position 6, demonstrating that this highly conserved polar asparagine residue is critical in the context of both HLA alleles, despite it being solvent-exposed in the B*81:01 structure and buried in the B*42:01 structure [156]. In addition, most TCR were sensitive to changes at position 4, indicating that this negatively charged, polar aspartic acid residue (which is solvent-exposed in both structures [156]) is critical for recognition; however, the B*81:01-derived clone 18A2 tolerated mutations at this residue, suggesting a distinct mechanism of interaction in this case. Structural flexibility is a crucial feature of the interaction between TCR and pHLA [177-179]; thus, changes in conformation induced upon TCR binding may be relevant to recognize TL9 variants in the context of both B*81:01 and B*42:01. Because such conformational rearrangements are difficult to predict [180], more detailed structural analyses will be necessary to explore this issue. In the absence of such data, we are unable to define structural determinants of cross-reactivity for the TCR clones examined in our study. Nevertheless, our results highlight peptide-recognition properties that may contribute to future studies of these and other TL9-specific TCRs.

This work extends prior efforts to examine TL9-specific CD8+ T cell responses. In particular, Leslie et al. [151] and Geldmacher et al. [152] observed enrichment of *TRBV12-3* usage in B*81:01 and some B*42:01 expressing individuals, while Leslie et al. [151] and Kloverpris et al [146] described public TCR ß sequences in B*42:01 expressing

individuals that correspond to the dual-reactive TCR clones 14A4 (CASSFSKNTEAFF) and 14D7 (CASSHSKNTEAFF) examined here and demonstrated that the presence of these public clones was associated with TL9 immunodominance [146]. These earlier reports suggested that CD8^{+} T cell responses in B*81:01 expressing individuals displayed broader recognition of TL9 variants, but individual T cell clones (or TCR clonotypes) were not explored. Here, we re-discovered public TCR ß clonotypes in B*42:01 expressing individuals by their dual HLA-reactive phenotypes. Extensive functional analyses of selected TCR clones demonstrated substantial diversity in their abilities to recognize TL9 variants. Our results emphasize the role of cross-reactive public TCR clones encoding *TRBV12-3* for effective TL9 responses in B*42:01 expressing individuals; however, differences in TL9 variant recognition among these public clones also suggests a functional hierarchy that may be clinically relevant. Furthermore, it should be noted that B*42:01-derived clone 7A10 encoded *TRBV12-3* but did not demonstrate dual-reactivity or broad recognition of TL9 escape variants, indicating that phenotypic differences among TCR were not driven entirely by V gene usage.

Several observations from this study are relevant for the design of vaccines or therapeutics. Vaccine antigens that can elicit effective cross-reactive TCR clonotypes might provide better protection against HIV-1 infection or enhance the ability of the immune system to recognize latent viral reservoirs encoding escape variants. We observed that public dual-reactive TCR clones from B*42:01 expressing individuals were unique in their ability to recognize a proline variant at TL9 position 3 (Q3P). It would be interesting to examine *ex vivo* responses to this rare TL9 variant as a surrogate marker for public dual-reactive T cells in HIV-infected individuals or vaccine recipients; or to consider vaccination with this variant TL9 sequence to elicit a more

broadly reactive T cell response in B*42:01 expressing individuals. We have also identified and validated the recognition profiles of eight TL9-specific TCR clones, including several with dual HLA-reactive phenotypes. These TCR clones may be attractive products for future T cell therapy strategies that aim to reduce or eliminate viral reservoirs encoding escape mutations in the context of HIV-1 subtype C infection.

In summary, we have identified characteristics of TCR clonotype sequence and function that are associated with variable control of HIV-1 infection in the context of B*81:01 and B*42:01. We observed a unique dual HLA-reactive CD8$^+$ T cell population that was highly enriched for a small number of public TCR clonotypes in B*42:01 expressing individuals. Mono- and dual-reactive TCR clones from individuals expressing the protective B*81:01 allele displayed broad recognition of TL9 variants, suggesting that they provide comparable abilities to contain HIV-1 Gag escape mutants. In contrast, only public dual-reactive TCR clones from B*42:01 expressing individuals displayed similar broad TL9 variant recognition, suggesting that these public clonotypes provide enhanced ability to control HIV-1 escape mutants in the context of this less protective HLA allele. While additional studies will be necessary to fully assess the structural mechanisms and clinical relevance of these observations, this work provides a strong foundation and rationale to further explore the impact of TCR clonotype differences on HIV-1 outcomes. Together, our results highlight the feasibility and use of detailed molecular analyses that link TCR sequences with functional characteristics to improve understanding of T cell responses against diverse and rapidly evolving pathogens. Similar investigations might be beneficial to enhance the development of vaccines and T cell-based immunotherapies against HIV or other human diseases.

2.6   Supplementary Data
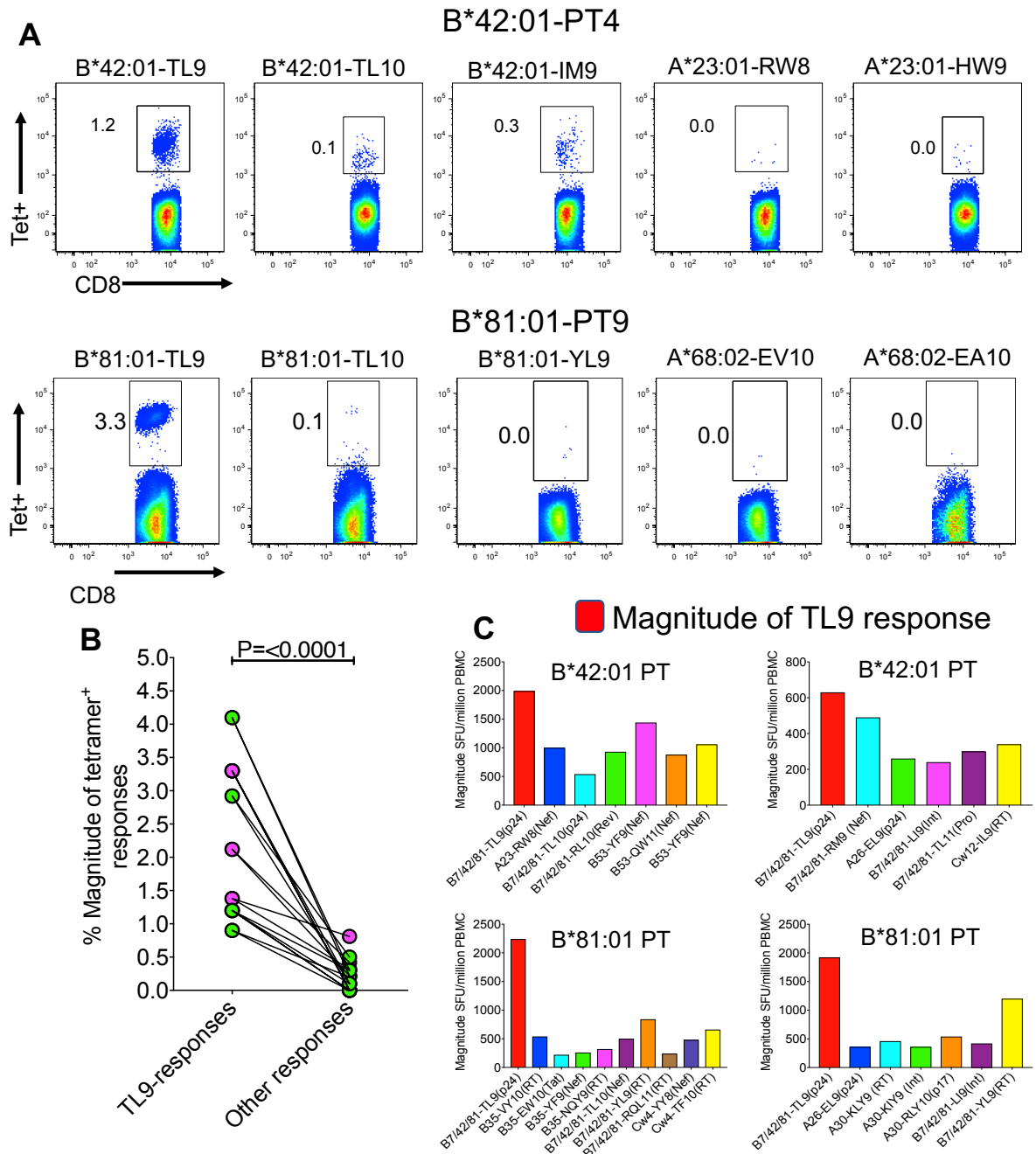
Supplementary Figure 2.1: Intra-patient comparison of TL9 response with responses restricted by other alleles. Flow plot showing HIV-specific responses in a B*81:01 and B*42:01 representative donors (A), and aggregate data of TL9 responses compared to other responses (B) showing that TL9 responses are maintained at significantly

higher frequencies than other responses. ELISPOT data showing the magnitude of

TL9 responses compared to other responses in B*81:01 and B*42:01 participants (C).
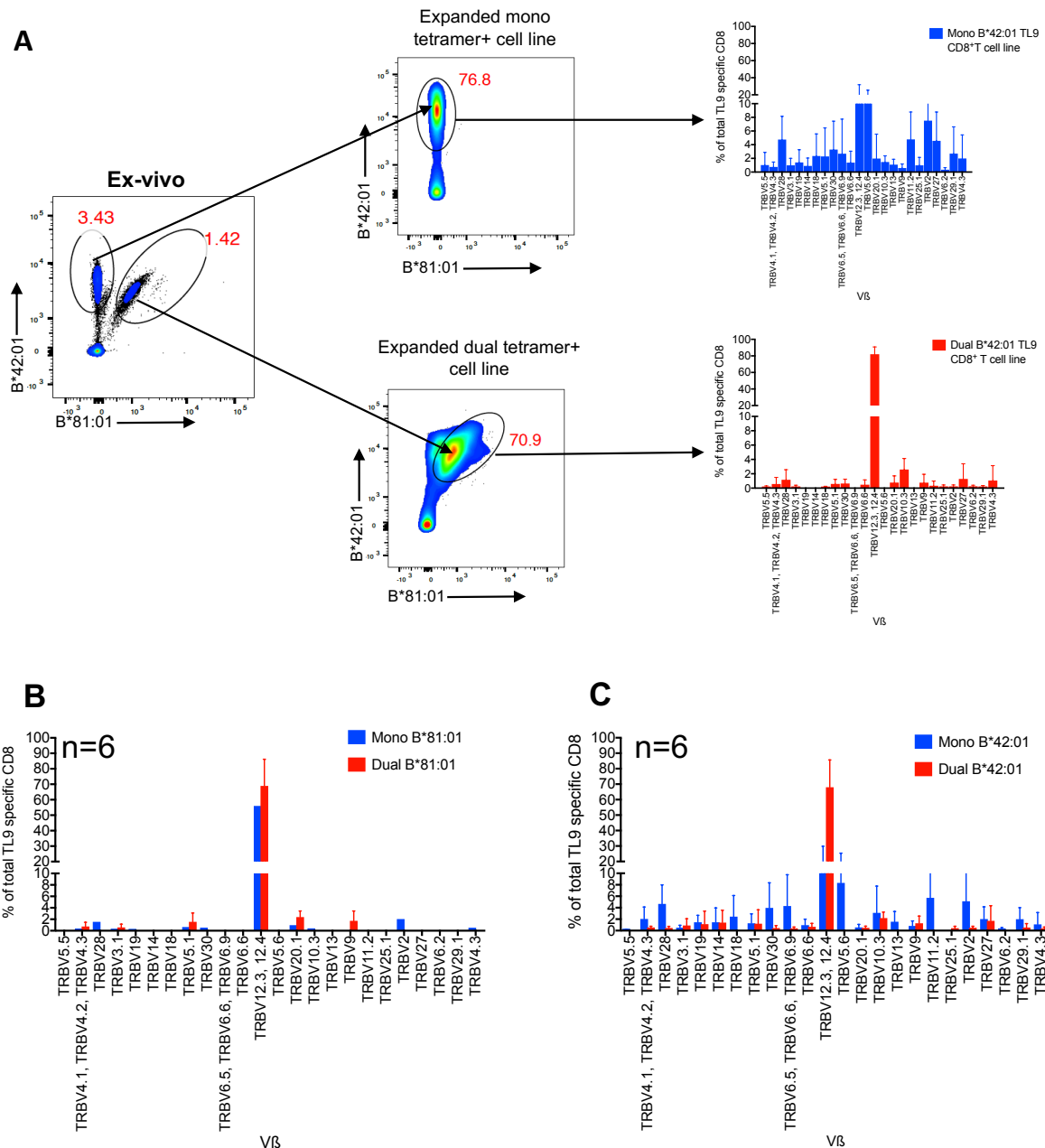
Supplementary Figure 2.2: TCR-Vβ is conserved in dual TL9 tetramer+ CD8^{+} T cell

lines. Representative flow plot and TCR-Vβ family usage is shown for mono- and dual-

reactive TL9 tetramer+ T cells isolated from a B*42:01 donor after expansion for 2

weeks (A). Aggregate data on TCR-Vβ family usage by mono-reactive compared to dual-reactive TL9 tetramer+ T cells in six B*81:01 donors (B) and six B*42:01 donors (C).

Peptide pulsed HLA-B*42 Target cells
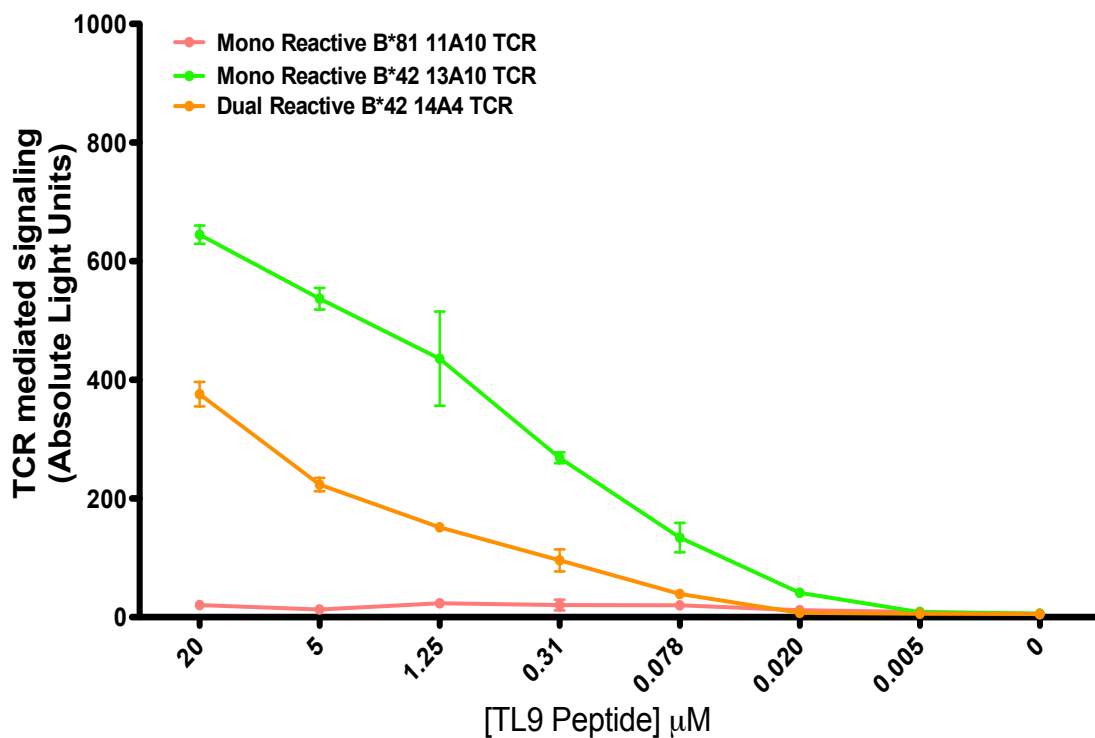
Supplementary Figure 2.3: TCR signalling in response to TL9 peptide dilutions. Mono-reactive TCR clones 11A10 (B*81; red) and 13A10 (B*42; green) and dual-reactive TCR clone 14A4 (B*42; orange) were tested using target cells expressing HLA-B*42:01. Similar mono- or dual-reactive phenotypes were observed over a range of TL9 peptide doses (5 nM to 20 μM). The mono-reactive B*42:01-derived clone 13A10 displayed greater signalling activity compared to the dual-reactive clone 14A4 at all peptide doses tested. In addition, the mono reactive B*81:01-derived clone 11A10 was

unable to recognize TL9 bound to HLA-B*42:01 at all peptide doses tested. Combined with data shown in Figure 4, these results confirm the mono- and dual-reactive phenotypes of these TCR clones and also suggest that antigen sensitivity is independent of dual-reactivity for the B*42:01-derived public TCR clones examined in this study.

Supplementary Table 2.1:

Frequencies of HIV specific CD8$^+$ T cell tetramer responses tested

PID	Class I HLA	Epitope tested	Tetramer response
PT4	A*23:01, A*29:02, B*53:01, B*42:01, C*03:04, C*17:00	**HLA-B*42:01 TL9**	**1.20**
		HLA-B*42:01 TL10	0.10
		HLA-B*42:01 IM9	0.30
		HLA-A*23:01 RW8	0.00
		HLA-A*23:01 HW9	0.00
PT5	A*30:01, A*34:02, B*35:01, B*42:01, C*02:10, C*17:01	**HLA-B*42:01 TL9**	**2.12**
		HLA-B*42:01 TL10	0.00
		HLA-B*42:01 IM9	0.00
		HLA-B*35:01 DL9	0.05
PT6	A*43:01, A*74:01, B*57:01, B*81:01, C*04:01, C*07:01	**HLA-B*81:01 TL9**	**2.08**
		HLA-B*81:01 TL10	0.00
		HLA-B*81:01 YL9	0.01
		HLA*C*07:01 KY11	0.53
PT9	A*23:01, A*68:02, B*14:02, B*81:01, C*08:02, C*18:00	**HLA-B*81:01 TL9**	**3.30**
		HLA-B*81:01 TL10	0.10
		HLA-B*81:01 YL9	0.00
		HLA-A*68:02 EV10	0.00
		HLA-A*68:02 EA10	0.00
PT10	A*02:05, A*33:01, B*42:01, B*15:03, C*07:01, B*17:01	**HLA-B*42:01 TL9**	**1.48**
		HLA-B*42:01 TL10	0.00
		HLA-B*15:03 FY10	0.81
		HLA-C*07:01 KY11	0.32
PT13	A*30:01, A*32:01, B*42:01, B*58:02, C*06:02, B*17:01	**HLA-B*42:01 TL9**	**4.70**
		HLA-B*42:01 TL10	0.00
		HLA-B*58:02 LF11	0.42
		HLA-B*58:02 QL11	0.30
PT14	A*02:01, A*30:01, B*42:01, B*45:07, C*16:01, B*17:01	**HLA-B*42:01 TL9**	**0.90**
		HLA-A*02:01 SL9	0.00
		HLA-B*42:01 TL10	0.20
		HLA-A*02:01 SV10	0.00
PT15	A*01:01, A*74:01, B*35:01, B*81:01, C*04:01, B*18:01	**HLA-B*81:01 TL9**	**1.38**
		HLA-B*42:01 TL10	0.10
		HLA-B*35:01 DL9	0.76
PT18	A*30:01, A*68:02, B*14:02, B*42:01, C*08:02, B*17:01	**HLA-B*42:01 TL9**	**4.60**
		HLA-B*42:01 TL10	0.10
		HLA-A*68:02 EA10	0.00
		HLA-A*68:02 EV10	0.20
PT19	A*23:01, A*30:01, B*42:01, B*57:02, C*07:01, B*17:00	**HLA-B*42:01 TL9**	**2.92**
		HLA-B*42:01 TL10	0.20
		HLA-B*57:02 TW10	0.10
		HLA-A*23:01 RW8	0.90
		HLA-C*07:01 KY11	0.50

All values are displayed as percent tetramer positive CD8$^+$ T cells. Tetramer responses tested were based on published epitopes restricted by HLA alleles of the study participants and tetramer availability.

2.7   References

1   Deeks, S. G. & Walker, B. D. Human immunodeficiency virus controllers: mechanisms of durable virus control in the absence of antiretroviral therapy. *Immunity* **27**, 406-416, doi:10.1016/j.immuni.2007.08.010 (2007).

2   Migueles, S. A. & Connors, M. Long-term nonprogressive disease among untreated HIV-infected individuals: clinical implications of understanding immune control of HIV. *Jama* **304**, 194-201, doi:10.1001/jama.2010.925 (2010).

3   Frater, A. J. *et al.* Effective T-cell responses select human immunodeficiency virus mutants and slow disease progression. *J Virol* **81**, 6742-6751, doi:10.1128/JVI.00022-07 (2007).

4   Kawashima, Y. *et al.* Adaptation of HIV-1 to human leukocyte antigen class I. *Nature* **458**, 641-645, doi:10.1038/nature07746 (2009).

5   Walker, B. & McMichael, A. The T-cell response to HIV. *Cold Spring Harbor perspectives in medicine* **2**, doi:10.1101/cshperspect.a007054 (2012).

6   Koup, R. A. *et al.* Temporal association of cellular immune responses with the initial control of viremia in primary human immunodeficiency virus type 1 syndrome. *J Virol* **68**, 4650-4655 (1994).

7   Borrow, P., Lewicki, H., Hahn, B. H., Shaw, G. M. & Oldstone, M. B. Virus-specific CD8+ cytotoxic T-lymphocyte activity associated with control of viremia in primary human immunodeficiency virus type 1 infection. *Journal of virology* **68**, 6103-6110 (1994).

8   Migueles, S. A. *et al.* HLA B*5701 is highly associated with restriction of virus replication in a subgroup of HIV-infected long term nonprogressors. *Proceedings of the National Academy of Sciences of the United States of America* **97**, 2709-2714, doi:10.1073/pnas.050567397 (2000).

9   Kiepiela, P. *et al.* Dominant influence of HLA-B in mediating the potential co-evolution of HIV and HLA. *Nature* **432**, 769-775, doi:10.1038/nature03113 (2004).

10   Kaslow, R. A. *et al.* Influence of combinations of human major histocompatibility complex genes on the course of HIV-1 infection. *Nature medicine* **2**, 405-411 (1996).

11   Gao, X. *et al.* Effect of a single amino acid change in MHC class I molecules on the rate of progression to AIDS. *The New England journal of medicine* **344**, 1668-1675, doi:10.1056/nejm200105313442203 (2001).

12   Draenert, R. *et al.* Constraints on HIV-1 evolution and immunodominance revealed in monozygotic adult twins infected with the same virus. *J Exp Med* **203**, 529-539 (2006).

13   Kosmrlj, A. *et al.* Effects of thymic selection of the T-cell repertoire on HLA class I-associated control of HIV infection. *Nature* **465**, 350-354, doi:10.1038/nature08997 (2010).

14   Leslie, A. J. *et al.* HIV evolution: CTL escape mutation and reversion after transmission. *Nat Med* **10**, 282-289 (2004).

15   Crawford, H. *et al.* Evolution of HLA-B*5703 HIV-1 escape mutations in HLA-B*5703-positive individuals and their transmission recipients. *J Exp Med* **206**, 909-921, doi:10.1084/jem.20081984 (2009).

16   Kiepiela, P. *et al.* CD8+ T-cell responses to different HIV proteins have discordant associations with viral load. *Nat Med* **13**, 46-53, doi:10.1038/nm1520 (2007).

17   Goonetilleke, N. *et al.* The first T cell response to transmitted/founder virus contributes to the control of acute viremia in HIV-1 infection. *The Journal of experimental medicine* **206**, 1253-1272, doi:10.1084/jem.20090365 (2009).

18   Yang, O. O. *et al.* Determinant of HIV-1 mutational escape from cytotoxic T lymphocytes. *J Exp Med* **197**, 1365-1375, doi:10.1084/jem.20022138 (2003).

19   Wright, J. K. *et al.* Gag-protease-mediated replication capacity in HIV-1 subtype C chronic infection: associations with HLA type and clinical parameters. *Journal of virology* **84**, 10820-10831, doi:10.1128/JVI.01084-10 (2010).

20   Brockman, M. A. *et al.* Early selection in Gag by protective HLA alleles contributes to reduced HIV-1 replication capacity that may be largely compensated for in chronic infection. *J Virol* **84**, 11937-11949, doi:10.1128/JVI.01086-10 (2010).

21   Davis, S. J. & van der Merwe, P. A. The structure and ligand interactions of CD2: implications for T-cell function. *Immunol Today* **17**, 177-187 (1996).

22   Turner, S. J., Doherty, P. C., McCluskey, J. & Rossjohn, J. Structural determinants of T-cell receptor bias in immunity. *Nature reviews. Immunology* **6**, 883-894, doi:10.1038/nri1977 (2006).

23   Nikolich-Zugich, J., Slifka, M. K. & Messaoudi, I. The many important facets of T-cell repertoire diversity. *Nature reviews. Immunology* **4**, 123-132, doi:10.1038/nri1292 (2004).

24   Lissina, A., Chakrabarti, L. A., Takiguchi, M. & Appay, V. TCR clonotypes: molecular determinants of T-cell efficacy against HIV. *Current opinion in virology* **16**, 77-85, doi:10.1016/j.coviro.2016.01.017 (2016).

25   Lee, K. H. *et al.* The immunological synapse balances T cell receptor signaling and degradation. *Science (New York, N.Y.)* **302**, 1218-1222, doi:10.1126/science.1086507 (2003).

26   Chen, H. *et al.* TCR clonotypes modulate the protective effect of HLA class I molecules in HIV-1 infection. *Nature immunology* **13**, 691-700, doi:10.1038/ni.2342 (2012).

27   Ladell, K. *et al.* A molecular basis for the control of preimmune escape variants by HIV-specific CD8+ T cells. *Immunity* **38**, 425-436, doi:10.1016/j.immuni.2012.11.021 (2013).

28   Iglesias, M. C. *et al.* Escape from highly effective public CD8+ T-cell clonotypes by HIV. *Blood* **118**, 2138-2149, doi:10.1182/blood-2011-01-328781 (2011).

29   Miles, J. J., Douek, D. C. & Price, D. A. Bias in the alphabeta T-cell repertoire: implications for disease pathogenesis and vaccination. *Immunology and cell biology* **89**, 375-387, doi:10.1038/icb.2010.139 (2011).

30   Turner, S. J., La Gruta, N. L., Kedzierska, K., Thomas, P. G. & Doherty, P. C. Functional implications of T cell receptor diversity. *Current opinion in immunology* **21**, 286-290, doi:10.1016/j.coi.2009.05.004 (2009).

31   Ntale, R. S. *et al.* Temporal association of HLA-B*81:01- and HLA-B*39:10-mediated HIV-1 p24 sequence evolution with disease progression. *Journal of virology* **86**, 12013-12024, doi:10.1128/jvi.00539-12 (2012).

32   Bihl, F. *et al.* Impact of HLA-B alleles, epitope binding affinity, functional avidity, and viral coinfection on the immunodominance of virus-specific CTL responses. *Journal of immunology* **176**, 4094-4101 (2006).

33   Carlson, J. M. *et al.* Correlates of protective cellular immunity revealed by analysis of population-level immune escape pathways in HIV-1. *J Virol* **86**, 13202-13216, doi:10.1128/JVI.01998-12 (2012).

34   Kloverpris, H. N. *et al.* CD8+ TCR Bias and Immunodominance in HIV-1 Infection. *Journal of immunology (Baltimore, Md. : 1950)* **194**, 5329-5345, doi:10.4049/jimmunol.1400854 (2015).

35   Moosa, Y. *et al.* Case report: mechanisms of HIV elite control in two African women. *BMC infectious diseases* **18**, 54, doi:10.1186/s12879-018-2961-8 (2018).

36   Koofhethile, C. K. *et al.* CD8+ T cell breadth and ex vivo virus inhibition capacity distinguish between viremic controllers with and without protective HLA class I alleles. *J Virol*, doi:10.1128/JVI.00276-16 (2016).

37   Sette, A. & Sidney, J. Nine major HLA class I supertypes account for the vast preponderance of HLA-A and -B polymorphism. *Immunogenetics* **50**, 201-212 (1999).

38   Sidney, J., Peters, B., Frahm, N., Brander, C. & Sette, A. HLA class I supertypes: a revised and updated classification. *BMC Immunol* **9**, 1, doi:10.1186/1471-2172-9-1 (2008).

39   Goulder, P. J. *et al.* Differential narrow focusing of immunodominant human immunodeficiency virus gag-specific cytotoxic T-lymphocyte responses in infected African and caucasoid adults and children. *J Virol* **74**, 5679-5690. (2000).

40   Leslie, A. *et al.* Differential selection pressure exerted on HIV by CTL targeting identical epitopes but restricted by distinct HLA alleles from the same HLA supertype. *Journal of immunology (Baltimore, Md. : 1950)* **177**, 4699-4708 (2006).

41   Geldmacher, C. *et al.* Minor viral and host genetic polymorphisms can dramatically impact the biologic outcome of an epitope-specific CD8 T-cell response. *Blood* **114**, 1553-1562, doi:10.1182/blood-2009-02-206193 (2009).

42   Kloverpris, H. N. *et al.* HIV control through a single nucleotide on the HLA-B locus. *J Virol* **86**, 11493-11500, doi:10.1128/JVI.01020-12 (2012).

43   Geldmacher, C. *et al.* CD8 T-cell recognition of multiple epitopes within specific Gag regions is associated with maintenance of a low steady-state viremia in human immunodeficiency virus type 1-seropositive patients. *J Virol* **81**, 2440-2448, doi:10.1128/JVI.01847-06 (2007).

44   Ntale, R. S. *et al.* Temporal association of HLA-B*81:01- and HLA-B*39:10-mediated HIV-1 p24 sequence evolution with disease progression. *J Virol* **86**, 12013-12024, doi:10.1128/JVI.00539-12 (2012).

45   Wright, J. K. *et al.* Impact of HLA-B*81-associated mutations in HIV-1 Gag on viral replication capacity. *J Virol* **86**, 3193-3199, doi:10.1128/JVI.06682-11 (2012).

46   Kloverpris, H. N. *et al.* A molecular switch in immunodominant HIV-1-specific CD8 T-cell epitopes shapes differential HLA-restricted escape. *Retrovirology* **12**, 20, doi:10.1186/s12977-015-0149-5 (2015).

47   Bunce, M. PCR-sequence-specific primer typing of HLA class I and class II alleles. *Methods in molecular biology (Clifton, N.J.)* **210**, 143-171 (2003).

48   Thobakgale, C. F. *et al.* Human immunodeficiency virus-specific CD8+ T-cell activity is detectable from birth in the majority of in utero-infected infants. *Journal of virology* **81**, 12775-12784, doi:10.1128/jvi.00624-07 (2007).

49   Bernal-Estevez, D., Sanchez, R., Tejada, R. E. & Parra-Lopez, C. Chemotherapy and radiation therapy elicits tumor specific T cell responses in a breast cancer patient. *BMC cancer* **16**, 591, doi:10.1186/s12885-016-2625-2 (2016).

50   Han, A., Glanville, J., Hansmann, L. & Davis, M. M. Linking T-cell receptor sequence to functional phenotype at the single-cell level. *Nature biotechnology* **32**, 684-692, doi:10.1038/nbt.2938 (2014).

51   Anmole, G. *et al.* A robust and scalable TCR-based reporter cell assay to measure HIV-1 Nef-mediated T cell immune evasion. *Journal of immunological methods* **426**, 104-113, doi:10.1016/j.jim.2015.08.010 (2015).

52   Brockman, M. A., Tanzi, G. O., Walker, B. D. & Allen, T. M. Use of a novel GFP reporter cell line to examine replication capacity of CXCR4- and CCR5-tropic HIV-1 by flow cytometry. *Journal of virological methods* **131**, 134-142, doi:10.1016/j.jviromet.2005.08.003 (2006).

53   Suzuki, R. & Shimodaira, H. Pvclust: an R package for assessing the uncertainty in hierarchical clustering. *Bioinformatics* **22**, 1540-1542, doi:10.1093/bioinformatics/btl117 (2006).

54   Leslie, A. *et al.* Additive contribution of HLA class I alleles in the immune control of HIV-1 infection. *Journal of virology* **84**, 9879-9888, doi:10.1128/jvi.00320-10 (2010).

55   Prentice, H. A. *et al.* HLA-B*57 versus HLA-B*81 in HIV-1 infection: slow and steady wins the race? *Journal of virology* **87**, 4043-4051, doi:10.1128/jvi.03302-12 (2013).

56   Goulder, P. J. *et al.* Evolution and transmission of stable CTL escape mutations in HIV infection. *Nature* **412**, 334-338, doi:10.1038/35085576 (2001).

57   Goulder, P. J. *et al.* Late escape from an immunodominant cytotoxic T-lymphocyte response associated with progression to AIDS. *Nature medicine* **3**, 212-217 (1997).

58   Pereyra, F. *et al.* HIV control is mediated in part by CD8+ T-cell targeting of specific epitopes. *Journal of virology* **88**, 12937-12948, doi:10.1128/jvi.01004-14 (2014).

59   Threlkeld, S. C. *et al.* Degenerate and promiscuous recognition by CTL of peptides presented by the MHC class I A3-like superfamily: implications for vaccine development. *Journal of immunology* **159**, 1648-1657 (1997).

60   Allen, T. M. *et al.* De novo generation of escape variant-specific CD8+ T-cell responses following cytotoxic T-lymphocyte escape in chronic human immunodeficiency virus type 1 infection. *Journal of virology* **79**, 12952-12960, doi:10.1128/jvi.79.20.12952-12960.2005 (2005).

61   Ueno, T., Idegami, Y., Motozono, C., Oka, S. & Takiguchi, M. Altering effects of antigenic variations in HIV-1 on antiviral effectiveness of HIV-specific CTLs. *Journal of immunology (Baltimore, Md. : 1950)* **178**, 5513-5523 (2007).

62   Almeida, J. R. *et al.* Antigen sensitivity is a major determinant of CD8+ T-cell polyfunctionality and HIV-suppressive activity. *Blood* **113**, 6351-6360, doi:10.1182/blood-2009-02-206557 (2009).

63   Akahoshi, T. *et al.* Selection and accumulation of an HIV-1 escape mutant by three types of HIV-1-specific cytotoxic T lymphocytes recognizing wild-type and/or escape mutant epitopes. *Journal of virology* **86**, 1971-1981, doi:10.1128/jvi.06470-11 (2012).

64   Gillespie, G. M. *et al.* Cross-reactive cytotoxic T lymphocytes against a HIV-1 p24 epitope in slow progressors with B*57. *AIDS* **16**, 961-972 (2002).

65   Sunshine, J. E. *et al.* Fitness-Balanced Escape Determines Resolution of Dynamic Founder Virus Escape Processes in HIV-1 Infection. *J Virol* **89**, 10303-10318, doi:10.1128/JVI.01876-15 (2015).

66   Henn, M. R. *et al.* Whole genome deep sequencing of HIV-1 reveals the impact of early minor variants upon immune recognition during acute infection. *PLoS Pathog* **8**, e1002529, doi:10.1371/journal.ppat.1002529 (2012).

67   Borbulevych, O. Y. *et al.* T cell receptor cross-reactivity directed by antigen-dependent tuning of peptide-MHC molecular flexibility. *Immunity* **31**, 885-896, doi:10.1016/j.immuni.2009.11.003 (2009).

68   Willcox, B. E. *et al.* TCR binding to peptide-MHC stabilizes a flexible recognition interface. *Immunity* **10**, 357-365 (1999).

69   Armstrong, K. M., Piepenbrink, K. H. & Baker, B. M. Conformational changes and flexibility in T-cell receptor recognition of peptide-MHC complexes. *Biochemistry Journal* **415**, 183-196, doi:10.1042/BJ20080850 (2008).

70   Miles, J. J., McCluskey, J., Rossjohn, J. & Gras, S. Understanding the complexity and malleability of T-cell recognition. *Immunology and cell biology* **93**, 433-441, doi:10.1038/icb.2014.112 (2015).

CHAPTER 3

Aim: Investigate the molecular mechanisms governing the expression of CXCR5 on CD8⁺ T cells isolated from lymphoid tissues of HIV-1 infected individuals.

Chapter 3 Overview

In chapter 2, we identified CD8⁺ T cell subsets in peripheral blood with diverse antigen-specific repertoires, and the potential to cross-recognize HIV-1 epitope variants. Even though these CD8⁺ T cells have a higher capability to control viral replication *in vivo*, their effect could be greatly enhanced if they efficiently accessed the micro-anatomical sites of HIV-1 replication, especially the B-cell follicles where HIV-1 replication persists even during highly active antiretroviral therapy (HAART). Indeed, animal studies have identified a unique subset of CD8⁺ T cells termed follicular CD8⁺ T cells (fCD8s) based on the expression of follicular homing marker CXCR5, and have demonstrated that fCD8s have the capacity to selectively enter B cell follicles and eradicate HIV-1 infected cells. In these studies, they identified a network of transcriptional factors that regulates the expression of CXCR5 on CD8⁺ T cells, but it is not clear if similar or additional regulatory elements are involved in regulating CXCR5 in human CD8⁺ T cells. In chapter 3 of this thesis, we describe the molecular regulation of CXCR5 in human CD8⁺ T cells. We showed that CXCR5 expression in human CD8⁺ T cells isolated from the lymphoid tissues of HIV-1 infected individuals is tightly regulated by distinct epigenetic and transcriptional mechanisms. We reported epigenetic and transcriptional targets that can be used to manipulate human CD8⁺ T cells to express

CXCR5 and infiltrate B cell follicles to clear viral reservoirs. This manuscript is under review by the co-authors.

CHAPTER 3: *CXCR5* gene expression in Human CD8^{+} T cells is regulated by DNA methylation and nucleosomal occupancy

Funsho J. Ogunshola[a,c], Werner Smidt[a,d], Anneta F. Naidoo[f], Thandeka Nkosi[a,c], Thandekile Ngubane[e], Trevor Khaba[c], Omolara O. Baiyegunhi[a,c], Sam Rasehlo[a], Ismail Jajbhay[e], Krista L. Dong[b], Veron Ramsuran[d], Johan Pansegrouw[e], Thumbi Ndung'u[a,c,g], Bruce D. Walker[b,c], Tulio Oliveria[d] and Zaza M. Ndhlovu[a,b,c*].

[a]Africa Health Research Institute (AHRI), Durban, South Africa.

[b]Ragon Institute of Massachusetts General Hospital, Massachusetts Institute of Technology, and Harvard University, Cambridge, MA, USA.

[c]HIV Pathogenesis Programme, Doris Duke Medical Research Institute, Nelson R. Mandela School of Medicine, University of KwaZulu-Natal, Durban, South Africa.

[d]KwaZulu-Natal Research Innovation and Sequencing Platform (KRISP), University of KwaZulu-Natal, Durban, South Africa.

[e]Prince Mshiyeni Memorial Hospital, Durban, South Africa

[f]HIV Vaccine Trial Network (HVTN), Cape Town, South Africa.

[g]Max Planck Institute for Infection Biology, Berlin, Germany.

*Corresponding author; Zaza Mtine Ndhlovu

zndhlovu@mgh.harvard.edu

3.1 Abstract

CD8$^+$ T cells located in B cell follicles play an important role in viral and tumor control. However, in human lymph nodes (LN), only a small subset of CD8$^+$ T cells called follicular CD8$^+$ T cells (fCD8s) express CXCR5, the chemokine receptor required for cell migration into B cell follicles. We investigated why most lymph node CD8$^+$ T cells (non-fCD8s) do not express CXCR5, and why there is reduced CXCR5 expression in fCD8s relative to Germinal centre T follicular helper cells (GCTfh). Our results show that DNA hypermethylation and closed chromatin at the transcriptional start site (*TSS*) prevent CXCR5 expression in non-fCD8s. We also found that greater nucleosomal density at the *CXCR5 TSS* is responsible for reduced CXCR5 expression in fCD8s relative to GCTfh. Together, these data provide critical insights into both the underlying molecular mechanisms that repress CXCR5 in non-fCD8s and the mechanisms responsible for the low CXCR5 expression in fCD8s, with implications for HIV cure strategy or eradication of B cell-derived tumors.

3.2   Introduction

Secondary lymphoid tissues (SLT) are the major site of human immunodeficiency virus (HIV) replication [1-3]. Germinal center follicular CD4$^+$ T cells (GCTfh) in the B cell follicles serve as major targets of infection [4-6]. The partial exclusion of the CD8$^+$ T cells from B cell follicles within lymph nodes (LN) [7,8] is thought to be partly responsible for HIV persistence in this compartment, particularly during suppressive antiretroviral therapy (ART) [9,10]. A recently described CXCR5 expressing CD8$^+$ T cell subset called fCD8 can infiltrate B cell follicles and eliminate HIV infected cells or tumor cells[11-13]. Human and animal studies have shown that the frequency of fCD8s inversely correlates with HIV or SIV viral load [11,14,15], suggesting that increased infiltration of fCD8s in B cell follicles can result in viral clearance. Detailed understanding of the mechanisms that govern the expression of CXCR5 in human CD8$^+$ T cells during differentiation can lead to the discovery of novel strategies for boosting fCD8s frequency in B cell follicles, required to suppress HIV replication or eliminate tumor cells.

Upon infection, viral antigens prime naïve CD8$^+$ T cells in the SLT to differentiate into effector cells and migrate to the site of infection, guided by chemokine-chemokine receptor interactions [16]. In the case of HIV infection, HIV-specific CD8$^+$ T cells need to be redirected to the B cell follicles. CXCR5 direct trafficking of CD8$^+$ T cells to LN germinal centers (GCs) where CXCL13 producing cells reside [17-19]. Paradoxically, only a proportion of HIV-specific cells differentiate into fCD8s and migrate to B cell follicles [14]. Molecular mechanisms that regulate the expression of CXCR5 in CD8$^+$ T cells during differentiation are poorly understood. Animal studies have attempted to define the transcriptional regulatory network that differentiate fCD8s from non-fCD8s. They

show that Blimp1 and BCL6 coupled with TCF1, Id2 and Id3 form a transcriptional circuit that govern fCD8 differentiation [11,20]. Additionally, an *in vitro* study in rhesus macaques showed that CD8^{+} T cell stimulation with inflammatory cytokines such as TGF-β, IL-12 and IL-23 promotes fCD8 differentiation [21], but the underlying molecular processes that govern fCD8 differentiation remain largely unknown. Moreover, most of what is currently known about fCD8 differentiation is derived from animal studies, such that the direct relevance to human diseases has not yet been fully established.

Here, we investigated how fCD8s are generated in the setting of HIV infection. We posit that epigenetic mechanisms are involved in regulation of CXCR5 in human CD8^{+} T cells. Epigenetic mechanisms such as DNA methylation can influence gene expression by affecting the binding affinity of transcriptional factors (TFs) [22]. This is evident in the enrichment for binding sites of effector-associated TFs within the demethylated regions of effector CD8^{+} T cells [23]. In addition, regulation of gene expression requires binding of TFs at specific regulatory loci, which is affected by chromatin state and accessibility [24,25]. Furthermore, the density and positioning of nucleosomes around the genomic DNA can regulate the levels of gene expression by modulating DNA accessibility to TFs [26].

Therefore, in this study we used DNA bisulphite sequencing in combination with the Assay for Transposase-Accessible Chromatin using Sequencing (ATAC-Seq) and RNA-Seq to define the epigenetic mechanisms underpinning *CXCR5* gene regulation in human CD8^{+} T cells. We found that the *CXCR5* gene was highly methylated around the transcription start site (*TSS*) in non-fCD8s. Treatment of non-fCD8s with a methyltransferase inhibitor (5-aza-2'-deoxycytidine) resulted in increased expression of CXCR5 mRNA transcripts, directly implicating DNA methylation in *CXCR5* gene

repression. Additionally, closed chromatin conformation was observed at the *TSS* of the *CXCR5* gene in non-fCD8s but not in fCD8s and GCTfh, signifying that there are addition epigenetic regulatory mechanism involved in *CXCR5* gene expression. Furthermore, we also investigated why CXCR5 expressing CD8$^+$ T cells (fCD8s) generally express less CXCR5 compared to GCTfh and GC B cells, which is thought to limit their migration into the interior of the B cell follicle. Computational analysis revealed a potential difference of both nucleosomal occupancy and positioning around the *TSS* of the *CXCR5* gene in fCD8s relative to GCTfh. This result suggests that fCD8s have high occupancy of nucleosomes around the *TSS,* which interfere with transcriptional efficiency leading to reduced CXCR5 mRNA levels. Together, these data demonstrate that *CXCR5* gene expression in human CD8$^+$ T cells is tightly regulated by multitiered processes involving DNA methylation, chromatin accessibility and nucleosomal occupancy. Importantly, our study describes potential mechanisms leading to the expression of CXCR5 in human CD8$^+$ T cells. This knowledge will be useful for targeted manipulation of CD8$^+$ T cells to induce and augment the expression of CXCR5 required to attract CD8$^+$ T cells into B cell follicles where they are needed to clear infections such as HIV and B-cell derived tumors.

3.3   Materials and Methods

3.3.1 Human samples

Fresh human inguinal lymph nodes (LNs) were obtained for research purposes from the Prince Memorial Mshiyeni Hospital, Umlazi township, Durban, South Africa. Most

of the LNs were from adults. Age, sex, treatment status and clinical parameters such as viral load and CD4 counts of the study participants are summarized in Table 1. A section of the excised LN was sliced and processed for tissue staining and the remaining section was meshed to isolate lymph node mononuclear cells (LNMCs). LNs were homogenized using a syringe plunger and passed through a cell strainer (BD, Biosciences Germany) to make a single-cell suspension. Mononuclear cells were isolated using RPMI medium (Sigma-Aldrich, St. Louis, MO) containing 10% heat-inactivated fetal calf serum (R10 medium). Extracted LNMCs were frozen for downstream experiments. All protocols were approved by the Biomedical Research Ethics Committee of the University of KwaZulu-Natal and the Massachusetts General Hospital Ethics committee.

3.3.2 Flow cytometry and cell sorting

For phenotypic characterization, cells were surface stained with cell-viability dye (Fixable Blue dead cell stain kit, Invitrogen), followed by anti-CD3-BV711 (Biolegend), anti-CD4-BV650 (BD Biosciences), anti-CD8-BV786 (BD Biosciences), anti-PD-1-BV421 (Biolegend), anti-CXCR5-AF488 (BD Biosciences), anti-CD45RA-A700 (Biolegend), anti-CCR7-PerCPcy5.5 (Biolegend). HIV-specific tetramers used in this study were conjugated to either PE or APC fluorochrome.

All cells were sorted for ATC-Seq and RNA-Seq using a BD FACSAria. Gating strategies for sorted subsets were as follows: fCD8; $CD3^+CD4^-CD8^+CD45RA^-CXCR5^+$, non-fCD8; $CD3^+CD4^-CD8^+CD45RA^-CXCR5^-$, Naïve $CD8^+$ T cells; $CD3^+CD4^-CD8^+CD45RA^+CCR7^+$, Tfh; $CD3^+CD4^+CD8^-PD-1^{high}CXCR5^{high}$. For RNA-Seq, cell subsets were sorted in RLT buffer (Qiangen, Invitrogen) containing 1% Beta-

mercaptoethanol. For ATAC-Seq, cell subsets were sorted in PBS containing 2% FCS for downstream processing.

3.3.3 Immunofluorescence staining

Localization of CD8^{+} T cell subsets was assessed as described by Banga et al., 2016 [5]. Briefly, slides were prepared from 4 µm sections of paraffin-embedded tissue blocks and immunostained using in-house optimized protocols. For each LN, serial sections were stained singly with antibodies against BCL6 and CD8 and a DAB DAB visualization kit (Envision Double Stain system, Dako; USA) for bright field microscopy. Alternatively, we used the Opal 4-Color Fluorescent IHC Kit (PerkinElmer, USA) for immunofluorescence microscopy light. Slides were mounted and viewed using the Axio observer and TissueFAXS imaging software (TissueGnostics). Quantitative imaging analysis was conducted with TissueQuest (TissueGnostics). Medians of the cell density in the scanned germinal centers were used to perform statistical analysis.

3.3.4 DNA methylation and drug treatment assays

Specific CpG within the *CXCR5* gene region was measured for DNA methylation according to a protocol from Paulin et al., 1998 [27]. Briefly, a minimum of 500ng of genomic DNA was bisulfide treated and amplified using a primer designed to cover 500bp around the *TSS*. Amplified product was then analysed using Agena MassArray platform.

Drug treatment was then performed on the same samples used for DNA methylation assay. Briefly, an average of 10,000 non-fCD8s was sorted from the lymph node tissues and treated with 10μM of 5'-aza-2-deoxycytidine; a drug that inhibits the activity of methyl-transferases genome-wide drugs for 24hrs. Thereafter, cells were washed, lysed and RNA were extracted and purified. cDNA was generated from the purified RNA using (BioRAD). CXCR5 mRNA transcripts were then measured from the generated cDNA using digital droplet PCR (ddPCR).

3.3.5 Chemotaxis assay

Chemotaxis assay were performed as previously described by Allen et al., 2004 [28]. Briefly, LNMCs were suspended at a density of 1×10^6 in RPMI 1640 medium containing L-glutamine, antibiotics, 10 mM HEPES buffer and 0.5% fatty acid-free BSA. Cells were re-sensitized for 30-60 min at 37 ^{0}C before being plated in trans-well inserts with a pore size of 5 um and a diameter of 6.5 mm in 24-well plates (Corning Costar). 100ul cells (1×10^6) were added to the upper wells and 580 ul diluted CXCL-13 chemokine (Peprotech) at 50 ng/ml was placed in the bottom wells, and plates were incubated for 3 hours at 37 ^{0}C in 5% CO_2. Migrated cells were stained with viability dye, CD3, CD4, CD8, CXCR5 and PD-1 and counted using flow cytometry.

3.3.6 Assay for Transposase-Accessible Chromatin

Library preparations were performed as described by (Buenrostro et al., 2013). Briefly, an average of 20,000 cells was sorted from lymph node for GCTfh, Naïve CD8$^+$ T cells, CXCR5$^+$CD8$^+$ T cells and CXCR5$^-$CD8$^+$ T cells. Five biological replicates were

sorted for each subset. Sorted cells were lysed using lysis buffer (10mM Tris-HCL, pH 7.4, 10mM NaCl, 3mM MgCl$_2$, 0.1% IGEPAL CA-630). Lysed cells were treated with 2.5ul of Tn5 Transposase (Illumina, San Diego, CA) suspended in 50ul of 1X TD buffer for 30 minutes at 37°C. Thereafter, transposed DNA was purified using QiaQuick MiniElute columns (Qiagen, Valencia, CA). Purified transposed DNA was amplified by PCR using Nextera barcoded primers (Illumina, San Diego, CA) and NEBNext High-Fidelity 2X PCR Master mix (New England Biolabs) with 12 cycles. Barcoded amplified libraries were purified using QiaQuick MiniElute columns (Qiagen, Valencia, CA) and quantified with Kapa real-time library quantification kit (Kapa, Wilmington, Massachusetts). Paired-end sequencing was performed using high throughput NextSeq 550 (Illumina, San Diego, CA). Raw data from sequencer were stored in an on-onsite database and is available on request.

3.3.7 RNA-Sequencing

An average of 20,000 cells were sorted directly into lysis (RLT) buffer (Qiagen, Valencia, CA) for RNA-Seq. Subsets that were sorted are: GCTfh, Naïve CD8$^+$ T cells, CXCR5$^+$CD8$^+$ T cells and CXCR5$^-$CD8$^+$ T cells. Five biological replicates were used to perform this experiment. Total RNA was isolated from lysed cells using Qiagen RNeasy Mini columns (Qiagen, Valencia, CA) according to the manufacturer's instructions. Purified RNA was evaluated with BioAnalyzer RNA pico kit (Agilent Technologies Inc, Santa Clara, CA). Messenger RNA (mRNA) was isolated from total RNA using NEBNext oligo dT beads (New England Biolabs). Isolated mRNA was fragmented and thereafter reverse transcribed to cDNA using NEBNext ultra RNA library preparation kit (New England Biolabs). The cDNA products were purified using

AmpureXP beads (Beckman Coulter, Danvers, MA) and indexed using NEBNext multiplex oligo (New England Biolabs). Size distribution was evaluated using Agilent high-sensitivity DNA chip and initial quantification was performed using Qubit dsDNA high sensitive kit (ThermoFisher Scientist, Waltham, MA) and the median obtained on the Tapestation (Agilent Technologies Inc). KAPA kit was used for final quantification of obtained cDNA libraries molarity for sequencing. Index libraries were pooled and sequenced using high throughput NextSeq 550 (Illumina, San Diego, CA). Raw data from sequencer was stored in an on-onsite database and is available on request.

3.3.8 Statistical analysis

Statistical analyses were conducted using Prism software, version 6.0 (GraphPad, Inc.). Two-tailed tests were employed, and p-values less than 0.05 were considered to be significant. Other analysis on the next generation sequencing data is described in the Bioinformatics analysis below.

3.3.9 Assay for Transposase-Accessible Chromatin analysis

To detect open chromatin regions (OCR), ATAC-seq Illumina reads were first filtered and trimmed for quality using TrimGalore and passed through the Kundaje lab pipeline [29] that performed the necessary quality controls (filtering of duplicate reads, removing reads mapping to the mitochondria) and peak detection together with irreproducible discovery rate (IDR) analysis using the biological replicates for each cell type. A cutoff of 0.1 was chosen for IDR. An optimal set of peaks that was produced for each cell type by the Kundaje pipeline was used for downstream analysis. OCR regions were

compared between cell types using the DiffBind and EdgeR [30]. A cut-off of 0.05 was chosen for FDR. We calculated the differential OCR using only the cell subsets as contrasts and subsequently paired the samples according to the patient from which the cells were extracted. The second method proved to be more sensitive at the same FDR of 0.05. Principal component analysis (PCA) was performed using the top 1000 OCR by variance. The same sites were also used to construct a heatmap using the dba.heatMap function. Peak regions were annotated with the annotatePeak function from the ChIPseeker package [31]. Annotations further than 50kb upstream from the *TSS* or those 10kb beyond the 3'-end of the gene were excluded. Gene ontology (GO) term enrichment was calculated with the enrichGO function from clusterProfiler [31].

3.3.10 RNA-Sequencing analysis

RNA-Seq short reads were quantified using Kallisto (Bray et al., 2016). The Ensembl version 85 (GRCh37) was used as a transcriptome reference. Options were included to correct for "GC bias" and bootstrap sampling of 100. The Sleuth R package was used for downstream quantification and differential expression analysis [32]. Gene transcripts were aggregated to gene level using internal sleuth functions. Due to the natural variation of expression data between subjects, when doing pairwise comparisons (e.g. fCD8 vs non-fCD8), the design matrix was constructed in a way that would take this effect into account. Thus, the reduced design formula took the shape of *~pid*, while the full model *~ pid + condition*, where pid refers to the patient id and condition refers to the cell type. The likelihood ratio test of Sleuth was used to determine differential expression of genes by determining whether the *condition* variable added significant contribution in explaining the count data. The beta statistic

obtained from the Wald test was used as a proxy for log-fold differences in gene expression between conditions. For visualization purposes, the batch effects introduced by individual patients were removed using the remove Batch Effects function of the R package limma. Functional enrichment was determined using both the enrichGO and gseGO functions of the clusterProfiler package.

3.3.11 Transcription factor footprinting and enrichment

Wellington-bootstrap was used for footprint detection [33]. To increase sensitivity of footprint prediction, aligned reads in the form of BAM files were merged for each cell type: fCD8, non-fCD8, Naive CD8+T cells, GCTfh. For the HIV-Specific cell sets, reads were not merged to determine HIV-Specific footprinting sets. Predicted footprints were extended by 5 bp at each end and TF matching was performed using RGT [34]. We used both the HOCOMOCO [35] and JASPAR [36] databases to complement mutually exclusive transcription factors from each set, e.g. *Id2* is not included in JASPAR, but is included in HOCOMOCO. Predicted footprints were filtered if they were more than 50 kilobases upstream from the transcription start site. Transcription factors that did not have evidence of expression from the RNA-Seq data were also filtered. We determined TF enrichment by comparing the frequency of predicted TF motifs in footprints compared to a background random set generated by RGT using a Fisher exact test. FDR values were determined using the R package *qvalue* [37] and a cut-off of 0.01 was used to filter out non-significant hits. We contrasted subjects for differential enrichment of TF motifs detected within the predicted footprints. Furthermore, we used the Wellington Bootstrap method [38] to detect differential footprints that can indicate higher activity of a transcription factor at different footprint loci. Differential footprints were chosen on

the criteria of having a score >8 as produced by the *wellington_bootstrap.py* script or if a footprint was exclusively detected in a condition.

We calculated the differentially enriched TF motifs between all the cell types, i.e. fCD8, non-fCD8, Naive CD8+ T cells, GCTfh and each of the HIV-Specific sets, yielding 27 comparisons. For the fCD8 and non-fCD8 subsets, we compared the enrichment of TF footprints between up and down regulated genes. This was done for both the predicted footprints from the whole set as well as the footprints demonstrating differential signal produced by Wellington bootstrap. For the Wellington bootstrap, relative frequencies of TF motifs were calculated. We then clustered these relative frequencies and displayed them as a heatmap.

Plots for the footprints were generated based on the average Tn5 insertion sites 200bp around the predicted footprinting sites. Because Tn5 does have cleavage bias, the counts were corrected using the *tracks* module of the RGT-HINT package. Additional plots were generated for differential footprints.

3.3.12 Weighted correlation network analysis

We tested the modularity of gene expression using weighted correlation network analysis (WGCNA) [39]. For the RNA-Seq data, raw count data was first regularized with the variance stabilizing transformation (vst) function from DESeq2 [40]. Network construction with WGCNA was done with CEMiTool [41]. CEMiTool, by default, filters out the majority of input expression data to reduce complexity and noise. We augmented this set with additional genes that were predicted to be differentially expressed between fCD8 and non-fCD8 and were filtered out by CEMiTool. We next

performed an enrichment analysis on each subset (fCD8, non-fCD8, Naive CD8^{+} T cells, GCTfh and HIV-Specific samples). Module enrichment per condition was performed and visualized. In particular, we wanted to investigate in which subsets the module containing *CXCR5* was enriched or diminished.

To determine whether there are modules of OCR specific to expressed genes, a WGCNA network for the OCR regions from the ATAC-Seq data was also constructed. We used the read counts from the merged peaks calculated by DiffBind as input and also regularized the input with variance stabilizing transformation. We imagined that while OCR in and around genes would be largely correlated, certain OCRs may be in different modules depending on the subset/cell condition. To test this, we assigned all the OCRs to modules and then used the OCR annotation as a gene reference. We then specifically looked at genes that are differentially expressed in fCD8 and GCTfh compared to non-fCD8 and cross-referenced this with the ATAC-Seq WGCNA network modules. We then determined which modules are enriched or diminished in the different subsets. Next, we intersected differentially expressed genes with their respective ATAC-Seq modules fCD8 and GCTfh and filtered by modules that are enriched in either. Finally, we compared the ATAC-Seq modules specific to fCD8 and GCTfh.

3.3.13 Transcriptional network profiling

We used the results from the differential footprinting to determine which transcription factors either increase or decrease expression in fCD8 and non-fCD8. A network was constructed by linking TF closer than 50kb to the promoter region of the top differentially expressed genes. We focused on genes specific to the modules for

CXCR5 and CXCL13 (*CXCR5* chemokine attractant) that were differentially expressed.

3.3.14 Nucleosomal positioning

NucleoATAC [42] was used to predict nucleosome occupancy and position from the ATAC-Seq data. For each subset, MACS 2 was used with the *--broadPeak* option to localize regions for nucleosomal detection. These regions were further expanded by 200bp on either end. To improve signal, samples reads were merged within each subset.

To investigate differences in nucleosomal positioning within the promoter region of *CXCR5* between GCTfh and fCD8, the region matching the promoter of *TSS* was successively trimmed from the 3' end. With each successive trim, NucleoATAC was again run on that region to calculate nucleosomal occupancy signals and positions. The idea is that this trimming will bias the removed shorter reads and reveal temporal positioning of the nucleosome. Importantly, the fragment size distribution files and V-matrix files produced from the full peakset was used as input to eliminate fragment distribution bias, produce a BED file containing these overlapping regions. The smoothed signal was plotted and the combined position file was used for dyad positioning of the nucleosome.

3.4 Results

3.4.1 Phenotypic characterization of fCD8s in HIV infected subjects

Studies have demonstrated the potential role of fCD8s in clearing viral reservoirs and tumor cells in immune sanctuary sites such as B cell follicles [11-13]. More recently, fCD8s have also been described as tissue resident CD8$^+$ T cells [43]. To assess whether CD8$^+$ T cells that have a follicular-homing phenotype CXCR5$^+$CD45RA$^-$CD8$^+$ T cells (fCD8s) were indeed localized in the lymphoid tissues during HIV infection, we first used flow cytometry to measure the frequency of fCD8s in lymph node (LN) and in peripheral blood (PB) during HIV infection. Consistent with a recent study [43], we observed significantly higher frequency of fCD8s in LN compared to PB ($p < 0.0001$) (Fig. 3.1A).

We next assessed the localization of fCD8s within the LN using multicolour immunofluorescence analysis, a technique that simultaneously permits quantitative assessment of cellular phenotype and positioning in tissues [44]. We identified fCD8 as CXCR5$^+$CD8$^+$ and active germinal centers (GCs) were BCL6$^+$ region within the B cell follicles. Our imaging confirmed that fCD8s were preferentially localized in the GCs compared to non-GC regions (Fig. 3.1B). Notably, we observed a significant positive correlation between the density of fCD8 localized in GCs and the frequency of fCD8s measured by flowcytometry ($r = 0.87$, $p = 0.02$) (Fig. 3.1C), consistent with the notion that CXCR5$^+$CD8$^+$(fCD8s) localization in GCs.

Previous studies have shown that antigen-specific fCD8s expand during persistent viral infection in mice and humans [11,20]. Therefore, we evaluated the effect of HIV infection and treatment status on the induction of fCD8s in LNs obtained at least one year after treatment initiation in 12 early treated, 10 late treated and 6 untreated groups. The clinical characteristics of the study participants are summarized in Table 3.1. We observed a significant increase in the frequency of fCD8s in late treated (p=0.01) and untreated donors (p=0.02) compared to uninfected donors (Fig. 3.1D). However, no difference was observed between early treated and HIV negative donors (p=0.92) (Fig. 3.1D), suggesting that the HIV antigen load or inflammation [45] drives the differentiation of fCD8s during HIV infection.

Table 3.1: Demographic and clinical characteristics of the study participants

Participants	HIV-Negative	Early treated	Late treated	Untreated
n	9	12	10	6
Female n (%)	9 (100%)	12 (100%)	10 (100%)	5 (83.3%)
Age	21 (20.5-22)[a]	21 (19-22)[a]	26 (23-36)[a]	22 (18-26)[a]
CD4 counts, cells/mm^3	N/A	772 (657.5-833.5)[a]	667 (401-1189)[a]	436 (355-718)[a]
Viral load RNA copies/ml	N/A	<20	5343 (20-15000)[a]	15068 (1200-23000)[a]
Time post treatment to LN excision (weeks)	N/A	89 (52-179)[a]	98 (64-249)[a]	>1year

[a] Values expressed as median (interquartile range)
N/A means not applicable
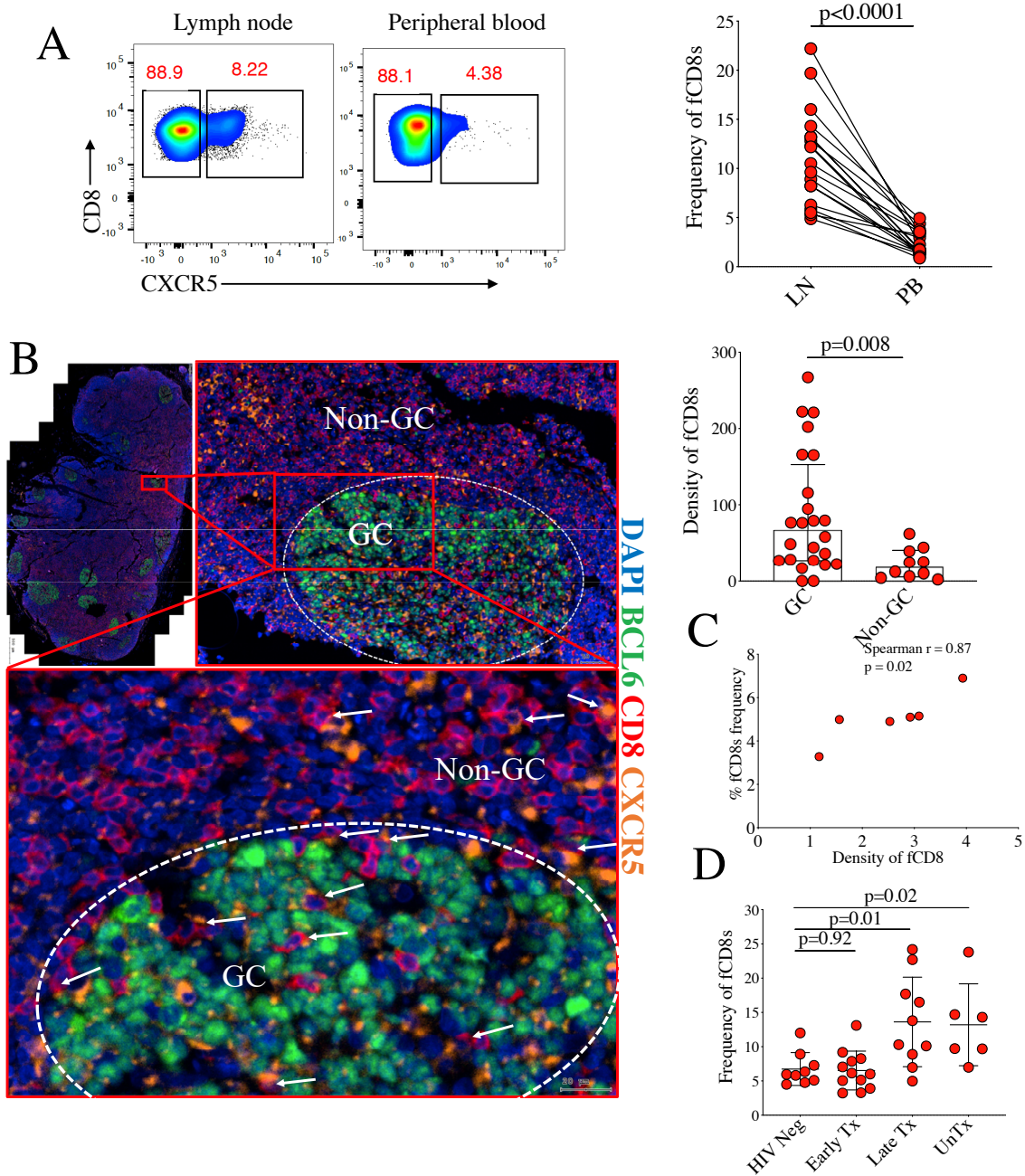
Figure 3.1: Phenotypic characterization of fCD8s during HIV-1 infection

(A) Paired comparative analysis of the frequency of fCD8s in lymph node (LN) and peripheral blood (PB) of HIV-1 infected individuals indicated significant increase of fCD8s in the LN compared to PB. (B) Tissue imaging showing the density of fCD8s infiltrating the germinal centre (GC) and statistical analysis showing significant

increase in the fCD8s localized in the GCs compared to non-GCs. (C) Correlation analysis showing significant positive correlation between the frequency of fCD8s measured by flow with the density of fCD8s in GCs quantified by TissueQuest. (D) Flow plot showing the frequency of fCD8s in HIV-1 infected individuals initiating treatment at different time points and statistical analysis showing significant increase in late treated and untreated groups when compared to HIV-1 negative individuals.

3.4.2 Transcriptional and epigenetic factors are differentially expressed between fCD8s and GCTfh

Recent animal studies have defined the regulatory networks that govern the expression of CXCR5 in CD8^{+} T cells [11,12,20,21]. However, it is not clear if similar regulatory networks regulate CXCR5 expression in human CD8^{+} T cells. To address this question, we performed RNA-Seq on sorted cells from the excised LN of five HIV infected individuals. Study participants were selected based on HIV infection status, high frequency of fCD8s and sample availability. The following cell populations were FACs sorted from each individual based on the following phenotypic markers; bulk fCD8s (CD3^{+}CD8^{+}CD45RA^{-}*CXCR5*^{+}), non-fCD8s (CD3^{+}CD8^{+}CD45RA^{-}*CXCR5*^{-}), naïve CD8^{+} T cells (CD3^{+}CD8^{+}CD45RA^{+}CCR7^{+}), and GCTfh (CD3^{+}CD4^{+}*CXCR5*^{+}PD1^{high}) (supplementary Fig. 3.1). GCTfh served as the positive control condition because they constitutively express high levels of CXCR5, whereas naïve CD8^{+} T cells were the negative control condition because they do not express CXCR5. Principal component analysis of 5 biological replicates separated all experimental groups in two dimensional space based on quantification of mRNA transcripts (Fig. 3.2A). fCD8s and non-fCD8s had minimal separation, understandably

so, given the phenotypic similarities between the two subsets. Nonetheless, there were 1,095 transcripts (FDR<0.1) that were differentially expressed between the two populations, which are mostly likely involved in *CXCR5* gene regulation.

To identify the key genes involved in *CXCR5* gene regulation, we first analysed genes that have previously been implicated in CXCR5 regulatory circuitry in animal studies. We started by analysing BCL6 because it has been described as the master regulator of CXCR5 expression in GCTfh and murine fCD8s [11,12,20,25,46-48]. We found that BCL6 was highly expressed in GCTfh, consistent with previous findings (Fig. 3.2B). However, fCD8s expressed very low BCL6 relative to GCTfh (p<0.00001), with no significant difference between fCD8s and non-fCD8s (p=0.64) (Fig. 3.2B). To determine if BCL6 expression levels seen by RNA-Seq correlate with protein levels, we measured BCL6 expression by flow cytometry. BCL6 expression in CD8$^+$ T cells is significantly lower in fCD8s compared to expression in GCTfh (p<0.0001) (Fig. 3.2C). Together, these data suggest that BCL6 may not be critical for CXCR5 expression in human CD8$^+$ T cells.

Next, we investigated other genes that were shown to be similarly expressed between murine fCD8s and GCTfh [20]. We determined the expression of *Id3* and *TCF1* genes that were implicated in the transcriptional circuitry that positively regulates fCD8s differentiation in murine studies [11]. Interestingly, Id3 and TCF1 were significantly downregulated in human fCD8s relative to GCTfh (*Id3*: p<0.0001, *TCF1*: p<0.0001), with no apparent difference between fCD8s and non-fCD8s (*Id3*: p=0.50, *TCF1*: p=0.90) (Fig 3.2D). Similarly, negative regulator Id2 was significantly higher in fCD8s compared to GCTfh (Id2: p=0.0005) and PRDM1 was significantly higher in fCD8s compared to GCTfh (p=0.0197, Log-fold change 0.76) (Fig. 3.2D). Together, these

data suggest that an alternative transcriptional circuitry may be involved in the regulation of fCD8s differentiation in human CD8$^+$ T cells.

To gain further insight into the transcriptional mechanisms responsible for the *CXCR5* gene regulation in human CD8$^+$ T cells, we focused on differentially expressed genes between fCD8s and non-fCD8s in our RNA-Seq data. We identified 43 genes (FDR<0.1) of differentially expressed epigenetic factors between fCD8s and non-fCD8s [49]. Interestingly, epigenetic factors such as JADE2 and SETD7 that antagonize DNA and histone methylation and participate in chromatin remodelling [50-52], were among the most highly differentially expressed genes between fCD8s and non-fCD8s (Fig. 3.2E and extended data in supplementary Fig. 3.2). This analysis gave us a strong hint that epigenetic mechanisms were heavily involved in *CXCR5* gene regulation.
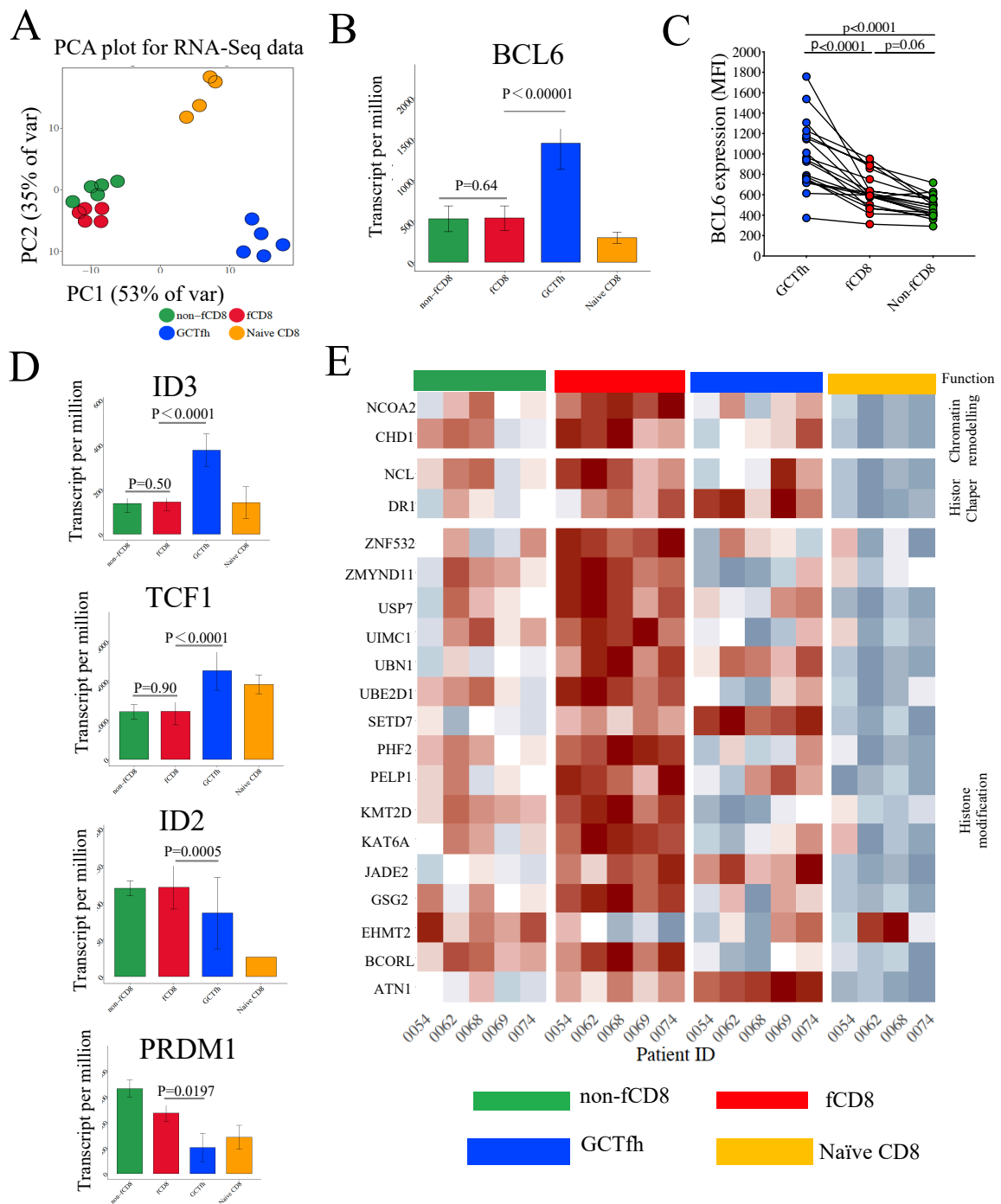
Figure 3.2: Differential expression of TF between fCD8s compared to GCTfh

(A) Principal component analysis of the RNA-Seq data from the four cell subsets, colour labeled according to cell subset. The top 500 genes by variance were used to construct the PCA plot. Clear separations are observed between most of the subsets,

with the fCD8s and non-fCD8s subsets showing closest proximity. (B) Statistical analysis showing significant increase of *BCL6* expression in GCTfh compared with fCD8s and non-fCD8s. (C) Statistical analysis showing mean fluorescence intensity (MFI) of BCL6 in GCTfh compared with fCD8s and non-fCD8s. (D) Expression values of CXCR5 regulating genes. Batch and patient corrected TPM values for genes previously shown to be involved in the regulation of CXCR5 expression. FDR values are obtained from the differential expression analysis using the sleuth package in the R statistical environment. (E) Ranked expression of selected epigenetic modifiers. Epigenetic modifiers were grouped according to functional attributes, i.e. chromatin remodeling, histone chaperone, histone modification and by Transcription activity. Genes were ranked from highest (red) to lowest (blue) expression. Each column represents the expression level for a particular patient and was labelled on the x-axis accordingly.

3.4.3 *CXCR5* gene is tightly regulated by DNA methylation and chromatin landscape in human CD8$^+$ T cells

Given that a large number of epigenetic regulation genes were among the most highly differentially expressed between fCD8s and non-fCD8s, we hypothesized that distinct epigenetic mechanisms such as DNA methylation and chromatin landscape regulate the expression of CXCR5 in human CD8$^+$ T cells. To test this hypothesis, we first investigated if DNA methylation was involved because it is the most common epigenetic regulatory mechanism [22,53]. We measured DNA methylation levels proximal to *CXCR5* gene using loci-specific bisulfite-treated sequencing of DNA samples extracted from the same cell populations used for RNA-Seq. This technology is

commonly used to detect DNA methylation at CpG sites within the genome regardless of chromatin structure [54-57]. Experimental details are described in the method section. Briefly, we FAC-sorted GCTfh, fCD8s, non-fCD8s and naïve CD8$^+$ T cells and extracted DNA from 3 biological replicates, followed by bisulfite treatment before sequencing. Bisulfite DNA treatment converts unmethylated cytosine to uracil giving rise to base-specific cleavage products that reflect underlying DNA methylation patterns [58]. We measured DNA methylation levels in CpG islands spanning 500bp (300bp upstream and 200bp downstream of the *TSS*) of the *CXCR5* gene. Interestingly, we observed significantly higher methylation levels proximal to the *CXCR5* promoter region as indicated by the shaded circles of naïve CD8$^+$ T cells (Average methylation 88%), non-fCD8s (Average methylation 69%). In contrast, fCD8s and GCTfh had minimal levels of methylation at equivalent sites; fCD8s (Average methylation 7%) and GCTfh population (Average 6%) (Fig. 3.3A and B). To verify if methylation was responsible for *CXCR5* gene silencing, we incubated FAC-sorted non-fCD8s with 10μM of 5'-aza-2-deoxycytidine (Aza drug), which inhibits the enzymatic activity of DNA methyl transferases [59]. After 24 hours of incubation, we measured CXCR5 mRNA transcript levels by digital droplet PCR (ddPCR). We found that Aza drug treatment significantly increased CXCR5 mRNA levels (p=0.002) (Fig. 3.3C). Together, these data strongly suggest that *CXCR5* gene locus-specific DNA methylation is involved in repressing the *CXCR5* gene in human non-fCD8s.

Although our data shows that DNA methylation was involved in repressing CXCR5, we noted that RNA-Seq data (Fig 3.2E), revealed several other differentially expressed genes that are involved in epigenetic regulatory processing such as chromatin remodelling and histone modification. This was a signal that other epigenetic regulatory mechanisms contribute to CXCR5 regulation. Thus, to gain

comprehensive mechanistic insights into the epigenetic processes that regulate *CXCR5* gene expression in CD8^{+} T cells, we used the Assay for Transposase-Accessible Chromatin using Sequencing (ATAC-Seq). We chose this technology because it provides a genome wide accessible regions and can be used to identify TF footprinting and nucleosomal positioning, all of which cooperatively regulate gene expression [60,61]. Briefly, ATAC-Seq analysis was performed on the DNA samples isolated from the same cell populations used for RNA-Seq studies diagrammed in (supplementary Fig. 3.1). We performed a principal component analysis on the top 10% variably accessible regions. We calculated a set of 66,514 open chromatin regions (OCRs) (see materials and methods). This analysis revealed clear delineation of cell subsets based on the chromatin accessibility profiles (Fig. 3.3D and supplementary Fig. 3.3A). The subset separation was strikingly similar to RNA-Seq data, suggesting that there is significant overlap between accessibility and gene expression. Indeed, there was a strong association between chromatin accessibility and gene expression between fCD8s and non-fCD8s (R^2= 0.6) (supplementary Fig. 3.3B). Next, we profiled accessibility of *CXCR5* gene and revealed a closed chromatin conformation at the *TSS* of *CXCR5* gene in non-fCD8s, and naïve CD8^{+} T cells. In contrast, fCD8s and GCTfh had opened chromatin conformation (track with peak in black box) at the equivalent site (Fig. 3.3E). These data confirm that chromatin accessibility also contributes to the repressed state of the *CXCR5* gene in non-fCD8s and naïve CD8^{+} T cells. The observed DNA methylation and closed chromatin structure of the *CXCR5 TSS* are consistent with the notion that DNA methylation promotes nucleation of repressed chromatin structure [26,62].

To gain more mechanistic insight into the molecular processes that govern DNA methylation and chromatin accessibility, we performed differential expression analysis

on epigenetic modifying factors. Interestingly, JADE2 and SETD7 were among the most significantly differentially expressed between fCD8 and non-fCD8s (Fig. 3.3F). The two genes are known to play a key role in regulating gene expression via DNA and histone methylation [51,63,64]. Our differential mRNA expression data suggest that JADE2 and SETD7 might be involved in regulating chromatin accessibility of the *CXCR5* gene in human CD8^{+} T cells, however, more direct evidence will be required to ascertain their precise role.
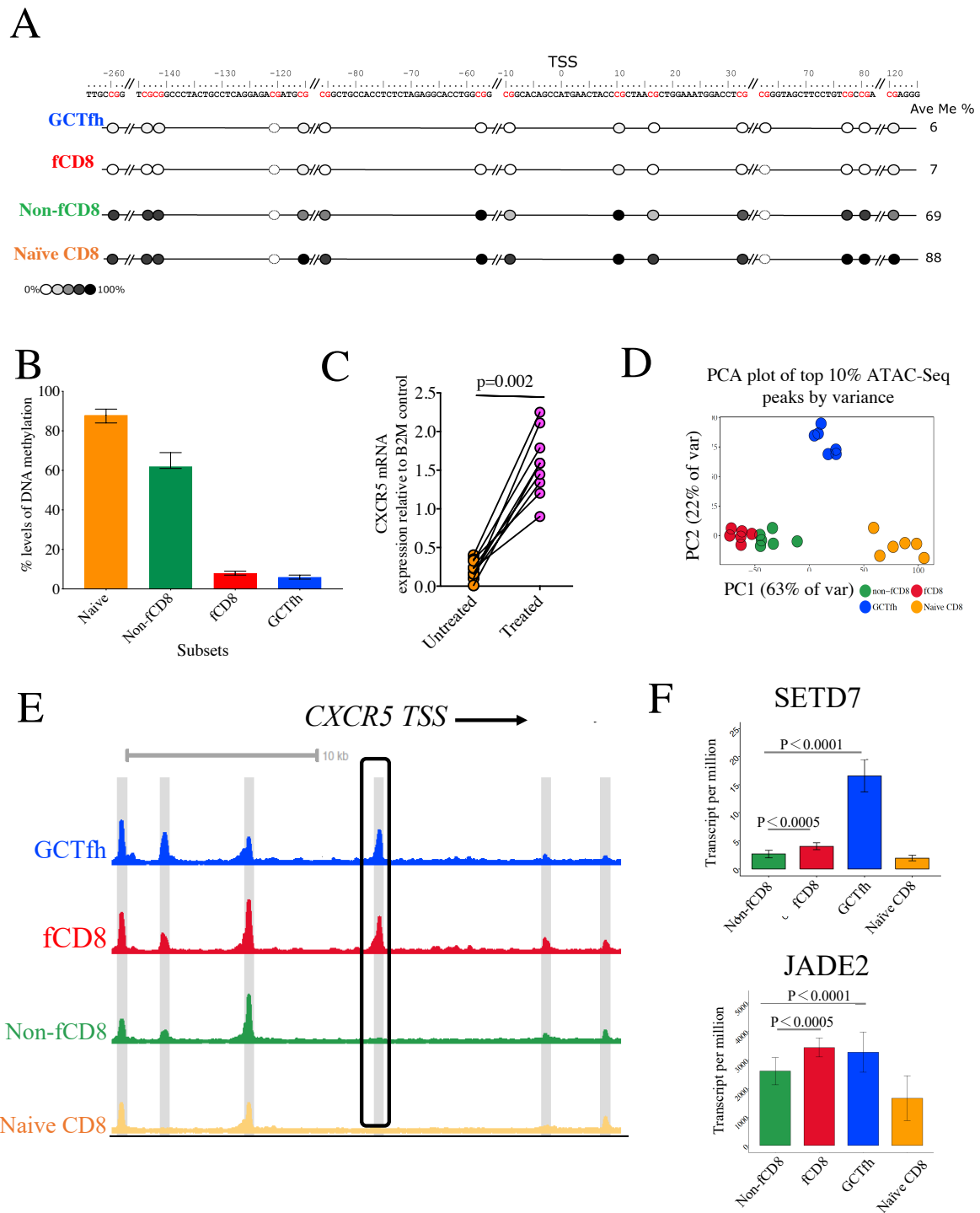
Figure 3.3: Epigenetic regulation of CXCR5 expression

(A) Quantitative measurement of DNA methylation levels within specific cell subsets; GCTfh, fCD8s, Non-fCD8s and Naïve-CD8^{+} T cells were determined using the EpiTYPER® DNA Methylation Analysis. Methylation levels were measured from bi

sulfite treated genomic DNA, followed by PCR amplification of a 500bp fragment containing 15 CpG sites (red). The naïve- and non-fCD8s cells show higher levels of methylation within several sites (darker circles), while the GCTfh and fCD8s show lower levels of methylation (lighter circles). The position of CpG sites are represented relative to the transcription start site (*TSS*). (B) Percentage levels of methylation are depicted in bar graph for each subset analyzed across the 15 CpG sites. (C) Non-fCD8s were FAC-sorted and treated with $10\mu M$ 5-aza-2'-deoxycytidine (Aza drug), a DNA methyltransferase inhibitor that causes hypomethylation of DNA, for 24 hours. Fold change relative to the B2M house keeping control indicated significant increase in the CXCR5 expression levels after treatment. (D) PCA plots obtained from the ATAC-Seq cut count data. The top 10% of ATAC-Seq peaks (merged between subsets) by variance were used to create the PCA plot. (E) Overview of the ATAC-Seq signal around the CXCR5 gene loci. ATAC-Seq signal is shown for different marked (in grey) loci where differential binding was detected in at least one sample. The black box shows the *TSS* region where there is clear equivalence between fCD8s and GCTfh ATAC-Seq signals, while very low signal was observed for both non-fCD8s and Naive CD8$^+$ T cells. (F) Expression values of *SETD7* and *JADE2* showing significant increase in fCD8s and GCTfh.

3.4.4 Similar potential TF binding sites are shared around the *TSS* of *CXCR5* gene between fCD8s and GCTfh

To identify epigenetic factors that may directly regulate chromatin accessibility of the *CXCR5* gene, we performed a TF motif search around the *CXCR5 TSS.* We restricted the motif search to regions that were inputted to have TF footprint proximal to the *TSS*

[33,38]. Our analysis revealed that fCD8s and GCTfh shared binding motifs at the *CXCR5* gene *TSS* for several epigenetic regulatory proteins namely, *POU3F1*, *POU3F3*, *E2F6*, and *ZNF384* (Fig. 3.4A). Given that POUs-TFs function as pioneering factors that interact with the closed chromatin at enhancer and/or promoter regions to open-up the regions for transcriptional activities [24,65-67], and the fact that *POU3F1* and *POU3F3* binding sites were observed for both fCD8s and GCTfh, suggest that these two pioneering factors are more likely be directly involved in opening the chromatin structure at the *CXCR5 TSS*.

Opening chromatin structure is not sufficient to drive gene expression. Several TFs are needed to bind to open chromatin and recruit the transcription machinery that drive mRNA expression [68]. Therefore, we next investigated the potential transcription factors that drive *CXCR5* gene expression. A larger proportion of the regulatory information that is necessary for gene expression is confined to the enhancer and promoter gene regions usually located upstream of *TSS* [69]. Our ATAC-seq data identified two peak regions upstream of *CXCR5 TSS*, which mostly likely represent enhancer regions. We labelled them *U1* (-6.5kb), and *U2* (-11kb) (supplementary Fig. 3.4A). We performed a TF motif search within these regions for each subset to identify specific TFs that bind in this region and found that *MAFB* was highly enriched in fCD8s and GCTfh, while *TGIF1* and *TGIF2* were enriched in fCD8s but not in GCTfh (Fig. 3.4B). Together, these data suggest that *POUs* pioneer the opening of chromatin around the *CXCR5 TSS,* which allows key TF such as *MAFB*, *TGIF1* and *TGIF2* to bind around the TSS and recruit the transcription machinery to drive CXCR5 expression in human CD8^{+} T cells.
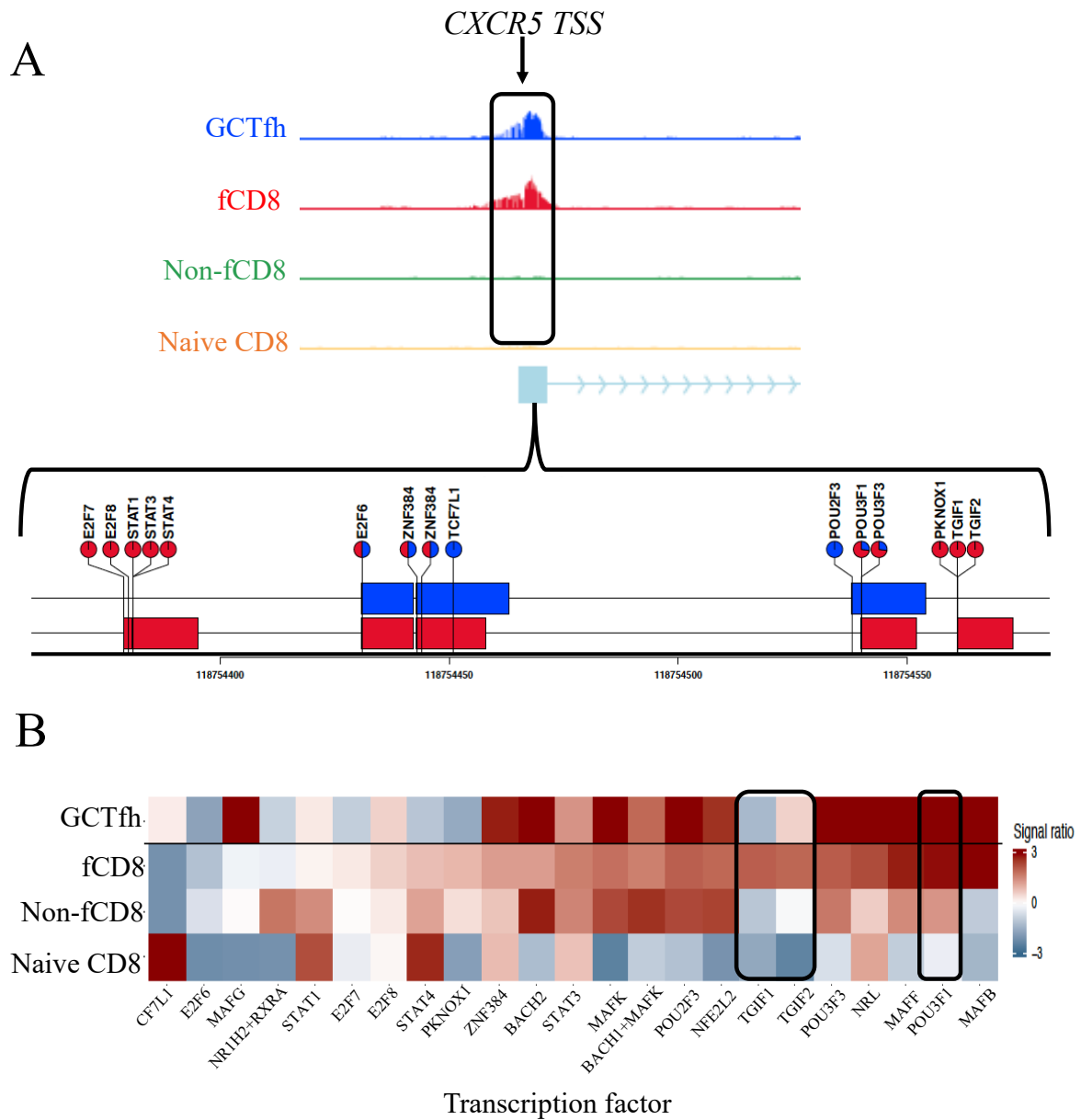
Figure 3.4: Shared and different transcriptional factors footprint proximal to the CXCR5 gene.

(A) Footprints in selected regions predicted footprinted regions respective cell subsets. The pie charts show the relative wellington bootstrap scores for each subset against

all others acting as a proxy for the relative TF activity observed in that region. The bars indicate the extent of the predicted TF footprint, with colours assigned to each subset. Footprints with unassigned TFs are also included. (B) Assignment of TF to subsets. Enrichment of TF motifs (restricted differential footprints between subsets) of each subset is depicted in the heatmap. The TFs are sorted in ascending order of importance in the fCD8 subset.

3.4.5 WGCNA reveals alternative pathway involved in the expression of CXCR5 in human CD8^{+} T cells

Cell types are controlled by complex layers of regulators resulting in co-expression of multiple receptors which are used in eliciting their effector functions. To identify potential common and cell-type specific signatures in the epigenetic and transcriptional circuitry that regulates *CXCR5* gene in human CD8^{+} T cells, we performed Weighted Gene Correlated Network Analysis (WGCNA) on our ATAC-Seq and RNA-Seq data sets. WGCNA is a network analysis that is used to identify modules of highly co-expressed genes [39] or chromatin accessible gene networks. The program assigns colours to modules as an identification mark. We first applied this network analysis on our ATAC-Seq data to identify chromatin accessibility networks from the ATAC-Seq data. We hypothesized that the mechanisms governing chromatin accessibility may not act on open chromatin regions (OCRs) in isolation, but rather are grouped into programs that change the accessibility of multiple chromatin loci.

We performed WGCNA on 12000 ATAC-Seq peaks after excluding sites with high technical variance. The expected was that OCRs proximal to *CXCR5* gene would fall within the same module. Interestingly, we observed that the *CXCR5 TSS* and *U2*

OCRs were assigned by WGCNA to the same module called grey*60* module (Fig. 3.5A). This suggested that the *U2* (enhancer region) interacted with the *TSS* to promote *CXCR5* transcription. Notably, enrichment analysis on the grey*60* modules revealed striking similarity in accessibility pattern between fCD8s and GCTfh (Fig. 3.5B), in spite of very clear difference in overall genome-wide accessibility between the two cell subsets as depicted in ATAC-Seq PCA plot (Fig. 3.3D). These data suggest that accessible regions that drives the *CXCR5* gene expression (contained in the grey*60* module) are shared between fCD8s and GCTfh.

Given that gene accessibility does not always translate into gene expression, we repeated the WGCNA analysis on the RNA-Seq data to identify regulatory genes that are actually transcribed. We constructed the network using the four cell subsets. We included 20,987 genes that were found to be expressed in fCD8s and non-fCD8s. The resultant network consisted of 91 modules, each containing a set of highly co-expressed genes. We batch normalized the data to account for heterogeneity of expression between patients and used the expression values to calculate gene set enrichment analysis (GSEA) for each subset for the 91 detected modules. We observed a significant enrichment of *CXCR5*, *MAF*, *Id3*, *POU3F1* and *CXCL13* genes in the honeydew module which was shared by fCD8s and GCTfh (Fig. 3.5C). Interestingly, ATAC-Seq data identified footprinting motifs for the same set of genes in *U2* and *TSS* regions of the *CXCR5* gene (Fig. 3.4B and supplementary Fig. 3.4A). Notably, GSEA demonstrated significant enrichment of GCTfh and fCD8s subsets in honeydew module (Fig. 3.5D). Gene ontology (GO) analysis on the *CXCR5*-centric module, i.e, honeydew module showed enrichment of terms associated with "cell migration" (Fig. 3.5F), suggesting that a subset of genes governing the expression of CXCR5 in human CD8$^+$ T cells are intricately involved in cell migration. Collectively,

our data identify *MAF, Id3* and *POU3F1* act as a putative gene circuitry that are involved in driving the expression of CXCR5 in human CD8+ T cells.
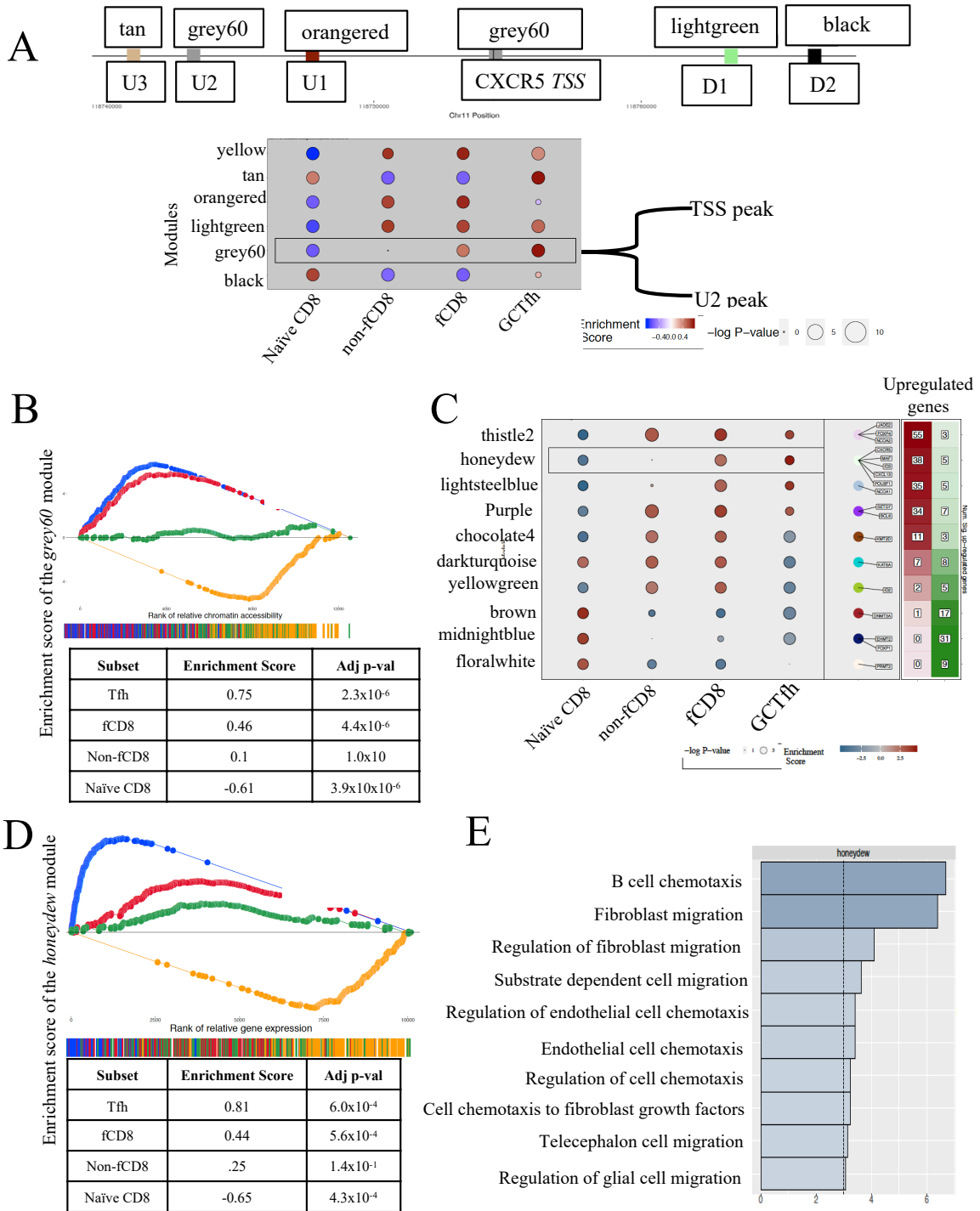
Figure 3.5: Regulatory pathways in CXCR5 expression

(A) The figure shows the OCR regions observed in at least one of the cell subsets. Peaks are either prefixed with U to indicate upstream, or D to indicate downstream of the CXCR5 TSS. The colors represent the WGCNA modules. The module names (as colors) appear above the peaks. ATAC-Seq WGCNA around the CXCR5 gene region. Modules are sized according to enrichment and significance. The highlighted grey60 module contains both the *TSS* of CXCR5 and the U2 region. (B) GSEA plot of the grey60 module of ATAC-Seq WGCNA enrichment values. Peaks belonging to the grey60 module for each subset are plotted according to the rank within each subset. High correspondence and enrichment are seen for the GCTfh and fCD8s subsets, while no enrichment is shown for non-fCD8s and negative enrichment is shown for naïve CD8$^+$ T cells. (C) Overview of the RNA-Seq WGNCA modules. Selected modules are shown. The modules are colored according to their Gene Set Enrichment Analysis (GSEA) score. Positive values indicating positive enrichment. The size of the module corresponds to the -log P-value. The panel to the right indicates the number of genes that are up-regulated in fCD8s and non-fCD8s for each module. (D) GSEA analysis shows the overall enrichment of the CXCR5 containing in honeydew module, with corresponding enrichment scores and significance values. The bottom bar shows the concentration of genes within a subset according to the rank of expression. (E) GO enrichment of the honeydew module showing positive enriched GO terms in the honey dew module ranked according to significance. Cell migration is an important factor in the honeydew module.

3.4.6 Reduced turnover rate of the nucleosome at the promoter region of CXCR5 could lead to lower levels of CXCR5 expression

CD8^{+} T cells do not typically express CXCR5, but even for fCD8 subset that do, the level of expression is generally much lower than GCTfh expression levels [15,70]. Consequently, this reduces their sensitivity to cognate chemoattractant CXCL13, resulting in inefficient infiltration into B cell follicles [20], where CXCL13 producing cells reside. To investigate epigenetic mechanism that regulate the level of CXCR5 expression, we first compared CXCR5 protein expression levels and found significantly higher expression in GCTfh compared to fCD8s (p=0.0001) (Fig. 3.6A). This was true for mRNA levels as well (Fig. 3.6B). A recent study reported similar results [45]. We then performed a trans-well experiment to assess if the expression of CXCR5 affects the rate of fCD8s chemotaxis towards a CXCL13 gradient. Indeed, fCD8s exhibited significantly lower chemotaxis capacity compared to GCTfh (p=0.01) (Fig. 3.6C). Moreover, a GO analysis on the RNA-Seq data showed enrichment of genes associated with cell migration/leukocyte migration in fCD8s relative non-fCD8s (Fig. 3.6D). Together, these data confirm that lower expression of CXCR5 reduces chemotaxis capacity of fCD8s towards CXCL13.

Given high frequency of methylated CpG islands in the *CXCR5* gene which tend to attract nucleosomes [26,71], we posit high nucleosomal occupancy at the *TSS* lowers CXCR5 expression in fCD8s. We reasoned that nucleosome positioning and occupancy around the *TSS* would interfere with transcription machinery resulting in mitigated gene expression [72]. To test this hypothesis, we used the recently developed NucleoATAC tool (Schep et al., 2015) to impute the presence of nucleosomes in and around the *CXCR5* gene. Interestingly, the presence of nucleosome was imputed in

both fCD8s and GCTfh at the *TSS*. However, nucleoATAC also reported higher nucleosomal occupancy in predicted TF footprint regions around the *TSS* in fCD8s, whereas GCTfh exhibit less nucleosomal occupancy in the same region (Fig. 3.6E). Computationally, the nucleosomal occupancy was calculated for a wider range upstream of the *TSS* in GCTfh than fCD8s (blue and red dotted lines), which extended beyond the point where a nucleosome may occupy TF binding regions (black dashed line) (Fig. 3.6E). Collectively, these data suggest higher nucleosomal occupancy in fCD8s at the *TSS*. Computational simulation of nucleosomal occupancy confirm the notion that nucleosomal occupancy interferes with transcriptional machinery, reducing the transcription of the *CXCR5* gene in fCD8s **(**supplementary Fig. 3.5).
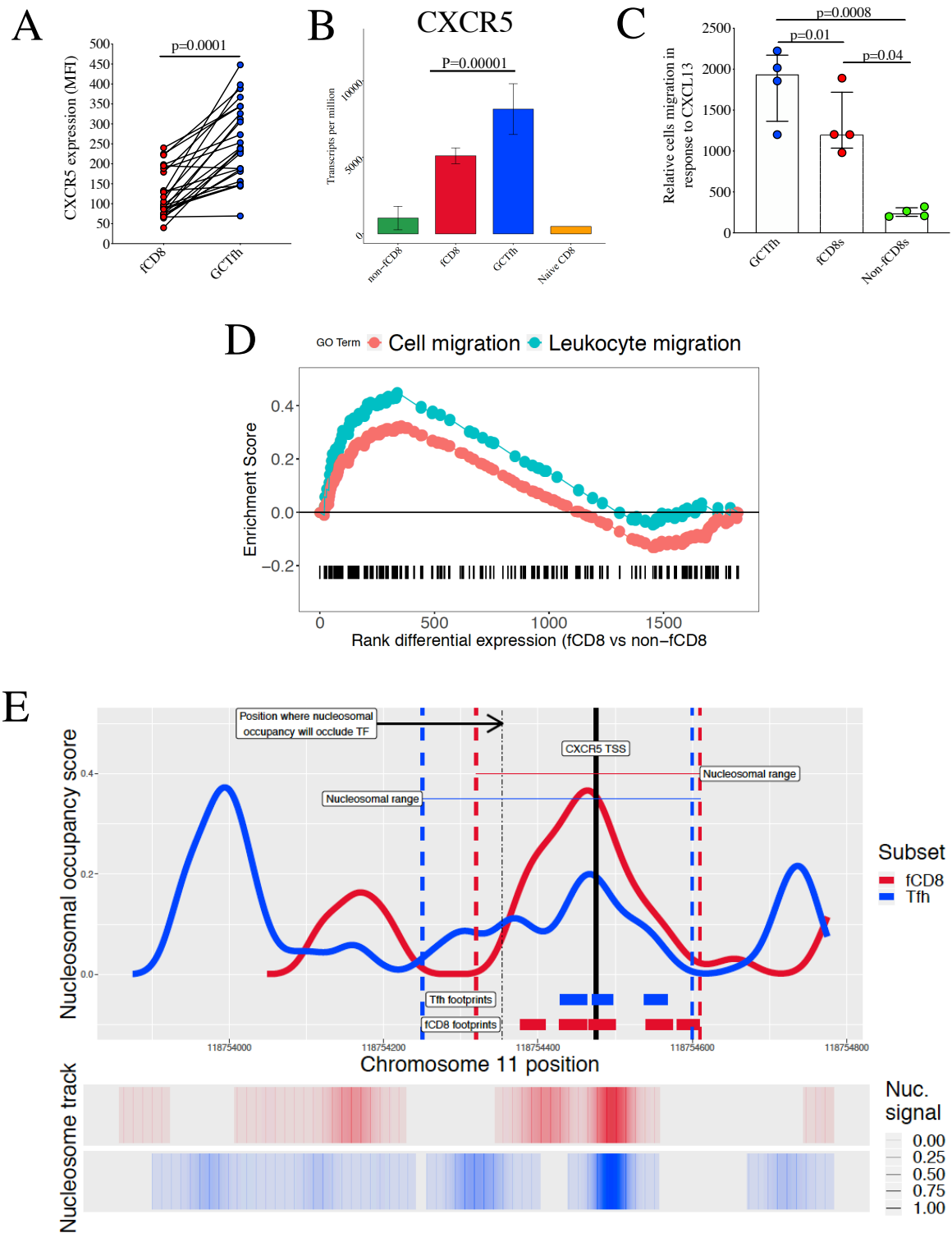
Figure 3.6: Nucleosome interfere with CXCR5 expression in fCD8s

(A) Mean fluorescence intensity (MFI) of CXCR5 on fCD8s and GCTfh shows

significant increase in the expression of CXCR5 on GCTfh compared to fCD8s. (B)

RNA-Seq expression values of CXCR5 showing the batch-normalized expression values in different cell subsets. (C) Relative migration of Tfh, fCD8s and non-fCD8s subsets in response to CXCL13; a ligand for CXCR5. Graph shows the number of cells that migrated in each subset after 3 hours (D) The GSEA plot of GO terms between fCD8s and non-fCD8s. Cell migration and Leukocyte migration shows the ranked differential expression of genes belonging to these terms between the fCD8s and non-fCD8s subsets. (E) The figure depicts the nucleosomal occupancy scores (top line plot) and the nucleosomal signal (bottom heatmap) as produced by NucleoATAC around the *TSS* region of CXCR5 in fCD8s (red) and GCTfh (blue) subsets. The colored vertical dashed lines show the range of predicted nucleosomal occupancy. The thin dashed line shows the approximate location of the nucleosomal dyad where the nucleosome will occlude the *TSS* region. Height of the occupancy score shows the fraction of nucleosomal sized fragments at the chromosome 11 position. Predicted transcription factor footprints are shown as bars for the respective cell subsets.

3.4.7.1 Proposed model of how human CD8⁺ T cells achieve CXCR5 expression

Based on experimental and computational evidence generated in this study, we propose a model of how *CXCR5* gene transcription is epigenetically regulated in human CD8⁺ T cells. In naïve CD8⁺ T cells, DNA methylation of CpG islands around the *TSS* stably silence *CXCR5* gene expression by attracting chromatin remodelling proteins and histone modifiers to the loci which compact chromatin around the *TSS* into heterochromatin state. Cell division following TCR stimulation results in passive DNA demethylation around the promoter region allowing for basal transcriptional

activity observed in non-fCD8s relative to naïve CD8$^+$ T cells. As the cells continue to divide, a small proportion of cells become more extensively demethylated at the *CXCR5* gene loci and gradually accumulate epigenetic regulatory proteins including pioneering factors (the POUs), namely POU3F3 and POU3F1 and methyltransferases (SETD7) which are recruited to the *TSS* proximal regions. These factors decondense the chromatin at the *TSS* thereby exposing unmethylated DNA for transcription, thus allowing the transcription machinery to bind and transcribe the *CXCR5* gene (Fig. 3.7A).

3.4.7.2   Proposed model of how the level of CXCR5 gene expression is moderated in human CD8$^+$ T cells

Nucleosomal positioning can dictate transcription efficiency. We postulate that fCD8s have less CXCR5 expression relative to GCTfh due to higher nucleosomal density around the *CXCR5 TSS*. The rationale is as follows, although, we detected primary nucleosomal signal over the *TSS* in both fCD8s and GCTfh, the secondary nucleosomal signal is closer to the *TSS* in fCD8s but further upstream in GCTfh (Fig. 3.7B). This suggest that the repositioning of the nucleosome further away from the *TSS*, in GCTfh, makes it easier for the transcriptional machinery to access the promoter and initiate transcription. Nucleosomes are pushed away from gene promoter regions by a family of proteins called nucloesomal remodellers. Some remodellers are more efficient at evicting nucleosomes from active gene loci than others [73]. Interestingly, fCD8s and GCTfh express different types of nucloesomal remodellers. Therefore, we postulate that nucleosomal remodellers in GCTfh are more efficient at pushing the nucleosome further upstream, which completely uncovers the

CXCR5 TSS for transcription whereas, fCD8s nucleosomal remodellers are less efficient at pushing the nucleosome away from the *TSS,* hence the attenuated *CXCR5* gene expression.
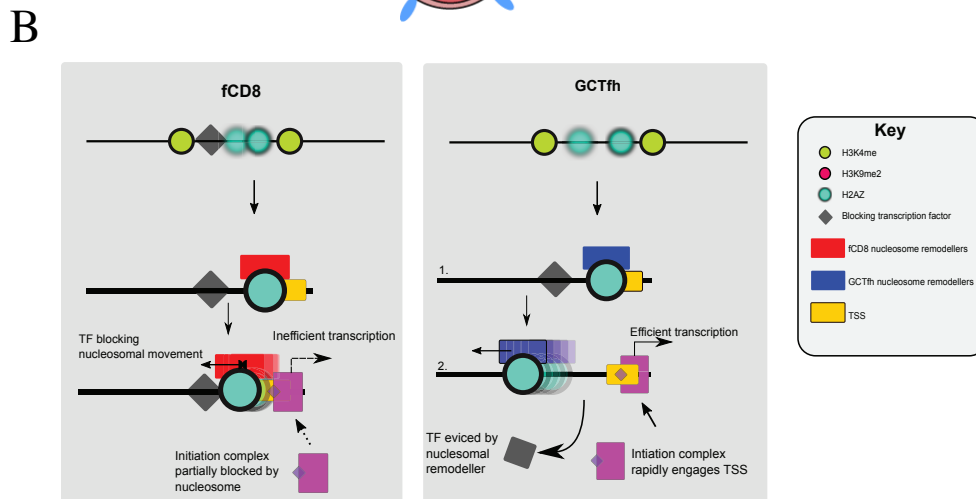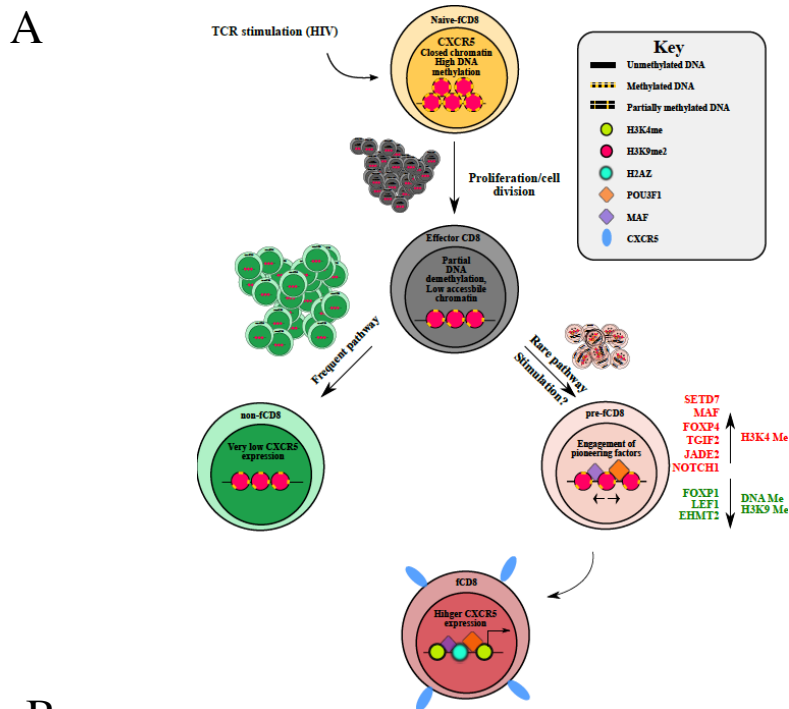
Figure 3.7: Proposed model for CXCR5 regulation in human CD8^{+} T cells

3.5 Discussion

Understanding how to increase trafficking of CD8$^+$ T cells to B cell follicles has far reaching implications for developing strategies to eradicate HIV infected cells in follicles for HIV cure and to treat B cell-derived malignancies. In this study, we assessed the epigenome and the transcriptome of human fCD8s and non-fCD8s to determine the molecular mechanisms that limit CXCR5 expression in human CD8$^+$ T cells. We show that CXCR5 expression in CD8$^+$ T cells is tightly controlled by at least three key epigenetic mechanisms; namely, DNA methylation, chromatin structure and organization and nucleosomal occupancy.

This study set out to address two key questions. First, why most CD8$^+$ T cells do not express CXCR5. Second, why fCD8s express low CXCR5 relative to GCTfh. To address the first question, we studied two antigen-experienced CD8$^+$ T cell subsets called fCD8s and non-fCD8s that were phenotypically matched except for the expression of CXCR5 on the cell surface. This meant that the difference in transcriptional expression and gene accessibility observed was more likely to be involved in *CXCR5* gene regulation. Interestingly, transcriptional analysis in combination with locus-specific bisulfite-treated sequencing and the genome-wide chromatin accessibility data identified DNA-hypermethylation and closed chromatin structure as the two epigenetic mechanisms that are involved in repressing CXCR5 expression in human non-fCD8s. To address the second question of why there is reduced expression of CXCR5 on fCD8s, relative to GCTfh, we focused our analysis CXCR5$^+$ subsets (fCD8s and GCTfh) because of the significant differences in their CXCR5 expression levels. We began by verifying in our setting that indeed fCD8s had reduced CXCR5 expression and were inefficient at trafficking towards CXCL13

chemokine compared to GCTfh. We went on to identify nucleosomal occupancy and positioning as a plausible mechanism that moderates the expression of CXCR5 in fCD8s.

Conceptualization of this study was motivated by three studies in mice that recently described a subset of CXCR5 expressing CD8^{+} T cells, which they termed fCD8s because of their ability to accumulate in B cells follicles [11,12,20]. The striking findings in murine models was that fCD8s were transcriptionally closely related to GCTfh and less so with non-fCD8s. More importantly they showed that following infection, these cells readily accumulated in B cells follicles and were able to eradicate infected GCTfh [11,12,20]. A subsequent rhesus macaques study showed similar results [21]. So, we wondered if CXCR5^{+}CD8^{+} T cells (fCD8s) were also increased in HIV infection in human lymph nodes (LN), and if their differentiation profile was similar to what was described in mice. Indeed, our data showed increased frequency of fCD8s in LN of HIV infected individuals compared to uninfected individuals. Early initiation of antiviral therapy mitigated the fCD8s response, suggesting that fCD8s induction is antigen driven as described in animal studies [15].

Given that mice studies identified several TFs that were common between fCD8s and GCTfh, including; BCL6, Id3, Id2, PRDM1 and TCF-1 [11,12,20,46,74]. We investigated whether similar TFs were operating in human LN CD8^{+} T cells in the setting of HIV infection. We sorted LN fCD8s and non-fCD8s from HIV infected and uninfected individuals. Our sorting panels were based on similar markers used in mice studies. RNA-Seq analysis showed that TF expression profiles in human GCTfh cells was similar to what was reported in mice [20]. However, unlike mice studies, we found significant differences in TF expression profiles between human GCTfh and fCD8s. In

fact, based on the reported TFs governing *CXCR5* expression, human fCD8s were more similar to non-fCD8s than GCTfh, suggesting that most of the TFs that were shown to be critical for fCD8 differentiation in mice might not be essential for human fCD8 differentiation. These results led us explore to other mechanisms that could possibly regulate *CXCR5* expression in human CD8$^+$ T cells.

The observation of many differentially regulatory epigenetic genes between fCD8s and non-fCD8s in our RNA-Seq data provided the first clue that epigenetic mechanisms might play a key role *CXCR5* gene regulation. Locus-specific bisulfite-treated sequencing revealed hypermethylation in CpG islands proximal to promoter regions of subsets that lack CXCR5 expression (non-fCD8s and naïve CD8$^+$T cells) and less methylation in *CXCR5*$^+$ cells (fCD8s and GCTfh). Moreover, inhibition of enzymatic activity of methyltransferase that is essential for re-methylation of DNA during cell division using aza drug treatment increased CXCR5 expression in CXCR5 negative cells, providing compelling evidence that DNA methylation was a major epigenetic mechanism involved in silencing CXCR5 expression [51]. Consistent with the notion that DNA methylation increases nucleosome compaction and rigidity [62], ATAC-Seq data revealed closed chromatin conformation at the *CXCR5 TSS* in non-fCD8s, further implicating condensed chromatin at the *TSS* as another epigenetic mechanism involved in *CXCR5* gene silencing.

Histone modification is essential in maintaining accessibility of gene regions. Our RNA-Seq studies identified several key epigenetic modifying enzymes that were significantly upregulated in fCD8s and GCTfh relative to non-fCD8s and naïve CD8$^+$ T cells. Two of such enzymes are SETD7 and JADE2 which have been shown to respectively mediate mono-methylation of lysine 4 on histone 3 (H3K4me1) and

counteract the activity of a gene silencing epigenetic enzyme called LSD1 [51,63]. It is therefore, not far-fetched to implicate SETD7 and JADE2 in orchestrating methylation of histone around *CXCR5* gene leading to opening of the chromatin for transcription of fCD8s and GCTfh. Furthermore, overlapping predicted footprints of *POU3F1* and *POU3F3* binding motif at the *TSS* of both fCD8s and GCTfh suggest that these factors could be initiating the decompaction of chromatin at the *CXCR5 TSS* following TCR stimulation [24,66,75].

To identify key genes and pathways involved in *CXCR5* gene regulation, we performed WGCNA on the ATAC-Seq and RNA-Seq data. This allowed us to identify circuits of correlated chromatin accessibility as well as gene expression. WGCNA analysis identified modules of highly correlated open chromatin regions that indicated chromatin accessibility of the *CXCR5* promoter region is part of a larger epigenetic circuit. We identify grey*60* module as an important module that contains the *TSS* and *U2* peaks (a putative enhancer region). Strikingly, this module was highly enriched in fCD8s and GCTfh which confirms similar epigenetic circuitry shared between fCD8s and GCTfh in the context of CXCR5. Further we used WGCNA to identify transcriptional modules that governs the expression of CXCR5 in human CD8^{+} T cells. An interesting module from this analysis is the honeydew module containing CXCR5, MAF, Id3, POU3F1 and CXCL13 which was enriched for fCD8s and GCTfh. GSEA on honeydew *module* confirms a stepwise significance of genes skewed for GCTfh and fCD8s and this corroborates with the expression pattern of CXCR5. Indeed, GO analysis of honeydew module clearly demonstrated chemotaxis and B cell migration as the key modules common to the two cell subsets. This implies that the transcriptional factors governing the expression of CXCR5 in human CD8^{+} T cells may

be present in honeydew modules of which Id3, MAF *and* POU3F1 are the key members more likely to be directly involved in regulating the gene.

Accumulation of high frequencies of CD8^{+} T cells in the B cell follicles is desirable for HIV cure. Our flow data and *in vitro* chemotaxis experiments suggest that lower expression level of CXCR5 in fCD8s contribute to the inefficient infiltration of B cell follicles observed in our imaging experiments. Importantly, nucleosomal occupancy emerged as a key molecular mechanism that most likely lowers CXCR5 expression in fCD8s. Recent studies have shown how two different chromatin remodellers, ISW1a and SWI/SWF have different capacities to shift nucleosomal position in yeasts [73,76,77]. The different potential of these remodellers to shift nucleosomes becomes apparent when an obstruction, such as a bound TF, is in the way (see cartoon in Figure 7). ISW1a lacks the ability to remove a bound TF and thus constrains the movement of the nucleosome, whereas SWI/SNF was shown to successfully dislodge the TF and move the nucleosome further away [78]. To test this hypothesis, future studies should use CRISPR-Cas9 technology to modify the nucleotides in the footprint region identified from the ATAC-Seq data to abrogate binding of TFs to this region and determine if this would lead to increase in CXCR5 expression.

Differential chromatin accessibility observed at the *TSS* of fCD8s but not in non-fCD8s suggests that there is a difference in histone modification pattern between the two subsets [53,79-84]. This can be confirmed by chromatin immunoprecipitation (ChIP-Seq) analysis. However, we could not perform ChIP-Seq because we did have not sufficient number of cells required for this assay. Nonetheless, ChIP-Seq data set on B cell line GM12787 (ENCODE Project Consortium 2012) shows H3K4me2 within the accessible regions around the *CXCR5* gene, which is consistent with our ATAC-Seq data. Also,

the differential positioning of a nucleosome transiently occupying the *TSS* region of *CXCR5* gene in fCD8s and GCTfh as imputed from the ATAC-Seq data is intriguing. However, we could not validate this phenomenon due to the technical difficulties associated with measuring nucleosomal positioning. Development of assays that can precisely track positioning of nucleosome is warranted.

In conclusion, our data provide evidence of coordinated epigenetic and transcriptional involvement in the tight regulation of the *CXCR5* gene in human CD8$^+$ T cells. Importantly, we identified a putative transcription circuitry that include Id3, MAF and POU3F1 TFs, SETD7, and JADE2 and epigenetic signatures such as DNA methylation and nucleosomal occupancy that could be manipulated to induce and maximize CXCR5 expression on CD8$^+$ T cells, which would enhance trafficking of CD8$^+$ T cells to B cell follicles where they are needed to eradicate HIV infected cells or cancerous cells.

Experimental setups for ATAC-Seq, RNA-Seq and DNA Methylation Assay

fCD8: CD3⁺CD8⁺CD45RA⁻CXCR5⁺

Non-fCD8: CD3⁺CD8⁺CD45RA⁻CXCR5⁻

Tfh: CD3⁺CD4⁺PD-1^high^CXCR5^high^

Naïve CD8: CD3⁺CD8⁺CD45RA⁺CCR7⁺
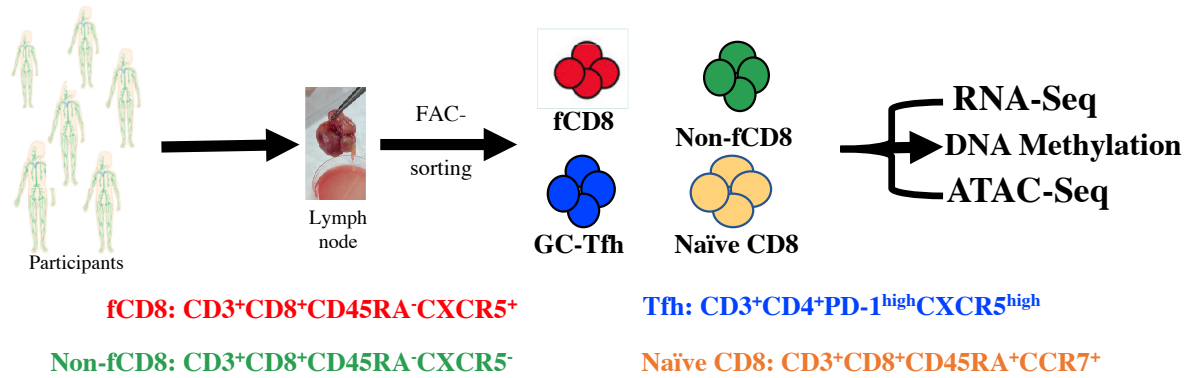
Supplementary Figure 3.1: Experimental design for ATAC-Seq, RNA-Seq and DNA methylation.
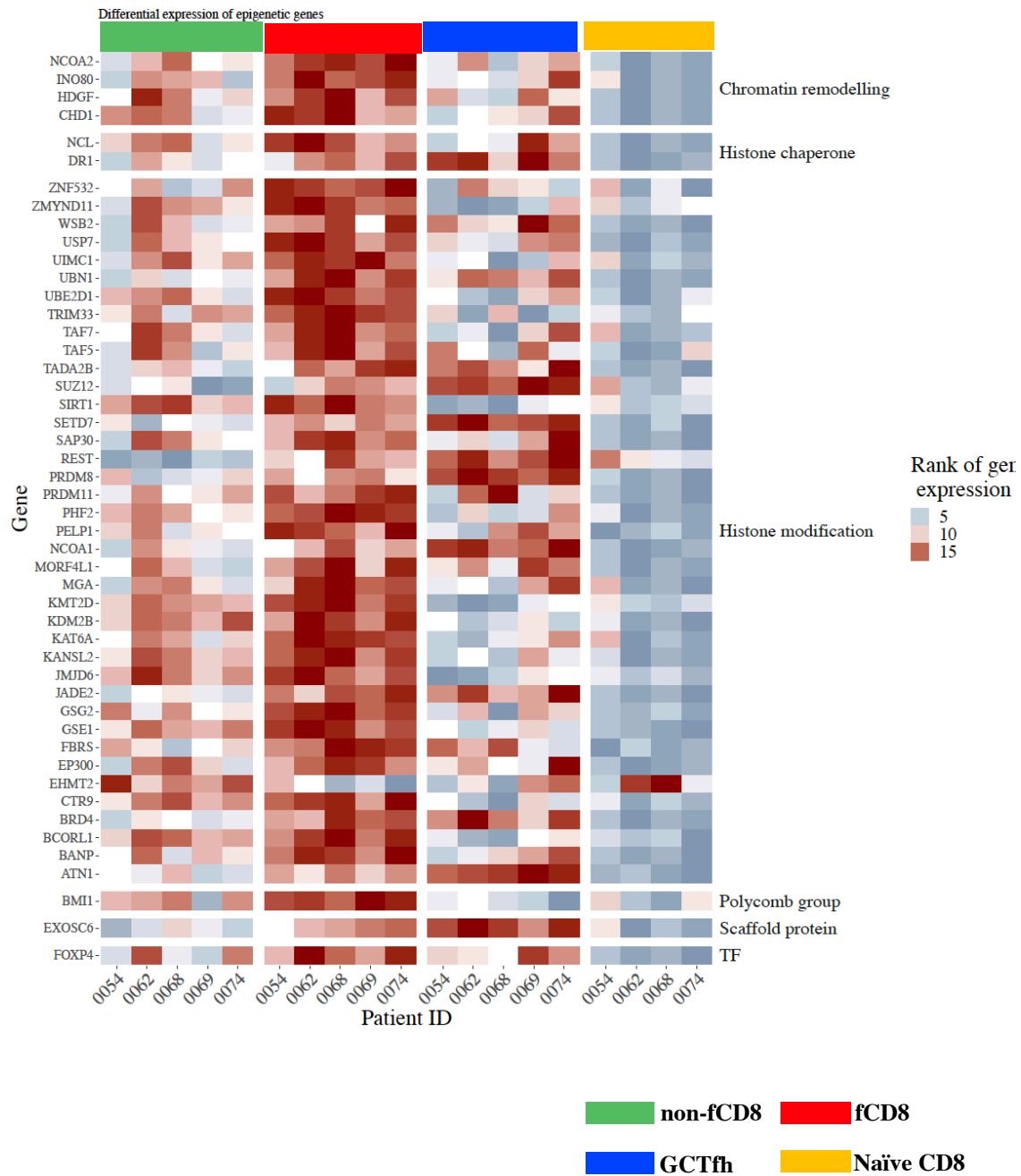
Supplementary Figure 3.2: Extended data for differentially expressed epigenetic factors

Heatmap of up-regulated genes with epigenetic function in fCD8s. The heatmap shows the relative rank of gene expression (after batch-adjustment) of the epigenetic

genes. Majority of the genes are involved in histone modification as shown in the heatmap.
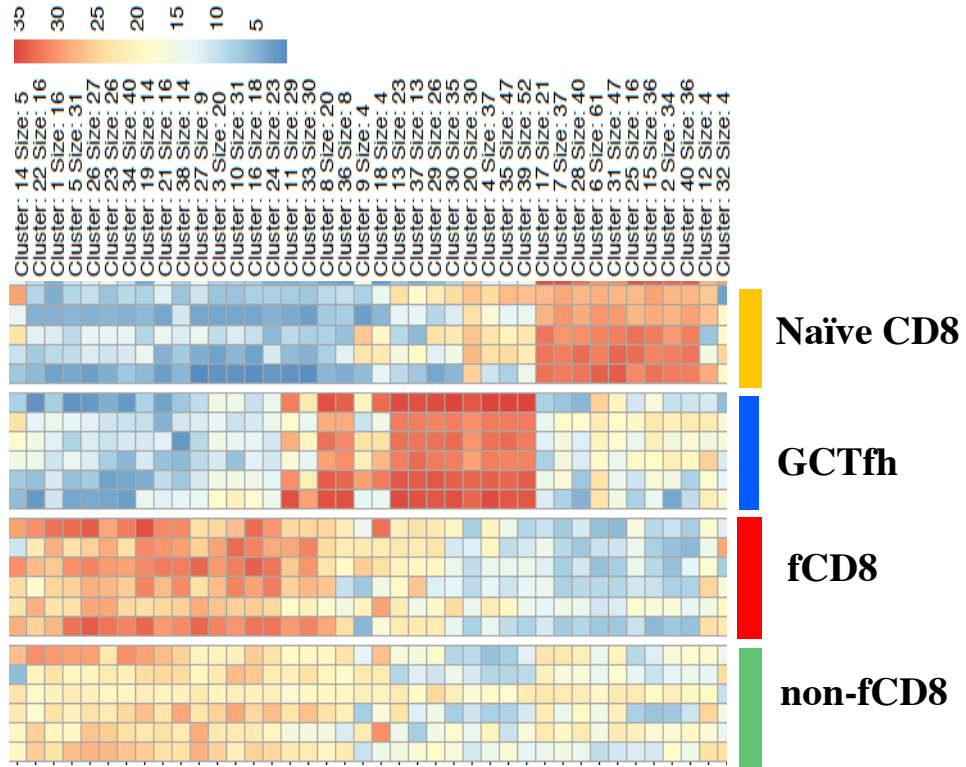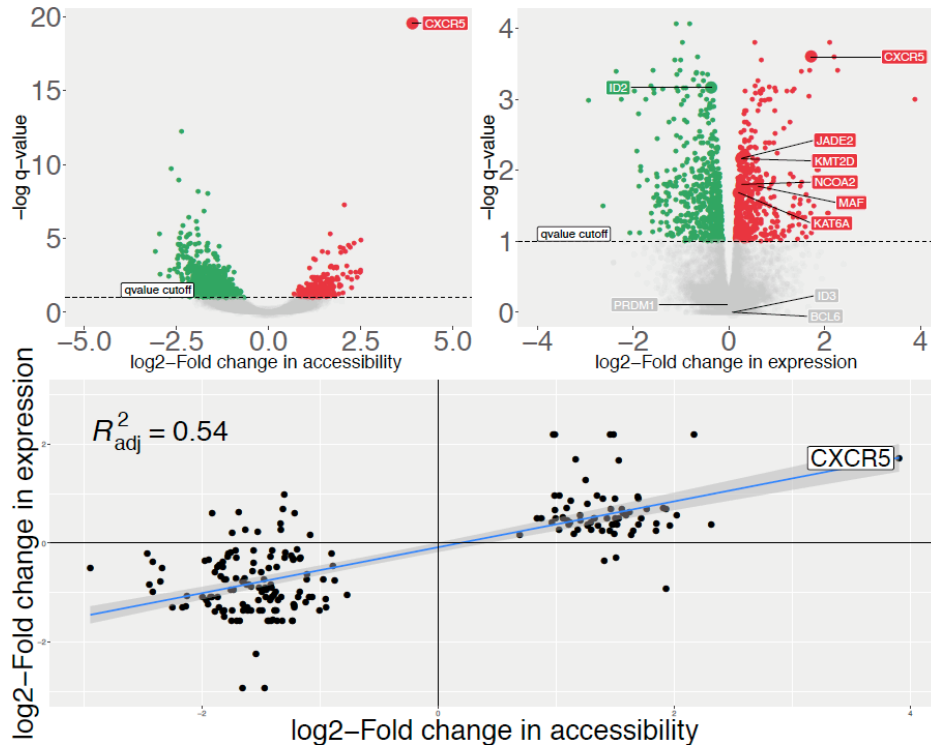
Supplementary Figure 3.3: ATAC-Seq signal and correlation between OCRs and gene expression

(A) The heatmap shows a condensed overview of ATAC-Seq signal of the top 10% ATAC-Seq peaks by variance. The clusters are organized in a hierarchical fashion showing subset specific clusters. (B) The figure shows deferentially expressed genes with corresponding differential accessibility OCRs between fCD8s and non-fCD8s. The y-axis represents the $\log_2$ fold change in gene expression, while the x-axis represents the log fold change in chromatin accessibility. A regularized regression line is fitted to the data. Example genes are annotated. The gene of interest, CXCR5 is coloured in red.

Supplementary Figure 3.4: Transcription factor footprinting track

(A) We determined the top TF enriched using WB for each subset and plotted the results on pie chart. ATAC-Seq peaks 11kb from the *TSS* region of *CXCR5* ATAC seq peaks within 11kb of the *TSS* of *CXCR5* are shown. The boxes indicate the named

upstream regions, i.e. U1 (-6.5kb) and U2 (-11kb). (B) Set enrichment of TF. We ranked ATAC-Seq signals of OCRs within the grey60 module with the representative *eigengene* of the *grey60*. Regions were sorted in descending order depending on their correlation with the *grey60* module. For each subset, we used the calculated TF footprints in each region and determined by *set enrichment analysis* whether these TFs were likely enriched in regions higher correlated with the *grey60* eigengene. That is, we hypothesize TF showing higher SEA enrichment with the *grey60* eigengene to be more associated with the hub regions that are purported to be central in governing accessibility programs across this module. TF were aggregated at family level. From the figures, it becomes apparent that there is a progressive enrichment of *MAF-family* related factors from non-fCD8s to the enrichment of pioneering *POU-family* transcription factors in fCD8s with *GCTfh* sharing these *TFs*. High enrichment is shown as positive (red) values, while negative enrichment (i.e. TF depleted *grey60* OCRs) are shown in blue.

3.7 References

1   Pantaleo, G. *et al.* HIV infection is active and progressive in lymphoid tissue during the clinically latent stage of disease. *Nature* **362**, 355-358, doi:10.1038/362355a0 (1993).

2   Folkvord, J. M., Armon, C. & Connick, E. Lymphoid follicles are sites of heightened human immunodeficiency virus type 1 (HIV-1) replication and reduced antiretroviral effector mechanisms. *AIDS research and human retroviruses* **21**, 363-370, doi:10.1089/aid.2005.21.363 (2005).

3   Horiike, M. *et al.* Lymph nodes harbor viral reservoirs that cause rebound of plasma viremia in SIV-infected macaques upon cessation of combined antiretroviral therapy. *Virology* **423**, 107-118, doi:10.1016/j.virol.2011.11.024 (2012).

4   Perreau, M. *et al.* Follicular helper T cells serve as the major CD4 T cell compartment for HIV-1 infection, replication, and production. *The Journal of experimental medicine* **210**, 143-156, doi:10.1084/jem.20121932 (2013).

5   Banga, R. *et al.* PD-1(+) and follicular helper T cells are responsible for persistent HIV-1 transcription in treated aviremic individuals. *Nature medicine* **22**, 754-761, doi:10.1038/nm.4113 (2016).

6   Kohler, S. L. *et al.* Germinal Center T Follicular Helper Cells Are Highly Permissive to HIV-1 and Alter Their Phenotype during Virus Replication. *Journal of immunology (Baltimore, Md. : 1950)* **196**, 2711-2722, doi:10.4049/jimmunol.1502174 (2016).

7   Connick, E. *et al.* CTL fail to accumulate at sites of HIV-1 replication in lymphoid tissue. *Journal of immunology (Baltimore, Md. : 1950)* **178**, 6975-6983 (2007).

8   Fukazawa, Y. *et al.* B cell follicle sanctuary permits persistent productive simian immunodeficiency virus infection in elite controllers. *Nature medicine* **21**, 132-139, doi:10.1038/nm.3781 (2015).

9   Streeck, H. AIDS virus seeks refuge in B cell follicles. *Nature medicine* **21**, 111-112, doi:10.1038/nm.3795 (2015).

10   Velu, V., Mylvaganam, G., Ibegbu, C. & Amara, R. R. Tfh1 Cells in Germinal Centers During Chronic HIV/SIV Infection. *Frontiers in immunology* **9**, 1272, doi:10.3389/fimmu.2018.01272 (2018).

11   Leong, Y. A. *et al.* CXCR5(+) follicular cytotoxic T cells control viral infection in B cell follicles. *Nature immunology* **17**, 1187-1196, doi:10.1038/ni.3543 (2016).

12   He, R. *et al.* Follicular CXCR5- expressing CD8(+) T cells curtail chronic viral infection. *Nature* **537**, 412-428, doi:10.1038/nature19317 (2016).

13   Chu, F. *et al.* CXCR5(+)CD8(+) T cells are a distinct functional subset with an antitumor activity. *Leukemia*, doi:10.1038/s41375-019-0464-2 (2019).

14   Reuter, M. A. *et al.* HIV-Specific CD8(+) T Cells Exhibit Reduced and Differentially Regulated Cytolytic Activity in Lymphoid Tissue. *Cell reports* **21**, 3458-3470, doi:10.1016/j.celrep.2017.11.075 (2017).

15   Petrovas, C. *et al.* Follicular CD8 T cells accumulate in HIV infection and can kill infected cells in vitro via bispecific antibodies. *Science translational medicine* **9**, doi:10.1126/scitranslmed.aag2285 (2017).

16   Luster, A. D., Alon, R. & von Andrian, U. H. Immune cell migration in inflammation: present and future therapeutic targets. *Nature immunology* **6**, 1182-1190, doi:10.1038/ni1275 (2005).

17   Cyster, J. G. Chemokines and cell migration in secondary lymphoid organs. *Science (New York, N.Y.)* **286**, 2098-2102, doi:10.1126/science.286.5447.2098 (1999).

18   Moser, B. & Ebert, L. Lymphocyte traffic control by chemokines: follicular B helper T cells. *Immunology letters* **85**, 105-112 (2003).

19   Hansell, C. A., Simpson, C. V. & Nibbs, R. J. Chemokine sequestration by atypical chemokine receptors. *Biochemical Society transactions* **34**, 1009-1013, doi:10.1042/bst0341009 (2006).

20   Im, S. J. *et al.* Defining CD8+ T cells that provide the proliferative burst after PD-1 therapy. *Nature* **537**, 417-421, doi:10.1038/nature19330 (2016).

21   Mylvaganam, G. H. *et al.* Dynamics of SIV-specific CXCR5+ CD8 T cells during chronic SIV infection. *Proceedings of the National Academy of Sciences of the United States of America* **114**, 1976-1981, doi:10.1073/pnas.1621418114 (2017).

22   Jones, P. A. Functions of DNA methylation: islands, start sites, gene bodies and beyond. *Nature reviews. Genetics* **13**, 484-492, doi:10.1038/nrg3230 (2012).

23   Scharer, C. D., Barwick, B. G., Youngblood, B. A., Ahmed, R. & Boss, J. M. Global DNA methylation remodeling accompanies CD8 T cell effector function. *Journal of immunology (Baltimore, Md. : 1950)* **191**, 3419-3429, doi:10.4049/jimmunol.1301395 (2013).

24   Iwafuchi-Doi, M. & Zaret, K. S. Pioneer transcription factors in cell reprogramming. *Genes & development* **28**, 2679-2692, doi:10.1101/gad.253443.114 (2014).

25   Yu, B. *et al.* Erratum: Epigenetic landscapes reveal transcription factors that regulate CD8(+) T cell differentiation. *Nature immunology* **18**, 705, doi:10.1038/ni0617-705b (2017).

26   Collings, C. K. & Anderson, J. N. Links between DNA methylation and nucleosome occupancy in the human genome. *Epigenetics & chromatin* **10**, 18, doi:10.1186/s13072-017-0125-5 (2017).

27   Paulin, R., Grigg, G. W., Davey, M. W. & Piper, A. A. Urea improves efficiency of bisulphite-mediated sequencing of 5'-methylcytosine in genomic DNA. *Nucleic acids research* **26**, 5009-5010, doi:10.1093/nar/26.21.5009 (1998).

28   Allen, C. D. *et al.* Germinal center dark and light zone organization is mediated by CXCR4 and CXCR5. *Nature immunology* **5**, 943-952, doi:10.1038/ni1100 (2004).

29   Sloan, C. A. *et al.* ENCODE data at the ENCODE portal. *Nucleic acids research* **44**, D726-732, doi:10.1093/nar/gkv1160 (2016).

30   Robinson, M. D., McCarthy, D. J. & Smyth, G. K. edgeR: a Bioconductor package for differential expression analysis of digital gene expression data. *Bioinformatics (Oxford, England)* **26**, 139-140, doi:10.1093/bioinformatics/btp616 (2010).

31   Yu, G., Wang, L. G. & He, Q. Y. ChIPseeker: an R/Bioconductor package for ChIP peak annotation, comparison and visualization. *Bioinformatics (Oxford, England)* **31**, 2382-2383, doi:10.1093/bioinformatics/btv145 (2015).

32   Pimentel, H., Bray, N. L., Puente, S., Melsted, P. & Pachter, L. Differential analysis of RNA-seq incorporating quantification uncertainty. *Nature methods* **14**, 687-690, doi:10.1038/nmeth.4324 (2017).

33   Piper, J. *et al.* Wellington: a novel method for the accurate identification of digital genomic footprints from DNase-seq data. *Nucleic acids research* **41**, e201, doi:10.1093/nar/gkt850 (2013).

34   Gusmao, E. G., Allhoff, M., Zenke, M. & Costa, I. G. Analysis of computational footprinting methods for DNase sequencing experiments. *Nature methods* **13**, 303-309, doi:10.1038/nmeth.3772 (2016).

35   Kulakovskiy, I. V. *et al.* HOCOMOCO: towards a complete collection of transcription factor binding models for human and mouse via large-scale ChIP-Seq analysis. *Nucleic acids research* **46**, D252-d259, doi:10.1093/nar/gkx1106 (2018).

36   Khan, A. *et al.* JASPAR 2018: update of the open-access database of transcription factor binding profiles and its web framework. *Nucleic acids research* **46**, D1284, doi:10.1093/nar/gkx1188 (2018).

37   Storey, J. D. & Tibshirani, R. Statistical significance for genomewide studies. *Proceedings of the National Academy of Sciences of the United States of America* **100**, 9440-9445, doi:10.1073/pnas.1530509100 (2003).

38   Piper, J. *et al.* Wellington-bootstrap: differential DNase-seq footprinting identifies cell-type determining transcription factors. *BMC genomics* **16**, 1000, doi:10.1186/s12864-015-2081-4 (2015).

39   Langfelder, P. & Horvath, S. WGCNA: an R package for weighted correlation network analysis. *BMC bioinformatics* **9**, 559, doi:10.1186/1471-2105-9-559 (2008).

40   Love, M. I., Huber, W. & Anders, S. Moderated estimation of fold change and dispersion for RNA-seq data with DESeq2. *Genome biology* **15**, 550, doi:10.1186/s13059-014-0550-8 (2014).

41   Russo, P. S. T. *et al.* CEMiTool: a Bioconductor package for performing comprehensive modular co-expression analyses. *BMC bioinformatics* **19**, 56, doi:10.1186/s12859-018-2053-1 (2018).

42   Schep, A. N., Wu, B., Buenrostro, J. D. & Greenleaf, W. J. chromVAR: inferring transcription-factor-associated accessibility from single-cell epigenomic data. *Nature methods* **14**, 975-978, doi:10.1038/nmeth.4401 (2017).

43   Buggert, M. *et al.* Identification and characterization of HIV-specific resident memory CD8(+) T cells in human lymphoid tissue. *Science immunology* **3**, doi:10.1126/sciimmunol.aar4526 (2018).

44   Gerner, M. Y., Kastenmuller, W., Ifrim, I., Kabat, J. & Germain, R. N. Histo-cytometry: a method for highly multiplex quantitative tissue imaging analysis applied to dendritic cell subset microanatomy in lymph nodes. *Immunity* **37**, 364-376, doi:10.1016/j.immuni.2012.07.011 (2012).

45   Ferrando-Martinez, S. *et al.* Accumulation of follicular CD8+ T cells in pathogenic SIV infection. *The Journal of clinical investigation* **128**, 2089-2103, doi:10.1172/jci96207 (2018).

46   Johnston, R. J. *et al.* Bcl6 and Blimp-1 are reciprocal and antagonistic regulators of T follicular helper cell differentiation. *Science (New York, N.Y.)* **325**, 1006-1010, doi:10.1126/science.1175870 (2009).

47   Nurieva, R. I. *et al.* Bcl6 mediates the development of T follicular helper cells. *Science (New York, N.Y.)* **325**, 1001-1005, doi:10.1126/science.1176676 (2009).

48   Crotty, S., Johnston, R. J. & Schoenberger, S. P. Effectors and memories: Bcl-6 and Blimp-1 in T and B lymphocyte differentiation. *Nature immunology* **11**, 114-120, doi:10.1038/ni.1837 (2010).

49   Medvedeva, Y. A. *et al.* EpiFactors: a comprehensive database of human epigenetic factors and complexes. *Database : the journal of biological databases and curation* **2015**, bav067, doi:10.1093/database/bav067 (2015).

50   Litterst, C. M., Kliem, S., Marilley, D. & Pfitzner, E. NCoA-1/SRC-1 is an essential coactivator of STAT5 that binds to the FDL motif in the alpha-helical region of the STAT5 transactivation domain. *The Journal of biological chemistry* **278**, 45340-45351, doi:10.1074/jbc.M303644200 (2003).

51   Han, X. *et al.* Destabilizing LSD1 by Jade-2 promotes neurogenesis: an antibraking system in neural development. *Molecular cell* **55**, 482-494, doi:10.1016/j.molcel.2014.06.006 (2014).

52   Batista, I. A. A. & Helguero, L. A. Biological processes and signal transduction pathways regulated by the protein methyltransferase SETD7 and their

significance in cancer. *Signal transduction and targeted therapy* **3**, 19, doi:10.1038/s41392-018-0017-6 (2018).

53   Henning, A. N., Roychoudhuri, R. & Restifo, N. P. Epigenetic control of CD8(+) T cell differentiation. *Nature reviews. Immunology* **18**, 340-356, doi:10.1038/nri.2017.146 (2018).

54   Little, D. P., Braun, A., O'Donnell, M. J. & Koster, H. Mass spectrometry from miniaturized arrays for full comparative DNA analysis. *Nature medicine* **3**, 1413-1416 (1997).

55   Bocker, S. SNP and mutation discovery using base-specific cleavage and MALDI-TOF mass spectrometry. *Bioinformatics (Oxford, England)* **19 Suppl 1**, i44-53, doi:10.1093/bioinformatics/btg1004 (2003).

56   Hartmer, R. *et al.* RNase T1 mediated base-specific cleavage and MALDI-TOF MS for high-throughput comparative sequence analysis. *Nucleic acids research* **31**, e47, doi:10.1093/nar/gng047 (2003).

57   Stanssens, P. *et al.* High-throughput MALDI-TOF discovery of genomic sequence polymorphisms. *Genome research* **14**, 126-133, doi:10.1101/gr.1692304 (2004).

58   Ehrich, M. *et al.* Quantitative high-throughput analysis of DNA methylation patterns by base-specific cleavage and mass spectrometry. *Proceedings of the National Academy of Sciences of the United States of America* **102**, 15785-15790, doi:10.1073/pnas.0507816102 (2005).

59   Yang, J. *et al.* 5-Aza-2'-deoxycytidine, a DNA methylation inhibitor, induces cytotoxicity, cell cycle dynamics and alters expression of DNA methyltransferase 1 and 3A in mouse hippocampus-derived neuronal HT22 cells. *Journal of toxicology and environmental health. Part A* **80**, 1222-1229, doi:10.1080/15287394.2017.1367143 (2017).

60   Buenrostro, J. D., Giresi, P. G., Zaba, L. C., Chang, H. Y. & Greenleaf, W. J. Transposition of native chromatin for fast and sensitive epigenomic profiling of open chromatin, DNA-binding proteins and nucleosome position. *Nature methods* **10**, 1213-1218, doi:10.1038/nmeth.2688 (2013).

61   Winter, D. R., Jung, S. & Amit, I. Making the case for chromatin profiling: a new tool to investigate the immune-regulatory landscape. *Nature reviews. Immunology* **15**, 585-594, doi:10.1038/nri3884 (2015).

62   Choy, J. S. *et al.* DNA methylation increases nucleosome compaction and rigidity. *Journal of the American Chemical Society* **132**, 1782-1783, doi:10.1021/ja910264z (2010).

63   Wang, H. *et al.* Purification and functional characterization of a histone H3-lysine 4-specific methyltransferase. *Molecular cell* **8**, 1207-1217 (2001).

64   Wang, J. *et al.* The lysine demethylase LSD1 (KDM1) is required for maintenance of global DNA methylation. *Nature genetics* **41**, 125-129, doi:10.1038/ng.268 (2009).

65   Lee, M. T. *et al.* Nanog, Pou5f1 and SoxB1 activate zygotic gene expression during the maternal-to-zygotic transition. *Nature* **503**, 360-364, doi:10.1038/nature12632 (2013).

66   Leichsenring, M., Maes, J., Mossner, R., Driever, W. & Onichtchouk, D. Pou5f1 transcription factor controls zygotic gene activation in vertebrates. *Science (New York, N.Y.)* **341**, 1005-1009, doi:10.1126/science.1242527 (2013).

67   Iwafuchi-Doi, M. The mechanistic basis for chromatin regulation by pioneer transcription factors. *Wiley interdisciplinary reviews. Systems biology and medicine* **11**, e1427, doi:10.1002/wsbm.1427 (2019).

68   Chang, J. T., Wherry, E. J. & Goldrath, A. W. Molecular regulation of effector and memory T cell differentiation. *Nature immunology* **15**, 1104-1115, doi:10.1038/ni.3031 (2014).

69   Bulger, M. & Groudine, M. Functional and mechanistic diversity of distal transcription enhancers. *Cell* **144**, 327-339, doi:10.1016/j.cell.2011.01.024 (2011).

70   Yu, D. & Ye, L. A Portrait of CXCR5(+) Follicular Cytotoxic CD8(+) T cells. *Trends in immunology* **39**, 965-979, doi:10.1016/j.it.2018.10.002 (2018).

71   Lovkvist, C., Sneppen, K. & Haerter, J. O. Exploring the Link between Nucleosome Occupancy and DNA Methylation. *Frontiers in genetics* **8**, 232, doi:10.3389/fgene.2017.00232 (2017).

72   Svensson, J. P. *et al.* A nucleosome turnover map reveals that the stability of histone H4 Lys20 methylation depends on histone recycling in transcribed chromatin. *Genome research* **25**, 872-883, doi:10.1101/gr.188870.114 (2015).

73   Barisic, D., Stadler, M. B., Iurlaro, M. & Schubeler, D. Mammalian ISWI and SWI/SNF selectively mediate binding of distinct transcription factors. *Nature* **569**, 136-140, doi:10.1038/s41586-019-1115-5 (2019).

74   Benezra, R., Davis, R. L., Lockshon, D., Turner, D. L. & Weintraub, H. The protein Id: a negative regulator of helix-loop-helix DNA binding proteins. *Cell* **61**, 49-59, doi:10.1016/0092-8674(90)90214-y (1990).

75   Soufi, A., Donahue, G. & Zaret, K. S. Facilitators and impediments of the pluripotency reprogramming factors' initial engagement with the genome. *Cell* **151**, 994-1004, doi:10.1016/j.cell.2012.09.045 (2012).

76   Choi, J., Jeon, S., Choi, S., Park, K. & Seong, R. H. The SWI/SNF chromatin remodeling complex regulates germinal center formation by repressing Blimp-1 expression. *Proceedings of the National Academy of Sciences of the United States of America* **112**, E718-727, doi:10.1073/pnas.1418592112 (2015).

77   Menon, D. U., Shibata, Y., Mu, W. & Magnuson, T. Mammalian SWI/SNF collaborates with a polycomb-associated protein to regulate male germ line transcription in the mouse. *Development (Cambridge, England)*, doi:10.1242/dev.174094 (2019).

78   Li, M. *et al.* Dynamic regulation of transcription factors by nucleosome remodeling. *eLife* **4**, doi:10.7554/eLife.06249 (2015).

79   He, B. *et al.* CD8(+) T Cells Utilize Highly Dynamic Enhancer Repertoires and Regulatory Circuitry in Response to Infections. *Immunity* **45**, 1341-1354, doi:10.1016/j.immuni.2016.11.009 (2016).

80   Rodriguez, R. M. *et al.* Epigenetic Networks Regulate the Transcriptional Program in Memory and Terminally Differentiated CD8+ T Cells. *Journal of immunology (Baltimore, Md. : 1950)* **198**, 937-949, doi:10.4049/jimmunol.1601102 (2017).

81   Araki, Y. *et al.* Genome-wide analysis of histone methylation reveals chromatin state-based regulation of gene transcription and function of memory CD8+ T cells. *Immunity* **30**, 912-925, doi:10.1016/j.immuni.2009.05.006 (2009).

82   Araki, Y., Fann, M., Wersto, R. & Weng, N. P. Histone acetylation facilitates rapid and robust memory CD8 T cell response through differential expression of effector molecules (eomesodermin and its targets: perforin and granzyme B). *Journal of immunology (Baltimore, Md. : 1950)* **180**, 8102-8108, doi:10.4049/jimmunol.180.12.8102 (2008).

83   Russ, B. E. *et al.* Distinct epigenetic signatures delineate transcriptional programs during virus-specific CD8(+) T cell differentiation. *Immunity* **41**, 853-865, doi:10.1016/j.immuni.2014.11.001 (2014).

84   Crompton, J. G. *et al.* Lineage relationship of CD8(+) T cell subsets is revealed by progressive changes in the epigenetic landscape. *Cellular & molecular immunology* **13**, 502-513, doi:10.1038/cmi.2015.32 (2016).

CHAPTER 4

4.1   General Discussion

Studies on T-cell function among HIV-1 infected persons revealed new insights into previously unknown mechanisms of HIV-1 immunopathogenesis. Induction of HIV-1 specific CD8^{+} T cell responses is expected to eliminate or significantly and durably control HIV-1 infected cells. However, there are barriers to CD8^{+} T cell mediated elimination or control of HIV-1 infected cells including: (i) HIV-1 continuous evolution to escape detection by CD8^{+} T cells, (ii) reduced frequency of CD8^{+} T cells infiltrating the sites of HIV-1 reservoirs within the lymphoid tissues, and (iii) inactive state of CD8^{+} T cells in the lymphoid tissues. Therefore, for CD8^{+} T cells to eliminate active HIV-1 infected cells, these barriers need to be overcome.

CD8^{+} T cell responses in natural control of HIV-1 is associated with specific class I HLA alleles, like B*27, B*57 and B*81 [111,253]. Class I HLA alleles dictate which epitopes from HIV-1 are presented to and recognized by CD8^{+} T cells, and "protective" HLA alleles [254] drive potent and effective CD8^{+} T cell responses [255]. Interestingly, some HIV-1 Gag epitopes presented by the protective alleles are also presented by less protective alleles due to the homology in their peptide binding grove [56,60,151]. Thus, we first investigated the mechanism of HIV-1 control by peripheral CD8^{+} T cells when presented with identical immunodominant Gag epitopes restricted by protective and less protective alleles. We reported a unique population of CD8^{+} T cells with greater capacity to recognize variant TL9 epitopes, and this was associated with lower viral load in protective and less protective individuals.

Responses of antiviral CD8^{+} T cells with greater capacity to recognize variant HIV-1 epitopes depend on their ability to traffic into tissue sites of active viral replication [114,115]. Indeed, studies have identified B-cell follicles in the secondary lymphoid organs as significant reservoirs of residual HIV-1, even in individuals that naturally control viremia [82,83,121,184,185,256,257]. The viral persistence is, at least in part, due to the apparent absence of effective antiviral CD8^{+} T cells responses inside the B-cell follicles [82,121,184,258]. This deficiency is attributed to a relative inability of CD8^{+} T cells to effectively traffic to B cell follicles within the secondary lymphoid tissues and suppress HIV-1 replication [121,184,258]. The movement of CD8^{+} T cells to different anatomical locations within the secondary lymphoid tissues is directed by the interplay of chemokine receptors and their endothelial ligands [6]. The chemokine receptor CXCR5 guides cells into B cell follicles in response to CXCL13 [259]. The CXCR5 receptor is usually not expressed on most CD8^{+} T cell subsets, but is required for their migration into B cell follicles. Recent studies in humans and mice have demonstrated that few CD8^{+} T cells express CXCR5 [187,188]. However, another study demonstrated that CXCR5 expressing CD8^{+} T cells are located predominantly outside the B cell follicles (Im et al., 2016), partly due to lower expression of CXCR5 on CD8^{+} T cells as compared to GCTfh. Improving our understanding of how CD8^{+} T cells express CXCR5 will be useful for redirecting antiviral CD8^{+} T cells to B cell follicles to eliminate HIV-1 infected cells. In our second study, we investigated why most lymph nodes CD8^{+} T cells do not express CXCR5 and why there is reduced CXCR5 expression in fCD8s relative to the GCTfh. We reported that DNA hypermethylation and a closed chromatin structure at the transcription start site (*TSS*) of *CXCR5* gene repress CXCR5 expression in non-follicular CD8^{+} T cells (non-fCD8s). We also found that greater nucleosomal density at the *TSS* of *CXCR5* gene which could be a plausible

mechanism responsible for the reduced expression of CXCR5 in fCD8s relative to GCTfh.

4.2   Study Implications and Future Directions

Overall, our studies describe important immune parameters that are useful for: (1) HIV-1 vaccine design, and (2) functional cure approaches that seek to redirect CD8$^+$ T cells to the B cell follicles within the lymphoid tissues and eliminate HIV-1 reservoirs. Our first study identified an unexpected population of CD8$^+$ T cells that responded to TL9 when presented by protective HLA-B*81 and the less protective HLA-B*42, even in individuals who lacked one allele. This dual-HLA reactive response was more common in protective HLA-B*81-expressing individuals and it was associated with lower plasma viral loads, indicating that it may contribute to control of HIV-1 infection. Detailed analysis of TL9 specific CD8$^+$ TCRs uncovered genetic and functional similarities between HLA-B*81-derived CD8$^+$ T cell responses and dual-HLA reactive responses from B*42 individuals. Notably, TCR clones isolated from dual-reactive cells in B*42 individuals displayed a broader ability to recognize TL9 polymorphisms that contribute to immune evasion. This study provides a possible mechanism for lower viremia in individuals expressing HLA-B*81:01. Furthermore, we identified TL9 position 3 (Q3P) variant that selectively stimulates dual-reactive TCRs. It would be interesting to further examine *ex vivo* responses to this TL9 variant which could be included in immunogen design that could induce dual tetramer populations with broad TCR cross recognition, even in less protective individuals. The TCR clones we described in this study are more cross reactive, meaning that CD8$^+$ T cells harbouring such TCRs may be better equipped to respond to not just the epitopes encoded by

the infecting virus but also variant epitopes that arise due to HIV-1's virus escape from CD8$^+$ T cell recognition. Together, the dual-reactive CD8$^+$ T cells we described in this study that can cross recognize variant TL9 epitopes, are vital for HIV vaccine design. A vaccine that can induce effective cross reactive TCR clones might provide better protection against HIV-1 infection. Cross reactive CD8$^+$ T cells as such, may be important effectors for functional cure, where CD8$^+$ T cells of an infected individual are redirected to immune sanctuary sites of HIV-1 replication and eliminate HIV-1 infected cells presenting variant epitopes. Efforts to identify variant epitopes that can induce such cross reactive responses in HIV-1 infected individuals will be important for future studies.

In the second part of this thesis, we identified molecular mechanisms governing the expression of CXCR5 in human CD8$^+$ T cells. The hypermethylation of DNA and closed chromatin conformation we observed around the *TSS* of the *CXCR5* gene strongly suggesting that epigenetic mechanisms are involved in silencing of *CXCR5* gene in human CD8$^+$ T cells. The increased expression of *CXCR5* mRNA we observed after treatment with Aza drug, provide strong evidence that *CXCR5* gene in human CD8$^+$ T cells is silenced by DNA methylation. Efforts to directly target methyltransferases involved in the methylation of this region will be important for future studies. Transcriptional factors have instructive roles in lineage determination. Exploration of *BCL6* gene, a known master regulator of CXCR5 expression in mice studies, revealed no difference between human fCD8s and non-fCD8s, suggesting that additional or different regulators maybe involved in the expression of CXCR5 in human CD8$^+$ T cells. Consistent with this notion, lower expression of *Id3*; a known established positive co-regulator of the *CXCR5 gene* was also observed in fCD8s compared to GCTfh. This further strengthens the notion that additional regulators may

be involved in expression of CXCR5 in human CD8$^+$ T cells. The *MAF* and *POU3F1* we observed in our study to be significantly upregulated in fCD8s compared to non-fCD8 and the upstream 2 (*U2*) with significant transcriptional activity of these factors in fCD8s gave us an insight on the regulation of the *CXCR5* gene in human CD8$^+$ T cells. Our studies indicate that the *U2* region may be an enhancer region for the *CXCR5* gene and cross-talk between the bound TFs in *U2* and the *TSS* could be an important pathway in the establishment of CXCR5 expression in human CD8$^+$ T cells. Another striking finding from our gene expression analysis was the differential expression of epigenetic factors between fCD8s and non-fCD8s, which further confirms the role of epigenetic mechanisms in the regulation of the *CXCR5* gene in human CD8$^+$ T cells. It makes sense that CD8$^+$ T cells in the lymph nodes should be epigenetically and transcriptionally programmed to silence the expression of CXCR5, because they could interfere with the process of affinity maturation of antibody-producing cells. Thus, failure of the majority of CD8$^+$ T cells to express CXCR5 during differentiation within lymphoid tissues likely results from the normal biology of lymphoid tissue microenvironment. Through this study, we have been able to identify some important epigenetic parameters that will need to be tested in the future studies to assess their roles in enhancing the expression of CXCR5 in human CD8$^+$ T cells.

It is important to note that the expression level of CXCR5 on fCD8s is lower when compared to GCTfh. The theory that nucleosomes and transcription factors (TFs) compete for access to DNA by regulatory machineries [260] holds in our study because we observed an increase in nucleosomal occupancy at the *TSS* region of *CXCR5* gene in fCD8s which was not present in GCTfh. This could be the reason why CXCR5 expression in fCD8s is lower compared to GCTfh, and lower expression of CXCR5 in fCD8s could impact localization of CD8$^+$ T cells to B cell follicles. Efforts to interrupt

nucleosome positioning at the *TSS* region of the *CXCR5* gene could enhance CXCR5 expression levels on CD8^{+} T cells and facilitate their migration to the B cell follicles. These findings have implications for HIV cure strategy that seek to redirect CD8^{+} T cells to B cell follicles and eliminate HIV reservoirs.

4.3   Concluding Remarks

The novel CD8^{+} T cell population we described in our first study highlights one of the mechanisms by which CD8^{+} T cell control HIV-1 infection. We have demonstrated that the CD8^{+} T cell receptor in protective individuals are better equipped at cross-recognizing epitope variant of immunodominant Gag-p24 TL9. A fraction of CD8^{+} T cells in less protective individuals harbouring such unique TCRs can be boosted, thus enhancing HIV-1 control. We identified TL9-epitope variants that can possibly be used to induce such novel populations even in less protective individuals. The novel CD8^{+} T cell population we described here is relevant for the design of HIV-1 vaccines.

In our second study, we described the pathways involved in the tight regulation of CXCR5 expression in human CD8^{+} T cells. We identified unique epigenetic mechanisms involved in repression of CXCR5 in human CD8^{+} T cells. We demonstrated that DNA methylation directly contributes to the tight regulation of CXCR5 expression in human CD8^{+} T cells. We also described the role of chromatin architecture in the regulation of *CXCR5* gene. Additionally, we computationally demonstrated the interference of nucleosome with transcriptional machineries in fCD8s. Together, our second study identified unique pathways involved in the tight regulation of the *CXCR5* gene in human CD8^{+} T cells. Efforts to interrupt pathways that antagonize the expression of CXCR5 in human CD8^{+} T cells will be important for

engineering CXCR5$^+$CD8$^+$ T cells that can safely infiltrate the B cell follicles and eliminate HIV-1 reservoirs.

In summary, we have described a novel mechanism by which HLA class I-restricted CD8$^+$ T cell responses contribute substantially to the control of HIV-1 replication in HIV-1 infected individuals. We also described molecular events limiting the recruitment of effector CD8$^+$ T cells to sites of HIV-1 persistence even during ART. Findings from these studies are useful in the generation of effective CD8$^+$ T cells with broad recognition of a highly variable pathogen, such as HIV-1 and for redirecting effector CD8$^+$ T cells to sites where they are needed to clear viral reservoirs. This information is useful for T cell based vaccine design and for functional cure strategies aimed at eliminating HIV-1 reservoirs from immune privilege sites, such as B cell follicles. Validation of the parameters highlighted in these studies should be an important focus for future studies.

4.4   References

1   De Cock, K. M., Jaffe, H. W. & Curran, J. W. The evolving epidemiology of HIV/AIDS. *Aids* **26**, 1205-1213, doi:10.1097/QAD.0b013e328354622a (2012).

2   UNAIDS. UNAIDS report on global AIDS epidemic update

. (2018).

3   Nyamweya, S. *et al.* Comparing HIV-1 and HIV-2 infection: Lessons for viral immunopathogenesis. *Reviews in medical virology* **23**, 221-240, doi:10.1002/rmv.1739 (2013).

4   Taylor, B. S. & Hammer, S. M. The challenge of HIV-1 subtype diversity. *The New England journal of medicine* **359**, 1965-1966, doi:10.1056/NEJMc086373 (2008).

5   Avert. Global information and education on HIV and AIDS. (2019).

6   Douek, D. C., Picker, L. J. & Koup, R. A. T cell dynamics in HIV-1 infection. *Annual review of immunology* **21**, 265-304, doi:10.1146/annurev.immunol.21.120601.141053 (2003).

7   Yuki, Y., Nochi, T. & Kiyono, H. Progress towards an AIDS mucosal vaccine: an overview. *Tuberculosis (Edinburgh, Scotland)* **87 Suppl 1**, S35-44, doi:10.1016/j.tube.2007.05.005 (2007).

8   Doms, R. W. Chemokine receptors and HIV entry. *Aids* **15 Suppl 1**, S34-35 (2001).

9   Munier, M. L. & Kelleher, A. D. Acutely dysregulated, chronically disabled by the enemy within: T-cell responses to HIV-1 infection. *Immunol Cell Biol* **85**, 6-15 (2007).

10   McMichael, A. J., Borrow, P., Tomaras, G. D., Goonetilleke, N. & Haynes, B. F. The immune response during acute HIV-1 infection: clues for vaccine development. *Nat Rev Immunol* **10**, 11-23 (2010).

11   Altfeld, M. & Walker, B. D. Less is more? STI in acute and chronic HIV-1 infection. *Nat Med* **7**, 881-884 (2001).

12   Mogensen, T. H., Melchjorsen, J., Larsen, C. S. & Paludan, S. R. Innate immune recognition and activation during HIV infection. *Retrovirology* **7**, 1742-4690 (2010).

13   Borrow, P., Lewicki, H., Hahn, B. H., Shaw, G. M. & Oldstone, M. B. Virus-specific CD8+ cytotoxic T-lymphocyte activity associated with control of viremia in primary human immunodeficiency virus type 1 infection. *Journal of virology* **68**, 6103-6110 (1994).

14   Koup, R. A. *et al.* Temporal association of cellular immune responses with the initial control of viremia in primary human immunodeficiency virus type 1 syndrome. *J Virol* **68**, 4650-4655 (1994).

15   Pantaleo, G. *et al.* Major expansion of CD8+ T cells with a predominant V beta usage during the primary immune response to HIV. *Nature* **370**, 463-467 (1994).

16   Wilson, J. D. *et al.* Direct visualization of HIV-1-specific cytotoxic T lymphocytes during primary infection. *Aids* **14**, 225-233 (2000).

17   Ndhlovu, Z. M. *et al.* Magnitude and Kinetics of CD8(+) T Cell Activation during Hyperacute HIV Infection Impact Viral Set Point. *Immunity* **43**, 591-604, doi:10.1016/j.immuni.2015.08.012 (2015).

18   Ndhlovu, Z. M. *et al.* Magnitude and Kinetics of CD8+ T Cell Activation during Hyperacute HIV Infection Impact Viral Set Point. *Immunity* **43**, 591-604, doi:10.1016/j.immuni.2015.08.012 (2015).

19   Bernardin, F., Kong, D., Peddada, L., Baxter-Lowe, L. A. & Delwart, E. Human immunodeficiency virus mutations during the first month of infection are preferentially found in known cytotoxic T-lymphocyte epitopes. *J Virol* **79**, 11523-11528, doi:10.1128/jvi.79.17.11523-11528.2005 (2005).

20   Salazar-Gonzalez, J. F. *et al.* Genetic identity, biological phenotype, and evolutionary pathways of transmitted/founder viruses in acute and early HIV-1 infection. *J Exp Med* **206**, 1273-1289, doi:10.1084/jem.20090378 (2009).

21   Appay, V. & Sauce, D. Immune activation and inflammation in HIV-1 infection: causes and consequences. *J Pathol* **214**, 231-241 (2008).

22   Paranjape, R. S. Immunopathogenesis of HIV infection. *Indian J Med Res* **121**, 240-255 (2005).

23   Derdeyn, C. A. & Silvestri, G. Viral and host factors in the pathogenesis of HIV infection. *Curr Opin Immunol* **17**, 366-373 (2005).

24   Chatterjee, K. Host genetic factors in susceptibility to HIV-1 infection and progression to AIDS. *J Genet* **89**, 109-116 (2010).

25   Mueller, Y. M. *et al.* Increased CD95/Fas-induced apoptosis of HIV-specific CD8(+) T cells. *Immunity* **15**, 871-882 (2001).

26   Kostense, S. *et al.* Persistent numbers of tetramer+ CD8(+) T cells, but loss of interferon-gamma+ HIV-specific T cells during progression to AIDS. *Blood* **99**, 2505-2511 (2002).

27   Phair, J. P. Determinants of the natural history of human immunodeficiency virus type 1 infection. *The Journal of infectious diseases* **179 Suppl 2**, S384-386, doi:10.1086/513839 (1999).

28   Cohen, D. E. & Walker, B. D. Human immunodeficiency virus pathogenesis and prospects for immune control in patients with established infection. *Clinical infectious diseases : an official publication of the Infectious Diseases Society of America* **32**, 1756-1768, doi:10.1086/320759 (2001).

29   Lehmann-Grube, F., Assmann, U., Loliger, C., Moskophidis, D. & Lohler, J. Mechanism of recovery from acute virus infection. I. Role of T lymphocytes in the clearance of lymphocytic choriomeningitis virus from spleens of mice. *J Immunol* **134**, 608-615 (1985).

30   Walker, B. D. *et al.* HIV-specific cytotoxic T lymphocytes in seropositive individuals. *Nature* **328**, 345-348 (1987).

31   Plata, F. *et al.* AIDS virus-specific cytotoxic T lymphocytes in lung disorders. *Nature* **328**, 348-351 (1987).

32   Nixon, D. F. *et al.* HIV-1 gag-specific cytotoxic T lymphocytes defined with recombinant vaccinia virus and synthetic peptides. *Nature* **336**, 484-487 (1988).

33   Dalod, M. *et al.* Weak anti-HIV CD8(+) T-cell effector activity in HIV primary infection. *J Clin Invest* **104**, 1431-1439 (1999).

34   Maecker, H. T. *et al.* Use of overlapping peptide mixtures as antigens for cytokine flow cytometry. *J Immunol Methods* **255**, 27-40 (2001).

35   Altman, J. D. *et al.* Phenotypic analysis of antigen-specific T lymphocytes. *Science (New York, N.Y.)* **274**, 94-96 (1996).

36   Ogg, G. S. *et al.* Quantitation of HIV-1-specific cytotoxic T lymphocytes and plasma load of viral RNA. *Science (New York, N.Y.)* **279**, 2103-2106, doi:10.1126/science.279.5359.2103 (1998).

37   Hersperger, A. R. *et al.* Perforin expression directly ex vivo by HIV-specific CD8 T-cells is a correlate of HIV elite control. *PLoS pathogens* **6**, e1000917, doi:10.1371/journal.ppat.1000917 (2010).

38   Gandhi, R. T. & Walker, B. D. Immunologic control of HIV-1. *Annu Rev Med* **53**, 149-172 (2002).

39   Rouvier, E., Luciani, M. F. & Golstein, P. Fas involvement in Ca(2+)-independent T cell-mediated cytotoxicity. *The Journal of experimental medicine* **177**, 195-200, doi:10.1084/jem.177.1.195 (1993).

40   Demers, K. R., Reuter, M. A. & Betts, M. R. CD8(+) T-cell effector function and transcriptional regulation during HIV pathogenesis. *Immunological reviews* **254**, 190-206, doi:10.1111/imr.12069 (2013).

41   Kagi, D. *et al.* Fas and perforin pathways as major mechanisms of T cell-mediated cytotoxicity. *Science (New York, N.Y.)* **265**, 528-530 (1994).

42   Betts, M. R. *et al.* HIV nonprogressors preferentially maintain highly functional HIV-specific CD8+ T cells. *Blood* **107**, 4781-4789, doi:10.1182/blood-2005-12-4818 (2006).

43   Streeck, H. *et al.* Antigen load and viral sequence diversification determine the functional profile of HIV-1-specific CD8+ T cells. *PLoS medicine* **5**, e100, doi:10.1371/journal.pmed.0050100 (2008).

44   Hersperger, A. R. *et al.* Increased HIV-specific CD8+ T-cell cytotoxic potential in HIV elite controllers is associated with T-bet expression. *Blood* **117**, 3799-3808, doi:10.1182/blood-2010-12-322727 (2011).

45   Yewdell, J. W., Reits, E. & Neefjes, J. Making sense of mass destruction: quantitating MHC class I antigen presentation. *Nat Rev Immunol* **3**, 952-961 (2003).

46   Jixin Zhong, J.-F. X., Ping Yang, Yi Liang and Cong-Yi Wang. Innate Immunity in the Recognition of β-Cell Antigens in Type 1 Diabetes, Type 1 Diabetes - Pathogenesis, Genetics and Immunotherapy. doi:10.5772/22264 (2011).

47   Davis, S. J. & van der Merwe, P. A. The structure and ligand interactions of CD2: implications for T-cell function. *Immunol Today* **17**, 177-187 (1996).

48   Turner, S. J., Doherty, P. C., McCluskey, J. & Rossjohn, J. Structural determinants of T-cell receptor bias in immunity. *Nature reviews. Immunology* **6**, 883-894, doi:10.1038/nri1977 (2006).

49   Rudolph, M. G., Stanfield, R. L. & Wilson, I. A. How TCRs bind MHCs, peptides, and coreceptors. *Annu Rev Immunol* **24**, 419-466 (2006).

50   Price, D. A. *et al.* T cell receptor recognition motifs govern immune escape patterns in acute SIV infection. *Immunity* **21**, 793-803 (2004).

51   Varela-Rohena, A. *et al.* Control of HIV-1 immune escape by CD8 T cells expressing enhanced T-cell receptor. *Nat Med* **14**, 1390-1395 (2008).

52   Chen, H. *et al.* TCR clonotypes modulate the protective effect of HLA class I molecules in HIV-1 infection. *Nat Immunol* **13**, 691-700 (2012).

53   Zoete, V., Irving, M., Ferber, M., Cuendet, M. A. & Michielin, O. Structure-Based, Rational Design of T Cell Receptors. *Frontiers in immunology* **4**, 268, doi:10.3389/fimmu.2013.00268 (2013).

54   Goulder, P. J. & Watkins, D. I. Impact of MHC class I diversity on immune control of immunodeficiency virus replication. *Nat Rev Immunol* **8**, 619-630 (2008).

55   Wright, J. K. *et al.* Impact of HLA-B*81-associated mutations in HIV-1 Gag on viral replication capacity. *Journal of virology* **86**, 3193-3199, doi:10.1128/jvi.06682-11 (2012).

56   Sidney, J., Peters, B., Frahm, N., Brander, C. & Sette, A. HLA class I supertypes: a revised and updated classification. *BMC Immunol* **9**, 1471-2172 (2008).

57   Madden, D. R. The three-dimensional structure of peptide-MHC complexes. *Annu Rev Immunol* **13**, 587-622 (1995).

58   Khan, A. R., Baker, B. M., Ghosh, P., Biddison, W. E. & Wiley, D. C. The structure and stability of an HLA-A*0201/octameric tax peptide complex with an empty conserved peptide-N-terminal binding site. *J Immunol* **164**, 6398-6405 (2000).

59   Mungall, A. J. *et al.* The DNA sequence and analysis of human chromosome 6. *Nature* **425**, 805-811 (2003).

60   Sette, A. & Sidney, J. Nine major HLA class I supertypes account for the vast preponderance of HLA-A and -B polymorphism. *Immunogenetics* **50**, 201-212 (1999).

61   Klein, J. & Sato, A. The HLA system. First of two parts. *N Engl J Med* **343**, 702-709 (2000).

62   Walker, B. & McMichael, A. The T-cell response to HIV. *Cold Spring Harbor perspectives in medicine* **2**, doi:10.1101/cshperspect.a007054 (2012).

63   Whitney, J. B. *et al.* Rapid seeding of the viral reservoir prior to SIV viraemia in rhesus monkeys. *Nature* **512**, 74-77, doi:10.1038/nature13594 (2014).

64   Goonetilleke, N. *et al.* The first T cell response to transmitted/founder virus contributes to the control of acute viremia in HIV-1 infection. *The Journal of experimental medicine* **206**, 1253-1272, doi:10.1084/jem.20090365 (2009).

65   Kim, J. *et al.* CD8(+) Cytotoxic T Lymphocyte Responses and Viral Epitope Escape in Acute HIV-1 Infection. *Viral immunology* **31**, 525-536, doi:10.1089/vim.2018.0040 (2018).

66   Yang, O. O. *et al.* Suppression of human immunodeficiency virus type 1 replication by CD8+ cells: evidence for HLA class I-restricted triggering of cytolytic and noncytolytic mechanisms. *Journal of virology* **71**, 3120-3128 (1997).

67   Chen, H. *et al.* Differential neutralization of human immunodeficiency virus (HIV) replication in autologous CD4 T cells by HIV-specific cytotoxic T lymphocytes. *Journal of virology* **83**, 3138-3149, doi:10.1128/jvi.02073-08 (2009).

68   Schmitz, J. E. *et al.* Control of viremia in simian immunodeficiency virus infection by CD8+ lymphocytes. *Science (New York, N.Y.)* **283**, 857-860 (1999).

69   Jin, X. *et al.* Dramatic rise in plasma viremia after CD8(+) T cell depletion in simian immunodeficiency virus-infected macaques. *The Journal of experimental medicine* **189**, 991-998, doi:10.1084/jem.189.6.991 (1999).

70   Schmitz, J. E. *et al.* Effect of CD8+ lymphocyte depletion on virus containment after simian immunodeficiency virus SIVmac251 challenge of live attenuated SIVmac239delta3-vaccinated rhesus macaques. *J Virol* **79**, 8131-8141 (2005).

71   Altfeld, M. *et al.* Cellular immune responses and viral diversity in individuals treated during acute and early HIV-1 infection. *J Exp Med* **193**, 169-180 (2001).

72   Cao, J. *et al.* Comprehensive analysis of human immunodeficiency virus type 1 (HIV-1)-specific gamma interferon-secreting CD8+ T cells in primary HIV-1 infection. *J Virol* **77**, 6867-6878 (2003).

73   Radebe, M. *et al.* Limited immunogenicity of HIV CD8+ T-cell epitopes in acute Clade C virus infection. *J Infect Dis* **204**, 768-776 (2011).

74   Altfeld, M. *et al.* Expansion of pre-existing, lymph node-localized CD8+ T cells during supervised treatment interruptions in chronic HIV-1 infection. *The Journal of clinical investigation* **109**, 837-843, doi:10.1172/jci14789 (2002).

75   Koibuchi, T. *et al.* Limited sequence evolution within persistently targeted CD8 epitopes in chronic human immunodeficiency virus type 1 infection. *J Virol* **79**, 8171-8181 (2005).

76   Reuter, M. A. *et al.* HIV-Specific CD8(+) T Cells Exhibit Reduced and Differentially Regulated Cytolytic Activity in Lymphoid Tissue. *Cell reports* **21**, 3458-3470, doi:10.1016/j.celrep.2017.11.075 (2017).

77   Bogle, G. & Dunbar, P. R. Agent-based simulation of T-cell activation and proliferation within a lymph node. *Immunology and cell biology* **88**, 172-179, doi:10.1038/icb.2009.78 (2010).

78   Willard-Mack, C. L. Normal structure, function, and histology of lymph nodes. *Toxicologic pathology* **34**, 409-424, doi:10.1080/01926230600867727 (2006).

79   Abbas, A. K., Murphy, K. M. & Sher, A. Functional diversity of helper T lymphocytes. *Nature* **383**, 787-793 (1996).

80   Roderick Nairn., M. H. *Immunology for Medical Students*. 2nd edition edn, 108-120 (Elsevier, 2007).

81   Andersson, J. *et al.* Low levels of perforin expression in CD8+ T lymphocyte granules in lymphoid tissue during acute human immunodeficiency virus type 1 infection. *The Journal of infectious diseases* **185**, 1355-1358, doi:10.1086/340124 (2002).

82   Folkvord, J. M., Armon, C. & Connick, E. Lymphoid follicles are sites of heightened human immunodeficiency virus type 1 (HIV-1) replication and reduced antiretroviral effector mechanisms. *AIDS research and human retroviruses* **21**, 363-370, doi:10.1089/aid.2005.21.363 (2005).

83   Banga, R. *et al.* PD-1(+) and follicular helper T cells are responsible for persistent HIV-1 transcription in treated aviremic individuals. *Nature medicine* **22**, 754-761, doi:10.1038/nm.4113 (2016).

84   Perreau, M. *et al.* Follicular helper T cells serve as the major CD4 T cell compartment for HIV-1 infection, replication, and production. *The Journal of experimental medicine* **210**, 143-156, doi:10.1084/jem.20121932 (2013).

85   Kaech, S. M. & Cui, W. Transcriptional control of effector and memory CD8+ T cell differentiation. *Nature reviews. Immunology* **12**, 749-761, doi:10.1038/nri3307 (2012).

86   Schluns, K. S., Kieper, W. C., Jameson, S. C. & Lefrancois, L. Interleukin-7 mediates the homeostasis of naive and memory CD8 T cells in vivo. *Nature immunology* **1**, 426-432, doi:10.1038/80868 (2000).

87   Joshi, N. S. & Kaech, S. M. Effector CD8 T cell development: a balancing act between memory cell potential and terminal differentiation. *Journal of immunology (Baltimore, Md. : 1950)* **180**, 1309-1315 (2008).

88   Surh, C. D. & Sprent, J. Homeostasis of naive and memory T cells. *Immunity* **29**, 848-862, doi:10.1016/j.immuni.2008.11.002 (2008).

89   Joshi, N. S. *et al.* Inflammation directs memory precursor and short-lived effector CD8(+) T cell fates via the graded expression of T-bet transcription factor. *Immunity* **27**, 281-295, doi:10.1016/j.immuni.2007.07.010 (2007).

90   Intlekofer, A. M. *et al.* Requirement for T-bet in the aberrant differentiation of unhelped memory CD8+ T cells. *The Journal of experimental medicine* **204**, 2015-2021, doi:10.1084/jem.20070841 (2007).

91   Pipkin, M. E. *et al.* Interleukin-2 and inflammation induce distinct transcriptional programs that promote the differentiation of effector cytolytic T cells. *Immunity* **32**, 79-90, doi:10.1016/j.immuni.2009.11.012 (2010).

92   Sullivan, B. M., Juedes, A., Szabo, S. J., von Herrath, M. & Glimcher, L. H. Antigen-driven effector CD8 T cell function regulated by T-bet. *Proceedings of the National Academy of Sciences of the United States of America* **100**, 15818-15823, doi:10.1073/pnas.2636938100 (2003).

93   Takemoto, N., Intlekofer, A. M., Northrup, J. T., Wherry, E. J. & Reiner, S. L. Cutting Edge: IL-12 inversely regulates T-bet and eomesodermin expression during pathogen-induced CD8+ T cell differentiation. *Journal of immunology (Baltimore, Md. : 1950)* **177**, 7515-7519, doi:10.4049/jimmunol.177.11.7515 (2006).

94   Joshi, N. S. *et al.* Increased numbers of preexisting memory CD8 T cells and decreased T-bet expression can restrain terminal differentiation of secondary effector and memory CD8 T cells. *Journal of immunology (Baltimore, Md. : 1950)* **187**, 4068-4076, doi:10.4049/jimmunol.1002145 (2011).

95   Banerjee, A. *et al.* Cutting edge: The transcription factor eomesodermin enables CD8+ T cells to compete for the memory cell niche. *Journal of immunology (Baltimore, Md. : 1950)* **185**, 4988-4992, doi:10.4049/jimmunol.1002042 (2010).

96   Henning, A. N., Roychoudhuri, R. & Restifo, N. P. Epigenetic control of CD8(+) T cell differentiation. *Nature reviews. Immunology* **18**, 340-356, doi:10.1038/nri.2017.146 (2018).

97   Ball, M. P. *et al.* Targeted and genome-scale strategies reveal gene-body methylation signatures in human cells. *Nature biotechnology* **27**, 361-368, doi:10.1038/nbt.1533 (2009).

98   Jones, P. A. Functions of DNA methylation: islands, start sites, gene bodies and beyond. *Nature reviews. Genetics* **13**, 484-492, doi:10.1038/nrg3230 (2012).

99   Scharer, C. D., Barwick, B. G., Youngblood, B. A., Ahmed, R. & Boss, J. M. Global DNA methylation remodeling accompanies CD8 T cell effector function. *Journal of immunology (Baltimore, Md. : 1950)* **191**, 3419-3429, doi:10.4049/jimmunol.1301395 (2013).

100   Rodriguez, R. M. *et al.* Epigenetic Networks Regulate the Transcriptional Program in Memory and Terminally Differentiated CD8+ T Cells. *Journal of*

immunology (Baltimore, Md. : 1950) **198**, 937-949, doi:10.4049/jimmunol.1601102 (2017).

101   Abdelsamed, H. A. *et al.* Human memory CD8 T cell effector potential is epigenetically preserved during in vivo homeostasis. *The Journal of experimental medicine* **214**, 1593-1606, doi:10.1084/jem.20161760 (2017).

102   He, B. *et al.* CD8(+) T Cells Utilize Highly Dynamic Enhancer Repertoires and Regulatory Circuitry in Response to Infections. *Immunity* **45**, 1341-1354, doi:10.1016/j.immuni.2016.11.009 (2016).

103   Nguyen, M. L. *et al.* Dynamic regulation of permissive histone modifications and GATA3 binding underpin acquisition of granzyme A expression by virus-specific CD8(+) T cells. *European journal of immunology* **46**, 307-318, doi:10.1002/eji.201545875 (2016).

104   Youngblood, B. *et al.* Cutting edge: Prolonged exposure to HIV reinforces a poised epigenetic program for PD-1 expression in virus-specific CD8 T cells. *Journal of immunology (Baltimore, Md. : 1950)* **191**, 540-544, doi:10.4049/jimmunol.1203161 (2013).

105   Youngblood, B., Hale, J. S. & Ahmed, R. T-cell memory differentiation: insights from transcriptional signatures and epigenetics. *Immunology* **139**, 277-284, doi:10.1111/imm.12074 (2013).

106   Zhang, F. *et al.* Epigenetic manipulation restores functions of defective CD8(+) T cells from chronic viral infection. *Molecular therapy : the journal of the American Society of Gene Therapy* **22**, 1698-1706, doi:10.1038/mt.2014.91 (2014).

107   Nag, M., De Paris, K. & J, E. F. Epigenetic Modulation of CD8(+) T Cell Function in Lentivirus Infections: A Review. *Viruses* **10**, doi:10.3390/v10050227 (2018).

108   Slaney, C. Y., Kershaw, M. H. & Darcy, P. K. Trafficking of T cells into tumors. *Cancer research* **74**, 7168-7174, doi:10.1158/0008-5472.Can-14-2458 (2014).

109   Chen, A., Engel, P. & Tedder, T. F. Structural requirements regulate endoproteolytic release of the L-selectin (CD62L) adhesion receptor from the cell surface of leukocytes. *The Journal of experimental medicine* **182**, 519-530, doi:10.1084/jem.182.2.519 (1995).

110   Nolz, J. C. Molecular mechanisms of CD8(+) T cell trafficking and localization. *Cellular and molecular life sciences : CMLS* **72**, 2461-2473, doi:10.1007/s00018-015-1835-0 (2015).

111   Kiepiela, P. *et al.* Dominant influence of HLA-B in mediating the potential co-evolution of HIV and HLA. *Nature* **432**, 769-775, doi:10.1038/nature03113 (2004).

112   Wright, J. K. *et al.* Gag-protease-mediated replication capacity in HIV-1 subtype C chronic infection: associations with HLA type and clinical parameters. *Journal of virology* **84**, 10820-10831, doi:10.1128/JVI.01084-10 (2010).

113   Carlson, J. M. *et al.* HIV transmission. Selection bias at the heterosexual HIV-1 transmission bottleneck. *Science (New York, N.Y.)* **345**, 1254031, doi:10.1126/science.1254031 (2014).

114   Cerwenka, A., Morgan, T. M. & Dutton, R. W. Naive, effector, and memory CD8 T cells in protection against pulmonary influenza virus infection: homing properties rather than initial frequencies are crucial. *Journal of immunology (Baltimore, Md. : 1950)* **163**, 5535-5543 (1999).

115   Cerwenka, A., Morgan, T. M., Harmsen, A. G. & Dutton, R. W. Migration kinetics and final destination of type 1 and type 2 CD8 effector cells predict protection against pulmonary virus infection. *The Journal of experimental medicine* **189**, 423-434, doi:10.1084/jem.189.2.423 (1999).

116   Charo, I. F. & Ransohoff, R. M. The many roles of chemokines and chemokine receptors in inflammation. *The New England journal of medicine* **354**, 610-621, doi:10.1056/NEJMra052723 (2006).

117   Luster, A. D., Alon, R. & von Andrian, U. H. Immune cell migration in inflammation: present and future therapeutic targets. *Nature immunology* **6**, 1182-1190, doi:10.1038/ni1275 (2005).

118   Cohen, O. J. *et al.* Pathogenic insights from studies of lymphoid tissue from HIV-infected individuals. *Journal of acquired immune deficiency syndromes and human retrovirology : official publication of the International Retrovirology Association* **10 Suppl 1**, S6-14 (1995).

119   Pantaleo, G. & Fauci, A. S. New concepts in the immunopathogenesis of HIV infection. *Annual review of immunology* **13**, 487-512, doi:10.1146/annurev.iy.13.040195.002415 (1995).

120   Iyengar, S., Chin, B., Margolick, J. B., Sabundayo, B. P. & Schwartz, D. H. Anatomical loci of HIV-associated immune activation and association with viraemia. *Lancet (London, England)* **362**, 945-950, doi:10.1016/s0140-6736(03)14363-2 (2003).

121   Connick, E. *et al.* CTL fail to accumulate at sites of HIV-1 replication in lymphoid tissue. *Journal of immunology (Baltimore, Md. : 1950)* **178**, 6975-6983 (2007).

122   Deeks, S. G. & Walker, B. D. Human immunodeficiency virus controllers: mechanisms of durable virus control in the absence of antiretroviral therapy. *Immunity* **27**, 406-416, doi:10.1016/j.immuni.2007.08.010 (2007).

123   Migueles, S. A. & Connors, M. Long-term nonprogressive disease among untreated HIV-infected individuals: clinical implications of understanding immune control of HIV. *Jama* **304**, 194-201, doi:10.1001/jama.2010.925 (2010).

124   Frater, A. J. *et al.* Effective T-cell responses select human immunodeficiency virus mutants and slow disease progression. *J Virol* **81**, 6742-6751, doi:10.1128/JVI.00022-07 (2007).

125   Kawashima, Y. *et al.* Adaptation of HIV-1 to human leukocyte antigen class I. *Nature* **458**, 641-645, doi:10.1038/nature07746 (2009).

126   Migueles, S. A. *et al.* HLA B*5701 is highly associated with restriction of virus replication in a subgroup of HIV-infected long term nonprogressors. *Proceedings of the National Academy of Sciences of the United States of America* **97**, 2709-2714, doi:10.1073/pnas.050567397 (2000).

127   Kaslow, R. A. *et al.* Influence of combinations of human major histocompatibility complex genes on the course of HIV-1 infection. *Nature medicine* **2**, 405-411 (1996).

128   Gao, X. *et al.* Effect of a single amino acid change in MHC class I molecules on the rate of progression to AIDS. *The New England journal of medicine* **344**, 1668-1675, doi:10.1056/nejm200105313442203 (2001).

129   Draenert, R. *et al.* Constraints on HIV-1 evolution and immunodominance revealed in monozygotic adult twins infected with the same virus. *J Exp Med* **203**, 529-539 (2006).

130   Kosmrlj, A. *et al.* Effects of thymic selection of the T-cell repertoire on HLA class I-associated control of HIV infection. *Nature* **465**, 350-354, doi:10.1038/nature08997 (2010).

131   Leslie, A. J. *et al.* HIV evolution: CTL escape mutation and reversion after transmission. *Nat Med* **10**, 282-289 (2004).

132   Crawford, H. *et al.* Evolution of HLA-B*5703 HIV-1 escape mutations in HLA-B*5703-positive individuals and their transmission recipients. *J Exp Med* **206**, 909-921, doi:10.1084/jem.20081984 (2009).

133   Kiepiela, P. *et al.* CD8+ T-cell responses to different HIV proteins have discordant associations with viral load. *Nature medicine* **13**, 46-53, doi:10.1038/nm1520 (2007).

134   Yang, O. O. *et al.* Determinant of HIV-1 mutational escape from cytotoxic T lymphocytes. *J Exp Med* **197**, 1365-1375, doi:10.1084/jem.20022138 (2003).

135   Brockman, M. A. *et al.* Early selection in Gag by protective HLA alleles contributes to reduced HIV-1 replication capacity that may be largely compensated for in chronic infection. *J Virol* **84**, 11937-11949, doi:10.1128/JVI.01086-10 (2010).

136   Nikolich-Zugich, J., Slifka, M. K. & Messaoudi, I. The many important facets of T-cell repertoire diversity. *Nature reviews. Immunology* **4**, 123-132, doi:10.1038/nri1292 (2004).

137   Lissina, A., Chakrabarti, L. A., Takiguchi, M. & Appay, V. TCR clonotypes: molecular determinants of T-cell efficacy against HIV. *Current opinion in virology* **16**, 77-85, doi:10.1016/j.coviro.2016.01.017 (2016).

138   Lee, K. H. *et al.* The immunological synapse balances T cell receptor signaling and degradation. *Science (New York, N.Y.)* **302**, 1218-1222, doi:10.1126/science.1086507 (2003).

139   Ladell, K. *et al.* A molecular basis for the control of preimmune escape variants by HIV-specific CD8+ T cells. *Immunity* **38**, 425-436, doi:10.1016/j.immuni.2012.11.021 (2013).

140   Iglesias, M. C. *et al.* Escape from highly effective public CD8+ T-cell clonotypes by HIV. *Blood* **118**, 2138-2149, doi:10.1182/blood-2011-01-328781 (2011).

141   Miles, J. J., Douek, D. C. & Price, D. A. Bias in the alphabeta T-cell repertoire: implications for disease pathogenesis and vaccination. *Immunology and cell biology* **89**, 375-387, doi:10.1038/icb.2010.139 (2011).

142   Turner, S. J., La Gruta, N. L., Kedzierska, K., Thomas, P. G. & Doherty, P. C. Functional implications of T cell receptor diversity. *Current opinion in immunology* **21**, 286-290, doi:10.1016/j.coi.2009.05.004 (2009).

143   Ntale, R. S. *et al.* Temporal association of HLA-B*81:01- and HLA-B*39:10-mediated HIV-1 p24 sequence evolution with disease progression. *Journal of virology* **86**, 12013-12024, doi:10.1128/jvi.00539-12 (2012).

144   Bihl, F. *et al.* Impact of HLA-B alleles, epitope binding affinity, functional avidity, and viral coinfection on the immunodominance of virus-specific CTL responses. *Journal of immunology* **176**, 4094-4101 (2006).

145   Carlson, J. M. *et al.* Correlates of protective cellular immunity revealed by analysis of population-level immune escape pathways in HIV-1. *J Virol* **86**, 13202-13216, doi:10.1128/JVI.01998-12 (2012).

146   Kloverpris, H. N. *et al.* CD8+ TCR Bias and Immunodominance in HIV-1 Infection. *Journal of immunology (Baltimore, Md. : 1950)* **194**, 5329-5345, doi:10.4049/jimmunol.1400854 (2015).

147   Moosa, Y. *et al.* Case report: mechanisms of HIV elite control in two African women. *BMC infectious diseases* **18**, 54, doi:10.1186/s12879-018-2961-8 (2018).

148   Koofhethile, C. K. *et al.* CD8+ T cell breadth and ex vivo virus inhibition capacity distinguish between viremic controllers with and without protective HLA class I alleles. *J Virol*, doi:10.1128/JVI.00276-16 (2016).

149   Sidney, J., Peters, B., Frahm, N., Brander, C. & Sette, A. HLA class I supertypes: a revised and updated classification. *BMC Immunol* **9**, 1, doi:10.1186/1471-2172-9-1 (2008).

150   Goulder, P. J. *et al.* Differential narrow focusing of immunodominant human immunodeficiency virus gag-specific cytotoxic T-lymphocyte responses in infected African and caucasoid adults and children. *J Virol* **74**, 5679-5690. (2000).

151   Leslie, A. *et al.* Differential selection pressure exerted on HIV by CTL targeting identical epitopes but restricted by distinct HLA alleles from the same HLA supertype. *Journal of immunology (Baltimore, Md. : 1950)* **177**, 4699-4708 (2006).

152   Geldmacher, C. *et al.* Minor viral and host genetic polymorphisms can dramatically impact the biologic outcome of an epitope-specific CD8 T-cell response. *Blood* **114**, 1553-1562, doi:10.1182/blood-2009-02-206193 (2009).

153   Kloverpris, H. N. *et al.* HIV control through a single nucleotide on the HLA-B locus. *J Virol* **86**, 11493-11500, doi:10.1128/JVI.01020-12 (2012).

154   Geldmacher, C. *et al.* CD8 T-cell recognition of multiple epitopes within specific Gag regions is associated with maintenance of a low steady-state viremia in human immunodeficiency virus type 1-seropositive patients. *Journal of virology* **81**, 2440-2448, doi:10.1128/jvi.01847-06 (2007).

155   Ntale, R. S. *et al.* Temporal association of HLA-B*81:01- and HLA-B*39:10-mediated HIV-1 p24 sequence evolution with disease progression. *J Virol* **86**, 12013-12024, doi:10.1128/JVI.00539-12 (2012).

156   Kloverpris, H. N. *et al.* A molecular switch in immunodominant HIV-1-specific CD8 T-cell epitopes shapes differential HLA-restricted escape. *Retrovirology* **12**, 20, doi:10.1186/s12977-015-0149-5 (2015).

157   Bunce, M. PCR-sequence-specific primer typing of HLA class I and class II alleles. *Methods in molecular biology (Clifton, N.J.)* **210**, 143-171 (2003).

158   Thobakgale, C. F. *et al.* Human immunodeficiency virus-specific CD8+ T-cell activity is detectable from birth in the majority of in utero-infected infants. *Journal of virology* **81**, 12775-12784, doi:10.1128/jvi.00624-07 (2007).

159   Bernal-Estevez, D., Sanchez, R., Tejada, R. E. & Parra-Lopez, C. Chemotherapy and radiation therapy elicits tumor specific T cell responses in a breast cancer patient. *BMC cancer* **16**, 591, doi:10.1186/s12885-016-2625-2 (2016).

160   Han, A., Glanville, J., Hansmann, L. & Davis, M. M. Linking T-cell receptor sequence to functional phenotype at the single-cell level. *Nature biotechnology* **32**, 684-692, doi:10.1038/nbt.2938 (2014).

161   Anmole, G. *et al.* A robust and scalable TCR-based reporter cell assay to measure HIV-1 Nef-mediated T cell immune evasion. *Journal of immunological methods* **426**, 104-113, doi:10.1016/j.jim.2015.08.010 (2015).

162   Brockman, M. A., Tanzi, G. O., Walker, B. D. & Allen, T. M. Use of a novel GFP reporter cell line to examine replication capacity of CXCR4- and CCR5-tropic HIV-1 by flow cytometry. *Journal of virological methods* **131**, 134-142, doi:10.1016/j.jviromet.2005.08.003 (2006).

163   Suzuki, R. & Shimodaira, H. Pvclust: an R package for assessing the uncertainty in hierarchical clustering. *Bioinformatics* **22**, 1540-1542, doi:10.1093/bioinformatics/btl117 (2006).

164   Leslie, A. *et al.* Additive contribution of HLA class I alleles in the immune control of HIV-1 infection. *Journal of virology* **84**, 9879-9888, doi:10.1128/jvi.00320-10 (2010).

165   Prentice, H. A. *et al.* HLA-B*57 versus HLA-B*81 in HIV-1 infection: slow and steady wins the race? *Journal of virology* **87**, 4043-4051, doi:10.1128/jvi.03302-12 (2013).

166   Goulder, P. J. *et al.* Evolution and transmission of stable CTL escape mutations in HIV infection. *Nature* **412**, 334-338, doi:10.1038/35085576 (2001).

167   Goulder, P. J. *et al.* Late escape from an immunodominant cytotoxic T-lymphocyte response associated with progression to AIDS. *Nature medicine* **3**, 212-217 (1997).

168   Pereyra, F. *et al.* HIV control is mediated in part by CD8+ T-cell targeting of specific epitopes. *Journal of virology* **88**, 12937-12948, doi:10.1128/jvi.01004-14 (2014).

169   Threlkeld, S. C. *et al.* Degenerate and promiscuous recognition by CTL of peptides presented by the MHC class I A3-like superfamily: implications for vaccine development. *Journal of immunology* **159**, 1648-1657 (1997).

170   Allen, T. M. *et al.* De novo generation of escape variant-specific CD8+ T-cell responses following cytotoxic T-lymphocyte escape in chronic human immunodeficiency virus type 1 infection. *Journal of virology* **79**, 12952-12960, doi:10.1128/jvi.79.20.12952-12960.2005 (2005).

171   Ueno, T., Idegami, Y., Motozono, C., Oka, S. & Takiguchi, M. Altering effects of antigenic variations in HIV-1 on antiviral effectiveness of HIV-specific CTLs. *Journal of immunology (Baltimore, Md. : 1950)* **178**, 5513-5523 (2007).

172   Almeida, J. R. *et al.* Antigen sensitivity is a major determinant of CD8+ T-cell polyfunctionality and HIV-suppressive activity. *Blood* **113**, 6351-6360, doi:10.1182/blood-2009-02-206557 (2009).

173   Akahoshi, T. *et al.* Selection and accumulation of an HIV-1 escape mutant by three types of HIV-1-specific cytotoxic T lymphocytes recognizing wild-type and/or escape mutant epitopes. *Journal of virology* **86**, 1971-1981, doi:10.1128/jvi.06470-11 (2012).

174   Gillespie, G. M. *et al.* Cross-reactive cytotoxic T lymphocytes against a HIV-1 p24 epitope in slow progressors with B*57. *AIDS* **16**, 961-972 (2002).

175   Sunshine, J. E. *et al.* Fitness-Balanced Escape Determines Resolution of Dynamic Founder Virus Escape Processes in HIV-1 Infection. *J Virol* **89**, 10303-10318, doi:10.1128/JVI.01876-15 (2015).

176 Henn, M. R. *et al.* Whole genome deep sequencing of HIV-1 reveals the impact of early minor variants upon immune recognition during acute infection. *PLoS Pathog* **8**, e1002529, doi:10.1371/journal.ppat.1002529 (2012).

177 Borbulevych, O. Y. *et al.* T cell receptor cross-reactivity directed by antigen-dependent tuning of peptide-MHC molecular flexibility. *Immunity* **31**, 885-896, doi:10.1016/j.immuni.2009.11.003 (2009).

178 Willcox, B. E. *et al.* TCR binding to peptide-MHC stabilizes a flexible recognition interface. *Immunity* **10**, 357-365 (1999).

179 Armstrong, K. M., Piepenbrink, K. H. & Baker, B. M. Conformational changes and flexibility in T-cell receptor recognition of peptide-MHC complexes. *Biochemistry Journal* **415**, 183-196, doi:10.1042/BJ20080850 (2008).

180 Miles, J. J., McCluskey, J., Rossjohn, J. & Gras, S. Understanding the complexity and malleability of T-cell recognition. *Immunology and cell biology* **93**, 433-441, doi:10.1038/icb.2014.112 (2015).

181 Pantaleo, G. *et al.* HIV infection is active and progressive in lymphoid tissue during the clinically latent stage of disease. *Nature* **362**, 355-358, doi:10.1038/362355a0 (1993).

182 Horiike, M. *et al.* Lymph nodes harbor viral reservoirs that cause rebound of plasma viremia in SIV-infected macaques upon cessation of combined antiretroviral therapy. *Virology* **423**, 107-118, doi:10.1016/j.virol.2011.11.024 (2012).

183 Kohler, S. L. *et al.* Germinal Center T Follicular Helper Cells Are Highly Permissive to HIV-1 and Alter Their Phenotype during Virus Replication. *Journal of immunology (Baltimore, Md. : 1950)* **196**, 2711-2722, doi:10.4049/jimmunol.1502174 (2016).

184 Fukazawa, Y. *et al.* B cell follicle sanctuary permits persistent productive simian immunodeficiency virus infection in elite controllers. *Nature medicine* **21**, 132-139, doi:10.1038/nm.3781 (2015).

185 Streeck, H. AIDS virus seeks refuge in B cell follicles. *Nature medicine* **21**, 111-112, doi:10.1038/nm.3795 (2015).

186 Velu, V., Mylvaganam, G., Ibegbu, C. & Amara, R. R. Tfh1 Cells in Germinal Centers During Chronic HIV/SIV Infection. *Frontiers in immunology* **9**, 1272, doi:10.3389/fimmu.2018.01272 (2018).

187 Leong, Y. A. *et al.* CXCR5(+) follicular cytotoxic T cells control viral infection in B cell follicles. *Nature immunology* **17**, 1187-1196, doi:10.1038/ni.3543 (2016).

188 He, R. *et al.* Follicular CXCR5- expressing CD8(+) T cells curtail chronic viral infection. *Nature* **537**, 412-428, doi:10.1038/nature19317 (2016).

189 Chu, F. *et al.* CXCR5(+)CD8(+) T cells are a distinct functional subset with an antitumor activity. *Leukemia*, doi:10.1038/s41375-019-0464-2 (2019).

190 Petrovas, C. *et al.* Follicular CD8 T cells accumulate in HIV infection and can kill infected cells in vitro via bispecific antibodies. *Science translational medicine* **9**, doi:10.1126/scitranslmed.aag2285 (2017).

191 Cyster, J. G. Chemokines and cell migration in secondary lymphoid organs. *Science (New York, N.Y.)* **286**, 2098-2102, doi:10.1126/science.286.5447.2098 (1999).

192 Moser, B. & Ebert, L. Lymphocyte traffic control by chemokines: follicular B helper T cells. *Immunology letters* **85**, 105-112 (2003).

193 Hansell, C. A., Simpson, C. V. & Nibbs, R. J. Chemokine sequestration by atypical chemokine receptors. *Biochemical Society transactions* **34**, 1009-1013, doi:10.1042/bst0341009 (2006).

194 Im, S. J. *et al.* Defining CD8+ T cells that provide the proliferative burst after PD-1 therapy. *Nature* **537**, 417-421, doi:10.1038/nature19330 (2016).

195 Mylvaganam, G. H. *et al.* Dynamics of SIV-specific CXCR5+ CD8 T cells during chronic SIV infection. *Proceedings of the National Academy of Sciences of the United States of America* **114**, 1976-1981, doi:10.1073/pnas.1621418114 (2017).

196 Iwafuchi-Doi, M. & Zaret, K. S. Pioneer transcription factors in cell reprogramming. *Genes & development* **28**, 2679-2692, doi:10.1101/gad.253443.114 (2014).

197 Yu, B. *et al.* Erratum: Epigenetic landscapes reveal transcription factors that regulate CD8(+) T cell differentiation. *Nature immunology* **18**, 705, doi:10.1038/ni0617-705b (2017).

198 Collings, C. K. & Anderson, J. N. Links between DNA methylation and nucleosome occupancy in the human genome. *Epigenetics & chromatin* **10**, 18, doi:10.1186/s13072-017-0125-5 (2017).

199 Allen, C. D. *et al.* Germinal center dark and light zone organization is mediated by CXCR4 and CXCR5. *Nature immunology* **5**, 943-952, doi:10.1038/ni1100 (2004).

200 Sloan, C. A. *et al.* ENCODE data at the ENCODE portal. *Nucleic acids research* **44**, D726-732, doi:10.1093/nar/gkv1160 (2016).

201 Robinson, M. D., McCarthy, D. J. & Smyth, G. K. edgeR: a Bioconductor package for differential expression analysis of digital gene expression data. *Bioinformatics (Oxford, England)* **26**, 139-140, doi:10.1093/bioinformatics/btp616 (2010).

202 Yu, G., Wang, L. G. & He, Q. Y. ChIPseeker: an R/Bioconductor package for ChIP peak annotation, comparison and visualization. *Bioinformatics (Oxford, England)* **31**, 2382-2383, doi:10.1093/bioinformatics/btv145 (2015).

203 Pimentel, H., Bray, N. L., Puente, S., Melsted, P. & Pachter, L. Differential analysis of RNA-seq incorporating quantification uncertainty. *Nature methods* **14**, 687-690, doi:10.1038/nmeth.4324 (2017).

204 Piper, J. *et al.* Wellington: a novel method for the accurate identification of digital genomic footprints from DNase-seq data. *Nucleic acids research* **41**, e201, doi:10.1093/nar/gkt850 (2013).

205 Gusmao, E. G., Allhoff, M., Zenke, M. & Costa, I. G. Analysis of computational footprinting methods for DNase sequencing experiments. *Nature methods* **13**, 303-309, doi:10.1038/nmeth.3772 (2016).

206 Kulakovskiy, I. V. *et al.* HOCOMOCO: towards a complete collection of transcription factor binding models for human and mouse via large-scale ChIP-Seq analysis. *Nucleic acids research* **46**, D252-d259, doi:10.1093/nar/gkx1106 (2018).

207 Khan, A. *et al.* JASPAR 2018: update of the open-access database of transcription factor binding profiles and its web framework. *Nucleic acids research* **46**, D1284, doi:10.1093/nar/gkx1188 (2018).

208 Storey, J. D. & Tibshirani, R. Statistical significance for genomewide studies. *Proceedings of the National Academy of Sciences of the United States of America* **100**, 9440-9445, doi:10.1073/pnas.1530509100 (2003).

209 Piper, J. *et al.* Wellington-bootstrap: differential DNase-seq footprinting identifies cell-type determining transcription factors. *BMC genomics* **16**, 1000, doi:10.1186/s12864-015-2081-4 (2015).

210 Langfelder, P. & Horvath, S. WGCNA: an R package for weighted correlation network analysis. *BMC bioinformatics* **9**, 559, doi:10.1186/1471-2105-9-559 (2008).

211 Love, M. I., Huber, W. & Anders, S. Moderated estimation of fold change and dispersion for RNA-seq data with DESeq2. *Genome biology* **15**, 550, doi:10.1186/s13059-014-0550-8 (2014).

212 Russo, P. S. T. *et al.* CEMiTool: a Bioconductor package for performing comprehensive modular co-expression analyses. *BMC bioinformatics* **19**, 56, doi:10.1186/s12859-018-2053-1 (2018).

213 Schep, A. N., Wu, B., Buenrostro, J. D. & Greenleaf, W. J. chromVAR: inferring transcription-factor-associated accessibility from single-cell epigenomic data. *Nature methods* **14**, 975-978, doi:10.1038/nmeth.4401 (2017).

214 Buggert, M. *et al.* Identification and characterization of HIV-specific resident memory CD8(+) T cells in human lymphoid tissue. *Science immunology* **3**, doi:10.1126/sciimmunol.aar4526 (2018).

215 Gerner, M. Y., Kastenmuller, W., Ifrim, I., Kabat, J. & Germain, R. N. Histo-cytometry: a method for highly multiplex quantitative tissue imaging analysis

applied to dendritic cell subset microanatomy in lymph nodes. *Immunity* **37**, 364-376, doi:10.1016/j.immuni.2012.07.011 (2012).

216   Ferrando-Martinez, S. *et al.* Accumulation of follicular CD8+ T cells in pathogenic SIV infection. *The Journal of clinical investigation* **128**, 2089-2103, doi:10.1172/jci96207 (2018).

217   Johnston, R. J. *et al.* Bcl6 and Blimp-1 are reciprocal and antagonistic regulators of T follicular helper cell differentiation. *Science (New York, N.Y.)* **325**, 1006-1010, doi:10.1126/science.1175870 (2009).

218   Nurieva, R. I. *et al.* Bcl6 mediates the development of T follicular helper cells. *Science (New York, N.Y.)* **325**, 1001-1005, doi:10.1126/science.1176676 (2009).

219   Crotty, S., Johnston, R. J. & Schoenberger, S. P. Effectors and memories: Bcl-6 and Blimp-1 in T and B lymphocyte differentiation. *Nature immunology* **11**, 114-120, doi:10.1038/ni.1837 (2010).

220   Medvedeva, Y. A. *et al.* EpiFactors: a comprehensive database of human epigenetic factors and complexes. *Database : the journal of biological databases and curation* **2015**, bav067, doi:10.1093/database/bav067 (2015).

221   Litterst, C. M., Kliem, S., Marilley, D. & Pfitzner, E. NCoA-1/SRC-1 is an essential coactivator of STAT5 that binds to the FDL motif in the alpha-helical region of the STAT5 transactivation domain. *The Journal of biological chemistry* **278**, 45340-45351, doi:10.1074/jbc.M303644200 (2003).

222   Han, X. *et al.* Destabilizing LSD1 by Jade-2 promotes neurogenesis: an antibraking system in neural development. *Molecular cell* **55**, 482-494, doi:10.1016/j.molcel.2014.06.006 (2014).

223   Batista, I. A. A. & Helguero, L. A. Biological processes and signal transduction pathways regulated by the protein methyltransferase SETD7 and their significance in cancer. *Signal transduction and targeted therapy* **3**, 19, doi:10.1038/s41392-018-0017-6 (2018).

224   Little, D. P., Braun, A., O'Donnell, M. J. & Koster, H. Mass spectrometry from miniaturized arrays for full comparative DNA analysis. *Nature medicine* **3**, 1413-1416 (1997).

225   Bocker, S. SNP and mutation discovery using base-specific cleavage and MALDI-TOF mass spectrometry. *Bioinformatics (Oxford, England)* **19 Suppl 1**, i44-53, doi:10.1093/bioinformatics/btg1004 (2003).

226   Hartmer, R. *et al.* RNase T1 mediated base-specific cleavage and MALDI-TOF MS for high-throughput comparative sequence analysis. *Nucleic acids research* **31**, e47, doi:10.1093/nar/gng047 (2003).

227   Stanssens, P. *et al.* High-throughput MALDI-TOF discovery of genomic sequence polymorphisms. *Genome research* **14**, 126-133, doi:10.1101/gr.1692304 (2004).

228   Ehrich, M. *et al.* Quantitative high-throughput analysis of DNA methylation patterns by base-specific cleavage and mass spectrometry. *Proceedings of the National Academy of Sciences of the United States of America* **102**, 15785-15790, doi:10.1073/pnas.0507816102 (2005).

229   Yang, J. *et al.* 5-Aza-2'-deoxycytidine, a DNA methylation inhibitor, induces cytotoxicity, cell cycle dynamics and alters expression of DNA methyltransferase 1 and 3A in mouse hippocampus-derived neuronal HT22 cells. *Journal of toxicology and environmental health. Part A* **80**, 1222-1229, doi:10.1080/15287394.2017.1367143 (2017).

230   Buenrostro, J. D., Giresi, P. G., Zaba, L. C., Chang, H. Y. & Greenleaf, W. J. Transposition of native chromatin for fast and sensitive epigenomic profiling of open chromatin, DNA-binding proteins and nucleosome position. *Nature methods* **10**, 1213-1218, doi:10.1038/nmeth.2688 (2013).

231   Winter, D. R., Jung, S. & Amit, I. Making the case for chromatin profiling: a new tool to investigate the immune-regulatory landscape. *Nature reviews. Immunology* **15**, 585-594, doi:10.1038/nri3884 (2015).

232   Choy, J. S. *et al.* DNA methylation increases nucleosome compaction and rigidity. *Journal of the American Chemical Society* **132**, 1782-1783, doi:10.1021/ja910264z (2010).

233   Wang, H. *et al.* Purification and functional characterization of a histone H3-lysine 4-specific methyltransferase. *Molecular cell* **8**, 1207-1217 (2001).

234   Wang, J. *et al.* The lysine demethylase LSD1 (KDM1) is required for maintenance of global DNA methylation. *Nature genetics* **41**, 125-129, doi:10.1038/ng.268 (2009).

235   Lee, M. T. *et al.* Nanog, Pou5f1 and SoxB1 activate zygotic gene expression during the maternal-to-zygotic transition. *Nature* **503**, 360-364, doi:10.1038/nature12632 (2013).

236   Leichsenring, M., Maes, J., Mossner, R., Driever, W. & Onichtchouk, D. Pou5f1 transcription factor controls zygotic gene activation in vertebrates. *Science (New York, N.Y.)* **341**, 1005-1009, doi:10.1126/science.1242527 (2013).

237   Iwafuchi-Doi, M. The mechanistic basis for chromatin regulation by pioneer transcription factors. *Wiley interdisciplinary reviews. Systems biology and medicine* **11**, e1427, doi:10.1002/wsbm.1427 (2019).

238   Chang, J. T., Wherry, E. J. & Goldrath, A. W. Molecular regulation of effector and memory T cell differentiation. *Nature immunology* **15**, 1104-1115, doi:10.1038/ni.3031 (2014).

239   Bulger, M. & Groudine, M. Functional and mechanistic diversity of distal transcription enhancers. *Cell* **144**, 327-339, doi:10.1016/j.cell.2011.01.024 (2011).

240   Yu, D. & Ye, L. A Portrait of CXCR5(+) Follicular Cytotoxic CD8(+) T cells. *Trends in immunology* **39**, 965-979, doi:10.1016/j.it.2018.10.002 (2018).

241   Lovkvist, C., Sneppen, K. & Haerter, J. O. Exploring the Link between Nucleosome Occupancy and DNA Methylation. *Frontiers in genetics* **8**, 232, doi:10.3389/fgene.2017.00232 (2017).

242   Svensson, J. P. *et al.* A nucleosome turnover map reveals that the stability of histone H4 Lys20 methylation depends on histone recycling in transcribed chromatin. *Genome research* **25**, 872-883, doi:10.1101/gr.188870.114 (2015).

243   Barisic, D., Stadler, M. B., Iurlaro, M. & Schubeler, D. Mammalian ISWI and SWI/SNF selectively mediate binding of distinct transcription factors. *Nature* **569**, 136-140, doi:10.1038/s41586-019-1115-5 (2019).

244   Benezra, R., Davis, R. L., Lockshon, D., Turner, D. L. & Weintraub, H. The protein Id: a negative regulator of helix-loop-helix DNA binding proteins. *Cell* **61**, 49-59, doi:10.1016/0092-8674(90)90214-y (1990).

245   Soufi, A., Donahue, G. & Zaret, K. S. Facilitators and impediments of the pluripotency reprogramming factors' initial engagement with the genome. *Cell* **151**, 994-1004, doi:10.1016/j.cell.2012.09.045 (2012).

246   Choi, J., Jeon, S., Choi, S., Park, K. & Seong, R. H. The SWI/SNF chromatin remodeling complex regulates germinal center formation by repressing Blimp-1 expression. *Proceedings of the National Academy of Sciences of the United States of America* **112**, E718-727, doi:10.1073/pnas.1418592112 (2015).

247   Menon, D. U., Shibata, Y., Mu, W. & Magnuson, T. Mammalian SWI/SNF collaborates with a polycomb-associated protein to regulate male germ line transcription in the mouse. *Development (Cambridge, England)*, doi:10.1242/dev.174094 (2019).

248   Li, M. *et al.* Dynamic regulation of transcription factors by nucleosome remodeling. *eLife* **4**, doi:10.7554/eLife.06249 (2015).

249   Araki, Y. *et al.* Genome-wide analysis of histone methylation reveals chromatin state-based regulation of gene transcription and function of memory CD8+ T cells. *Immunity* **30**, 912-925, doi:10.1016/j.immuni.2009.05.006 (2009).

250   Araki, Y., Fann, M., Wersto, R. & Weng, N. P. Histone acetylation facilitates rapid and robust memory CD8 T cell response through differential expression of effector molecules (eomesodermin and its targets: perforin and granzyme B). *Journal of immunology (Baltimore, Md. : 1950)* **180**, 8102-8108, doi:10.4049/jimmunol.180.12.8102 (2008).

251   Russ, B. E. *et al.* Distinct epigenetic signatures delineate transcriptional programs during virus-specific CD8(+) T cell differentiation. *Immunity* **41**, 853-865, doi:10.1016/j.immuni.2014.11.001 (2014).

252   Crompton, J. G. *et al.* Lineage relationship of CD8(+) T cell subsets is revealed by progressive changes in the epigenetic landscape. *Cellular & molecular immunology* **13**, 502-513, doi:10.1038/cmi.2015.32 (2016).

253   Troyer, R. M. *et al.* Variable fitness impact of HIV-1 escape mutations to cytotoxic T lymphocyte (CTL) response. *PLoS pathogens* **5**, e1000365, doi:10.1371/journal.ppat.1000365 (2009).

254   Goulder, P. J. & Walker, B. D. HIV and HLA class I: an evolving relationship. *Immunity* **37**, 426-440, doi:10.1016/j.immuni.2012.09.005 (2012).

255   Brennan, C. A. *et al.* Early HLA-B*57-restricted CD8+ T lymphocyte responses predict HIV-1 disease progression. *Journal of virology* **86**, 10505-10516, doi:10.1128/jvi.00102-12 (2012).

256   Fukazawa, Y. *et al.* Lymph node T cell responses predict the efficacy of live attenuated SIV vaccines. *Nature medicine* **18**, 1673-1681, doi:10.1038/nm.2934 (2012).

257   Deleage, C. *et al.* Defining HIV and SIV Reservoirs in Lymphoid Tissues. *Pathogens & immunity* **1**, 68-106 (2016).

258   Connick, E. *et al.* Compartmentalization of simian immunodeficiency virus replication within secondary lymphoid tissues of rhesus macaques is linked to disease stage and inversely related to localization of virus-specific CTL. *Journal of immunology (Baltimore, Md. : 1950)* **193**, 5613-5625, doi:10.4049/jimmunol.1401161 (2014).

259   Vinuesa, C. G. & Cyster, J. G. How T cells earn the follicular rite of passage. *Immunity* **35**, 671-680, doi:10.1016/j.immuni.2011.11.001 (2011).

260   Lickwar, C. R., Mueller, F., Hanlon, S. E., McNally, J. G. & Lieb, J. D. Genome-wide protein-DNA binding dynamics suggest a molecular clutch for transcription factor function. *Nature* **484**, 251-255, doi:10.1038/nature10985 (2012).

4.5   Funding Statement

4.6   Ethics Approval for the Studies

UNIVERSITY OF KWAZULU-NATAL
INYUVESI YAKWAZULU-NATALI

RESEARCH OFFICE
BIOMEDICAL RESEARCH ETHICS ADMINISTRATION
Westville Campus
Govan Mbeki Building
Private Bag X 54001
Durban
4000
KwaZulu-Natal, SOUTH AFRICA
Tel: 27 31 2604769 - Fax: 27 31 260-4609
Email: BREC@ukzn.ac.za
Website: http://research.ukzn.ac.za/Research-Ethics/Biomedical-Research-Ethics.aspx

26 April 2018

Mr Funsho Ogunshola
719 Umbilo Road
DDMRI, Level 1
Nelson R. Mandela School of Medicine
Congella
Durban
4013
fasio2002@gmail.com

Dear Mr Ogunshola

PROTOCOL: Analysis of viral inhibition activity of CD8 T cells targeting identical epitopes but restricted by different HLA class one alleles from the same HLA Supertype: Degree Purposes (MMedSc). BREC REF: BE305/14.

RECERTIFICATION APPLICATION APPROVAL NOTICE

Approved: 19 June 2018
Expiration of Ethical Approval: 18 June 2019

I wish to advise you that your application for Recertification on 10 April 2018 for the above protocol has been **noted and approved** by a sub-committee of the Biomedical Research Ethics Committee (BREC) for another approval period. The start and end dates of this period are indicated above.

If any modifications or adverse events occur in the project before your next scheduled review, you must submit them to BREC for review.   Except in emergency situations, no change to the protocol may be implemented until you have received written BREC approval for the change.

The approval will be **ratified** by a full Committee at a meeting to be held on **12 June 2018.**

Yours sincerely

Mrs A Marimuthu
Senior Administrator: Biomedical Research Ethics

cc: leslie@ukzn.ac.za

UNIVERSITY OF
KWAZULU-NATAL

INYUVESI
YAKWAZULU-NATALI

RESEARCH OFFICE
Biomedical Research Ethics Administration
Westville Campus, Govan Mbeki Building
Private Bag X 54001
Durban
4000
KwaZulu-Natal, SOUTH AFRICA
Tel: 27 31 2604769 - Fax: 27 31 2604609
Email: BREC@ukzn.ac.za
Website http://research.ukzn.ac.za/Research-Ethics/Biomedical-Research-Ethics.aspx

04 September 2018

Mr FJ Ogunshola (214584502)
HIV Pathogenesis Programme
School of Laboratory Medicine and Medical Sciences
Health Sciences
fashio2002@gmail.com

Title: Trafficking, phenotype and function of CD8 T cells in the lymphoid tissues during HIV-1 subtype C Infection.
Degree: PhD
BREC REF NO: BE582/16

RECERTIFICATION APPLICATION APPROVAL NOTICE
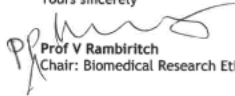
Approved: 17 November 2018
Expiration of Ethical Approval: 16 November 2019

I wish to advise you that your application for Recertification received on 31 August 2018 for the above protocol has been **noted and approved** by a sub-committee of the Biomedical Research Ethics Committee (BREC) for another approval period. The start and end dates of this period are indicated above.

If any modifications or adverse events occur in the project before your next scheduled review, you must submit them to BREC for review. Except in emergency situations, no change to the protocol may be implemented until you have received written BREC approval for the change.

The committee will be notified of the above approval at its next meeting to be held on 09 October 2018.

Yours sincerely

Prof V Rambiritch
Chair: Biomedical Research Ethics Committee

cc supervisor: ndhlovuz@ukzn.ac.za
cc postgraduate administrator: dudhrajhp@ukzn.ac.za
cc: leslie@ukzn.ac.za